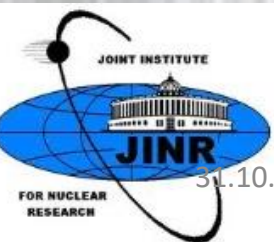




EXPERIMENTS AT CIRCULAR ELECTRON-POSITRON COLLIDER

PROPOSITION FOR JINR PROJECT



31.10.2024

Yuri Davydov¹⁾ Yuri Kulchitsky^{1),2)}

1) JINR, Dubna 2) IP NASB, Minsk, Belarus

31.10.2024 seminar DLNP, JINR, Dubna

❑ The SM describes the fundamental constituents of matter and their interactions

❑ The SM of particle physics is the theory describing **3 of the 4 known fundamental forces (electromagnetic, weak and strong interactions** — *excluding gravity*) in the universe and classifying all known elementary particles

QUARKS

UP mass 2,3 MeV/c ² charge 2/3 spin 1/2 u	CHARM 1,275 GeV/c ² 2/3 1/2 c	TOP 173,07 GeV/c ² 2/3 1/2 t
--	--	---

DOWN 4,8 MeV/c ² -1/3 1/2 d	STRANGE 95 MeV/c ² -1/3 1/2 s	BOTTOM 4,18 GeV/c ² -1/3 1/2 b
--	--	---

LEPTONS

ELECTRON 0,511 MeV/c ² -1 1/2 e	MUON 105,7 MeV/c ² -1 1/2 μ	TAU 1,777 GeV/c ² -1 1/2 τ
--	--	---

ELECTRON NEUTRINO <2,2 eV/c ² 0 1/2 ν_e	MUON NEUTRINO <0,17 MeV/c ² 0 1/2 ν_μ	TAU NEUTRINO <15,5 MeV/c ² 0 1/2 ν_τ
--	--	---

GAUGE BOSONS

GLUON 0 0 1 g

PHOTON 0 0 1 γ
--

Z BOSON 91,2 GeV/c ² 0 1 Z

W BOSON 80,4 GeV/c ² ±1 1 W
--

HIGGS BOSON
126 GeV/c²
0
0
H

❖ **Quantum chromodynamics sector**

❖ **Electroweak sector**

❖ **Higgs sector**

❖ **Yukawa sector**

$$\mathcal{L}_{\text{QCD}} = \sum_i \bar{\psi}_i \left(i\gamma^\mu (\partial_\mu \delta_{ij} - ig_s G_\mu^a T_{ij}^a) \right) \psi_j - \frac{1}{4} G_{\mu\nu}^a G_{\mu\nu}^a$$

$$\mathcal{L}_{\text{EW}} = \sum_\psi \bar{\psi} \gamma^\mu \left(i\partial_\mu - g' \frac{1}{2} Y_W B_\mu - g \frac{1}{2} \vec{\tau}_L \vec{W}_\mu \right) \psi - \frac{1}{4} W_{\mu\nu}^a W_{\mu\nu}^a - \frac{1}{4} B_{\mu\nu} B_{\mu\nu}$$

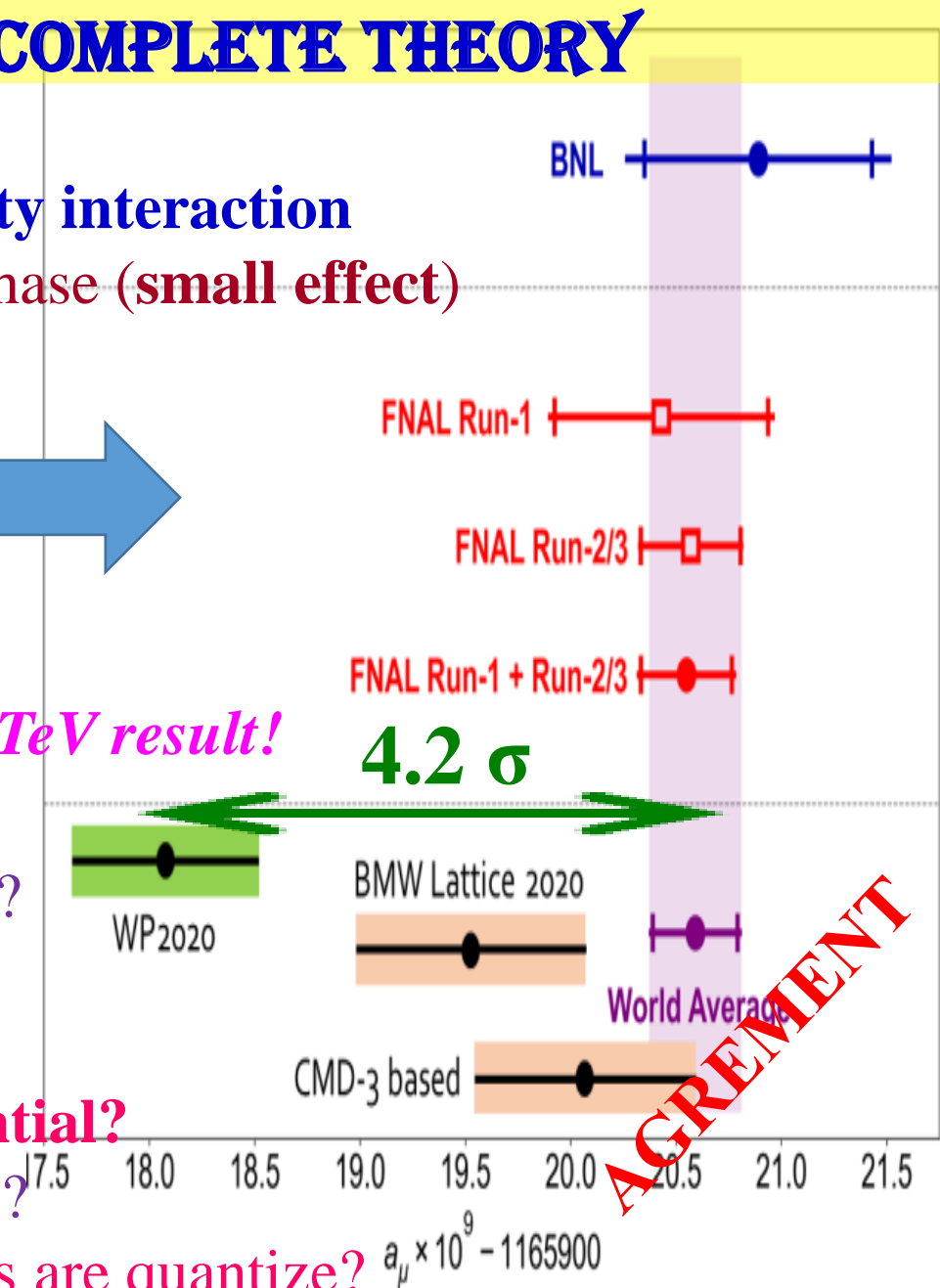
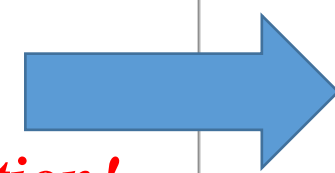
$$\mathcal{L}_H = \left| \left(\partial_\mu + \frac{i}{2} (g' Y_W B_\mu + g \vec{\tau} \vec{W}_\mu) \right) \varphi \right|^2 - \frac{\lambda^2}{4} (\varphi^\dagger \varphi - v^2)^2$$

$$\mathcal{L}_{\text{Yukawa}} = \bar{U}_L G_u U_R \varphi^0 - \bar{D}_L G_u U_R \varphi^- + \bar{U}_L G_d D_R \varphi^+ + \bar{D}_L G_d D_R \varphi^0 + \text{h. c.},$$

Interaction	Property	Fundamental Forces			
		Weak	Electromagnetic	Strong	
		Electroweak		Fundamental	Residual
Acts on:	Mass - Energy	Flavor	Electric charge	Color charge	Atomic nuclei
Particles experiencing:	All particles	quarks, lepton s	Electrically charged	Quarks, Gluons	Hadrons
Particles mediating:	Graviton (Not yet observed)	W ⁺ , W ⁻ and Z ⁰	γ (photon)	Gluons	Mesons
Strength at the scale of quarks:	10 ⁻⁴¹ (predicted)	10 ⁻⁴	1	60	Not applicable to quarks
Strength at the scale of protons/neutrons:	10 ⁻³⁶ (predicted) Yuri Kulchitsky, JINR	10 ⁻⁷	1	Not applicable to hadrons	20

STANDARD MODEL PROBLEMS: AN INCOMPLETE THEORY

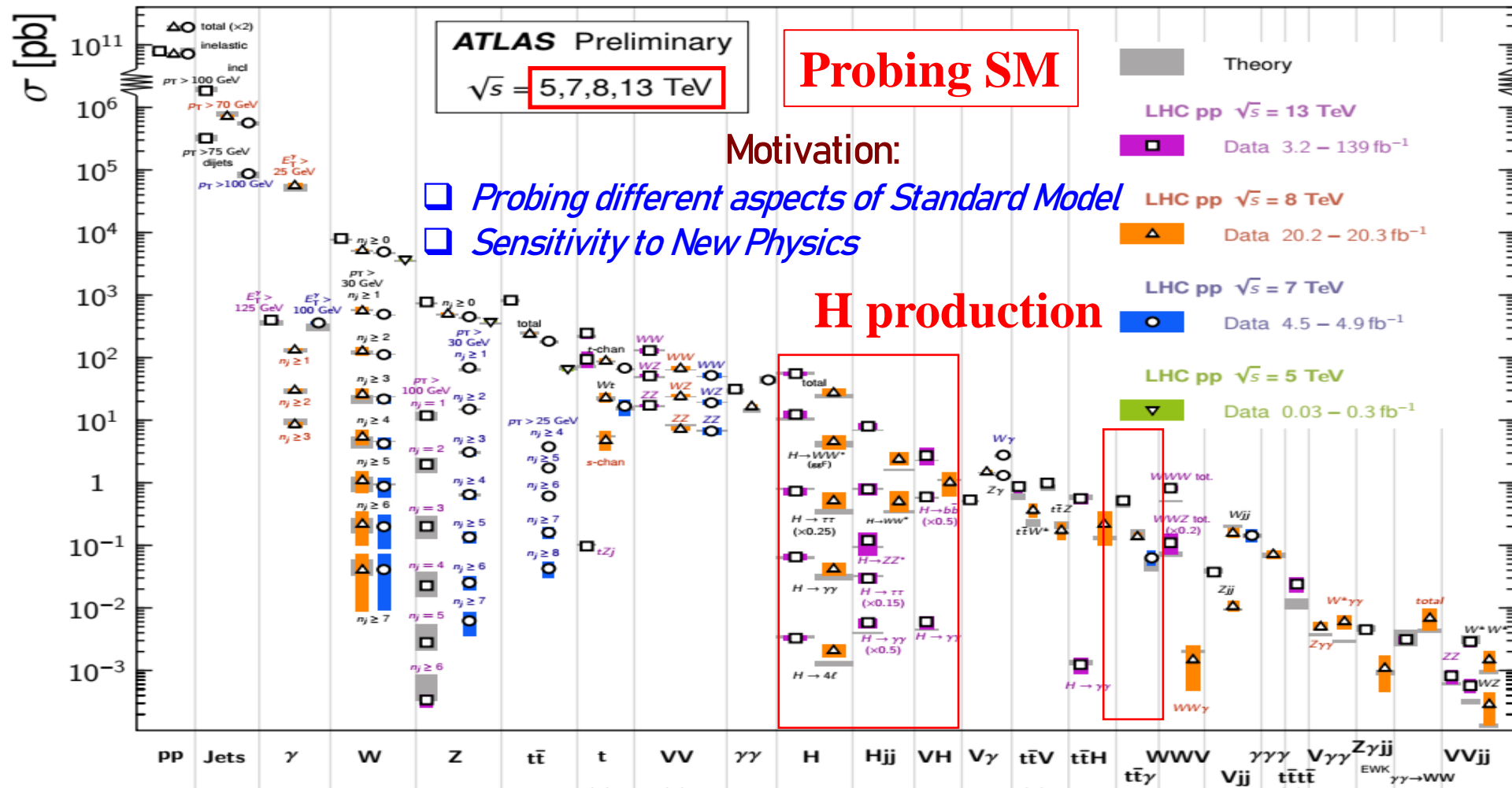
- ❑ Unknown nature of **Dark Matter**
- ❑ Very small cosmological constant and very weak gravity interaction
- ❑ CP violation Cabibbo–Kobayashi–Maskawa (CKM) phase (small effect)
- ❑ Particle–antiparticle asymmetry in the Universe
- ❑ Problem of neutrino masses, mixing, oscillations
- ❑ Muon (g-2) μ anomaly ($3.5\sigma \rightarrow 4.2\sigma$ BNL):
 $CMD-3 \sigma(e^+ e^- \rightarrow \pi^+ \pi^-) \rightarrow$ *new theoretical calculation!*
- ❑ B-anomalies (4.5σ): semi-leptonic B-decays
- ❑ CDF W-mass anomaly (7σ): *new ATLAS & CMS at 13 TeV result!*



- What is a generation? Why there are only 3 generations?
- What is a nature of **quark-lepton analogy**?
- Are there additional gauge symmetries?
- What is responsible for a formation of the Higgs potential?
- Why gravity is so weak comparing to other interactions?
- What is responsible for gauge symmetries, why charges are quantize?
- To which accuracy the Charge, Parity & Time reversal symmetry (CPT) is exact?

Standard Model Production Cross Section Measurements

Status: February 2022



ATLAS/CMS Results

1. Higgs boson discovery
2. Systematic study of pp-processes at 0.9 – 13.6 TeV & comparison with SM predictions
3. There was no discovery of the MSSM particles at 10 TeV region
4. There was no discovery of exotic models particles

Conclusion:
No BSM physics at 10 TeV

Review of Particle Physics,
PTEP 2022 083C01
Part 9: QCD; Figure 9.1

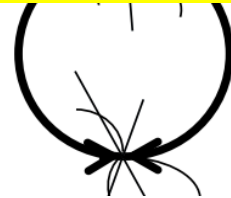
ATLAS: Summary of SM and fiducial production cross-section measurements in pp interactions at $\sqrt{s}=5, 7, 8, 13$ TeV, corrected for branching fractions, compared to the corresponding theoretical expectations

$$\mu_{if} = (\sigma_i / \sigma_i^{SM}) \times (B_f / B_f^{SM})$$

The inclusive Higgs boson production rate relative to the SM prediction is measured to be

$$\mu = 1.05 \pm 0.06 = 1.05 \pm 0.03 \text{ (stat.)} \pm 0.03 \text{ (exp.)} \pm 0.04 \text{ (sig. th.)} \pm 0.02 \text{ (bkg. th.)}$$

FUTURE COLLIDERS



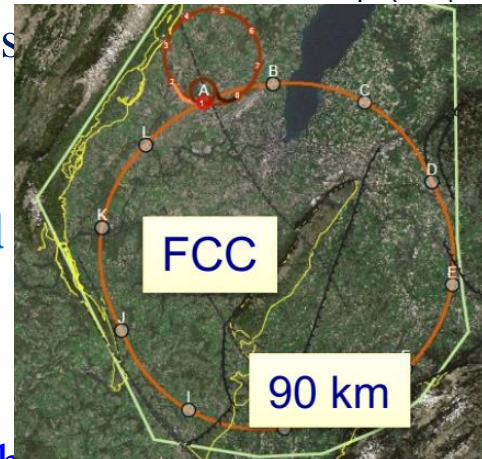
❖ ILC (Japan):

- Linear collider with high-gradient superconducting acceleration
- Ultimate: 0.5-1(?) TeV
- To secure funding: reduce cost by starting at 250 GeV (H factory)



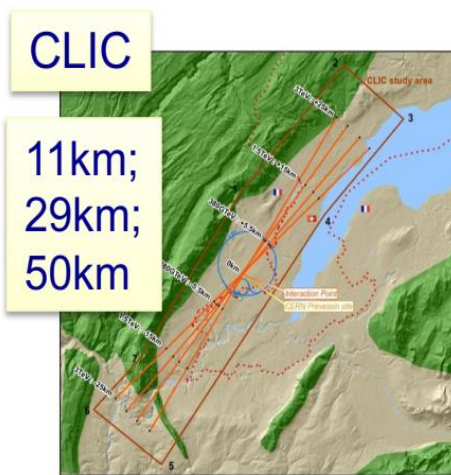
❖ FCC-ee/FCC-hh (CERN):

- Protons to extend energy frontier
- **90 km** ring with 16T magnets
- Use FCC-hh tunnel for e^+e^- collider
- Technology for ee: **standard**



❖ CLIC (CERN):

- Linear collider with high gradient normal-conducting acceleration
- Ultimate: multi-TeV (3) e^+e^- collisions
- Use technology to overcome challenges
- **Stages**, for physics and funding



❖ CEPC/SppC

- Essentially an FCC-ee, then hh with
 - more conservative luminosity estimates
 - in China



❖ Outliers:

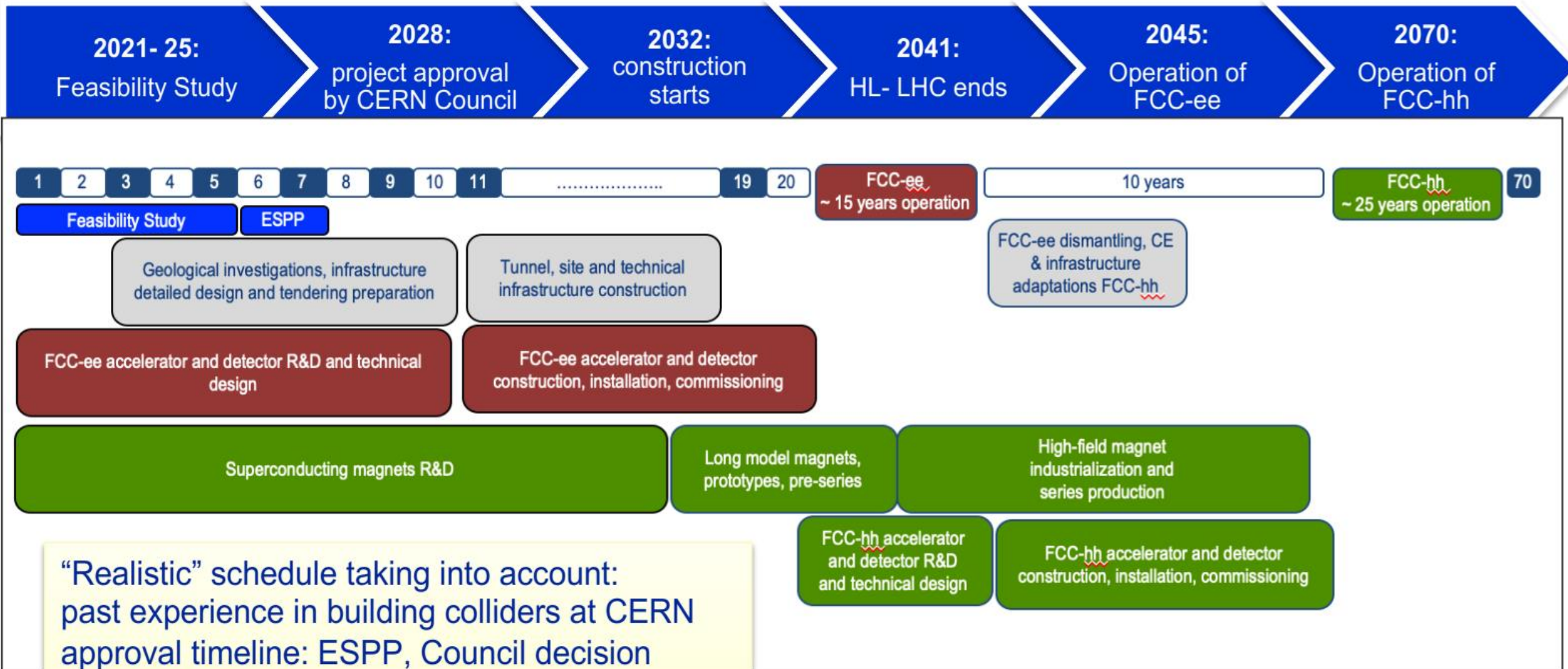
- “Low-field” (7T) magnets @FCC (?)
- Muon Collider (?)

CEPC: multiple candidate sites in China

FCC INTEGRATED PROGRAM - TIMELINE



FCCee Conceptual Design Study started in 2014 leading to Conceptual Design Report in 2018



“Realistic” schedule taking into account: past experience in building colliders at CERN approval timeline: ESPP, Council decision that HL-LHC will run until 2041

Can be accelerated if more resources available

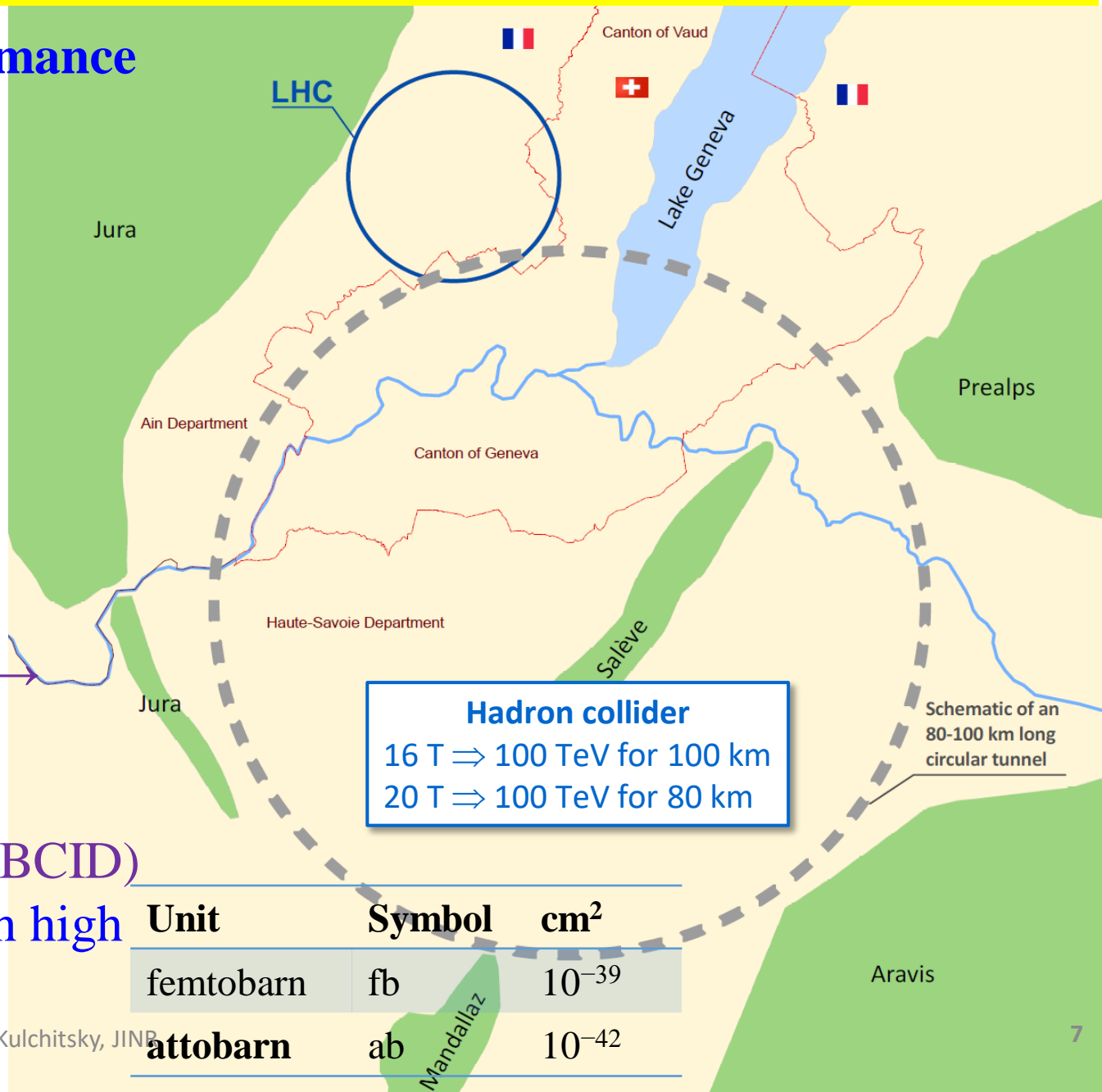
FCC INFRASTRUCTURE & OPERATION

Future Circulated Collider (FCC) performance

- Center of mass energy: **100 TeV**
- Peak luminosity ultimate: $\leq 30 \times 10^{34}$
- Bunch Crossing **<5 ns**
- Integrated luminosity ultimate $\sim 1000 \text{ fb}^{-1}$ (average per year)
- 25 years operation, leading to $\sim 20 \text{ ab}^{-1}$

Consequence on detectors

- Boosted objects \rightarrow up to $|\eta|=6$ coverage
- High pileup and fast Bunch-Crossing (BC) \rightarrow very fast and granular detectors
- Momentum resolution $\approx 15\%$ at $p_T=10 \text{ TeV}$
- **~1 ns** sharp Bunch-Crossing Identification (BCID)
- Particle flow capability for calorimeters with high granularity **25 mrad²**
- Fine timing against pileup \rightarrow **< 100 ps**

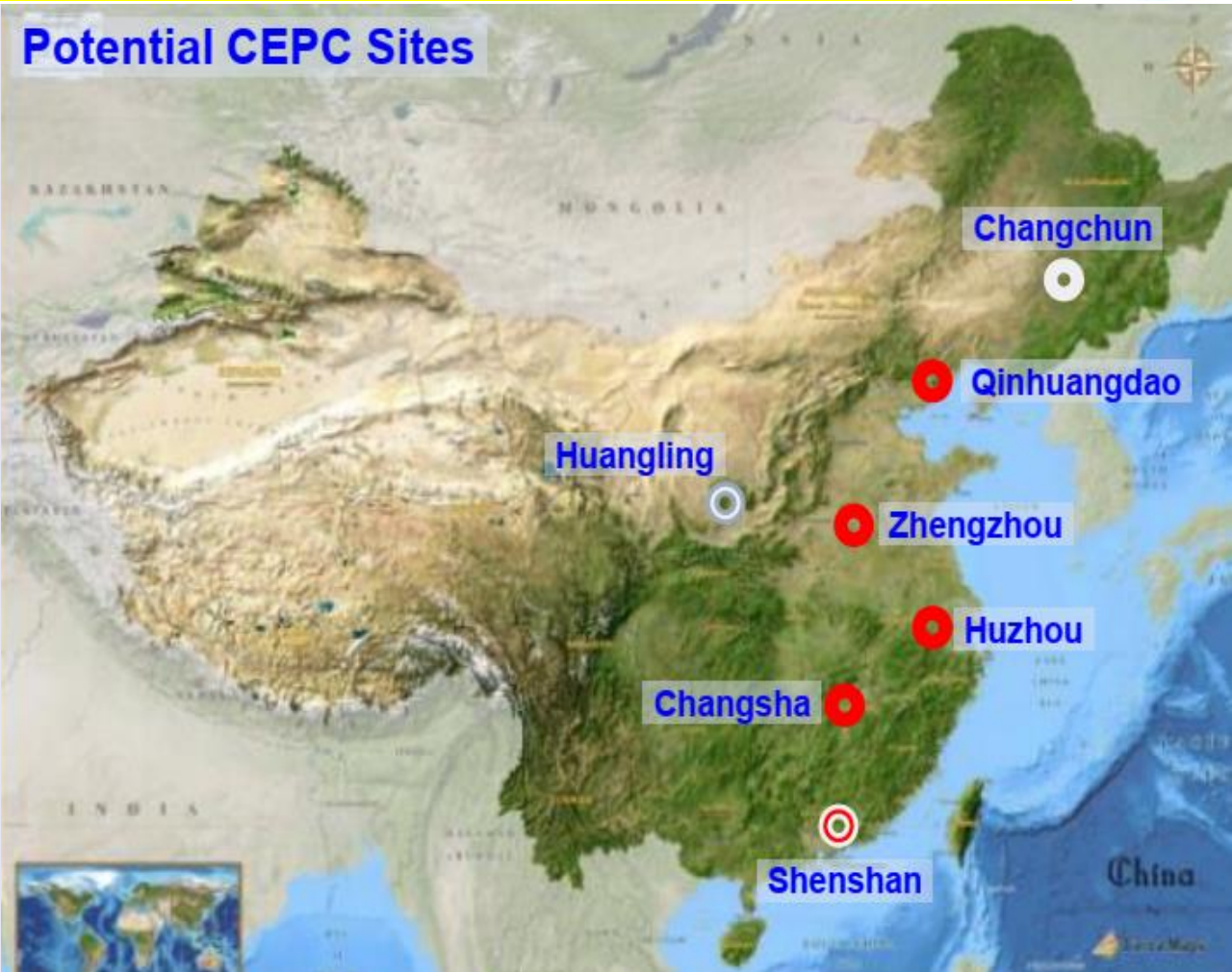
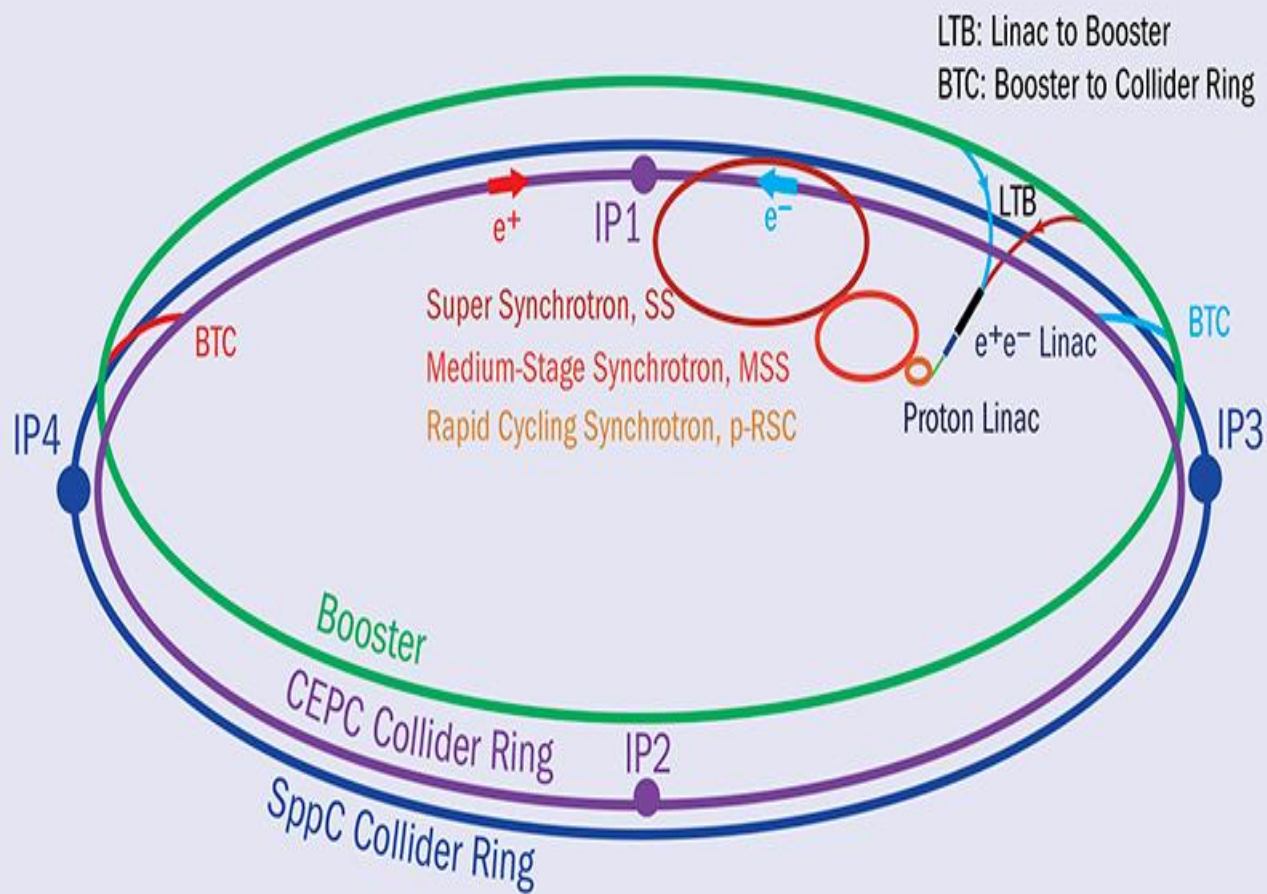


Hadron collider
 16 T \Rightarrow 100 TeV for 100 km
 20 T \Rightarrow 100 TeV for 80 km

Unit	Symbol	cm ²
femtobarn	fb	10 ⁻³⁹
attobarn	ab	10 ⁻⁴²



CIRCULATED ELECTRON-POSITRON COLLIDER (CEPC)



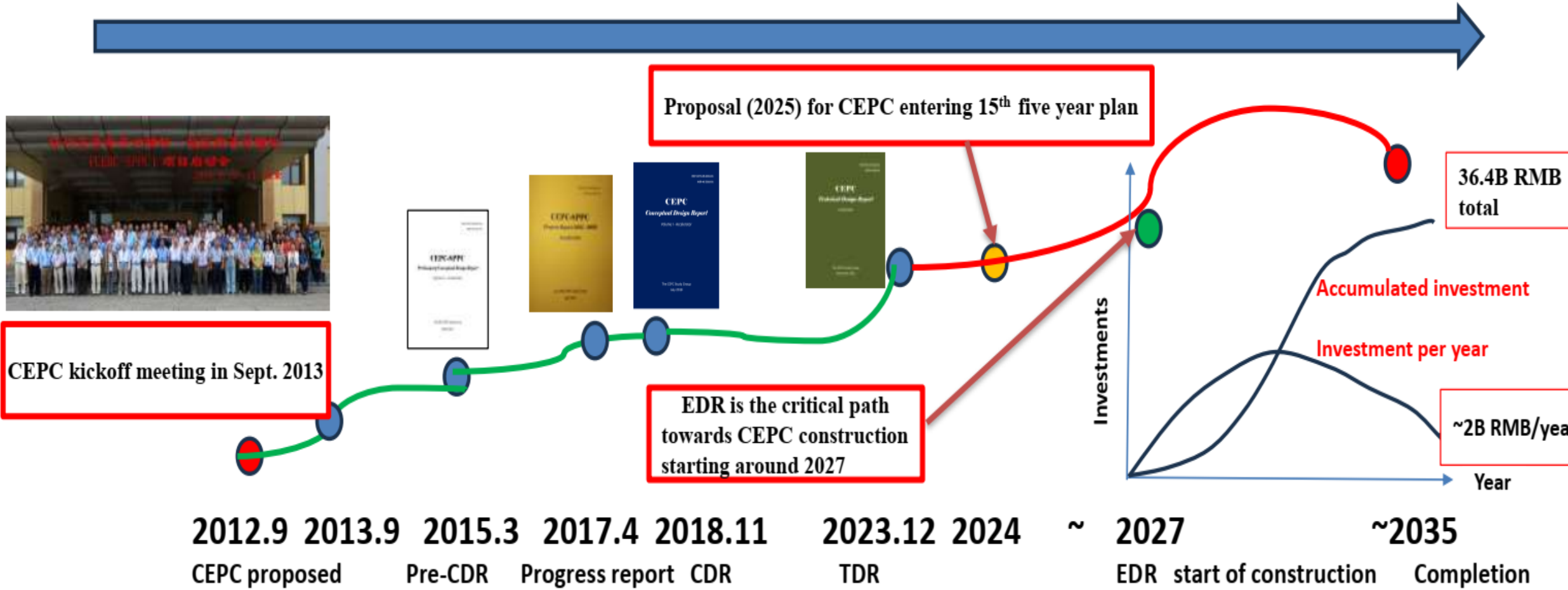
- ❖ The **CEPC** was proposed by the **Chinese HEP community in September 2012**
- ❖ The **CEPC** aims to start operation in 2035, as a **Higgs/Z/W/top factory**
- ❖ The **CEPC** to produce **Higgs/Z/W/top** for **high precision Higgs, EW measurements, studies of flavor physics & QCD, probes of BSM physics**



CIRCULATED ELECTRON-POSITRON COLLIDER (CEPC) MILESTONES



Year	2012	2013	2015	2017	2018	2023	2025	2027	2030	2035
------	------	------	------	------	------	------	------	------	------	------

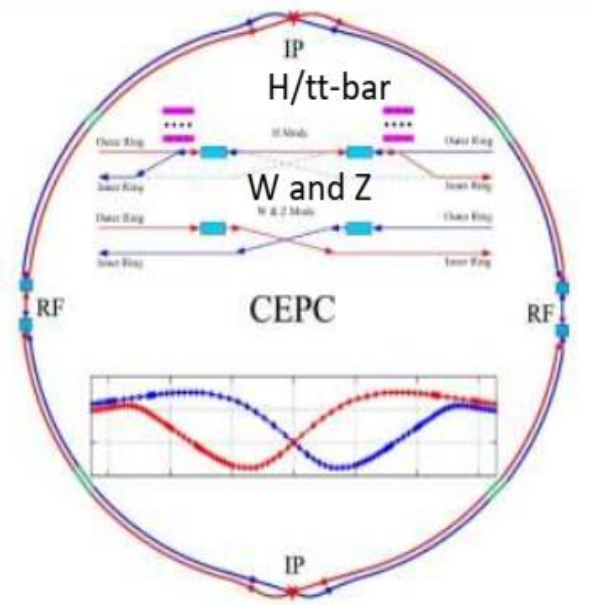




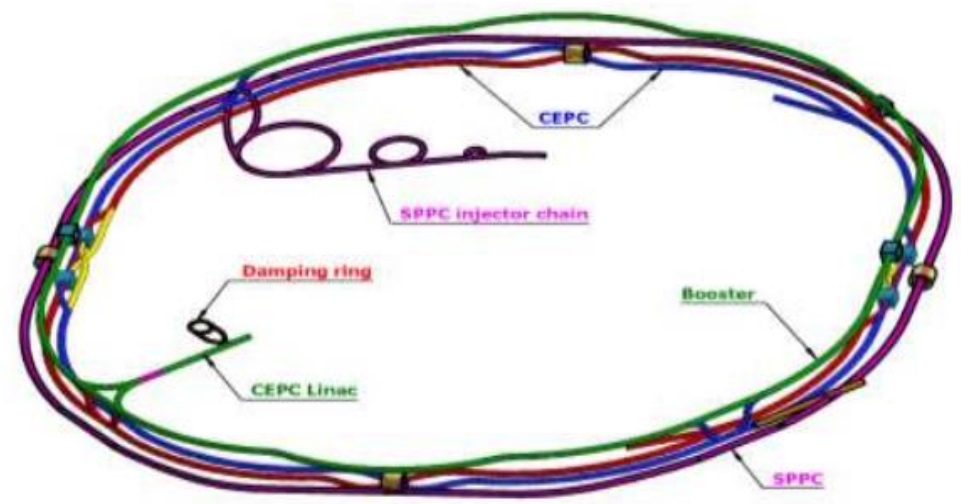
CEPC HIGGS FACTORY AND SPPC LAYOUT



CEPC as a Higgs Factory: **H, W, Z**, upgradable to **ttbar**, followed by a SppC (a Hadron collider) $\sim 125\text{TeV}$
30MW SR power per beam (upgradable to 50MW), high energy gamma ray 100KeV \sim 100MeV

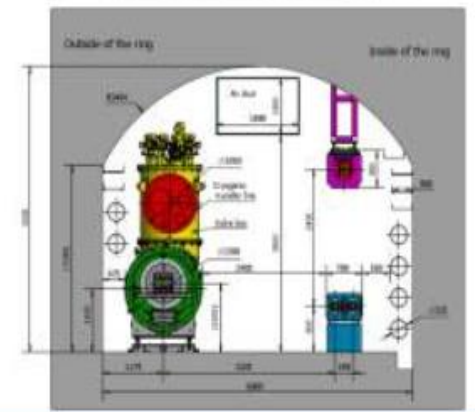
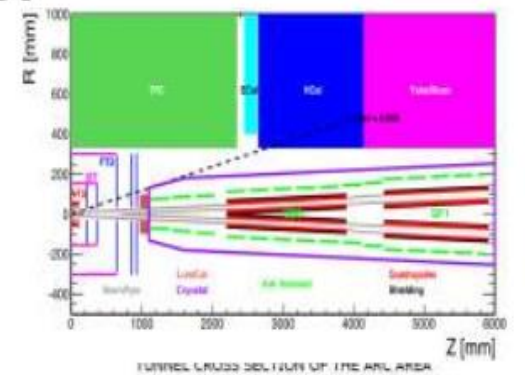
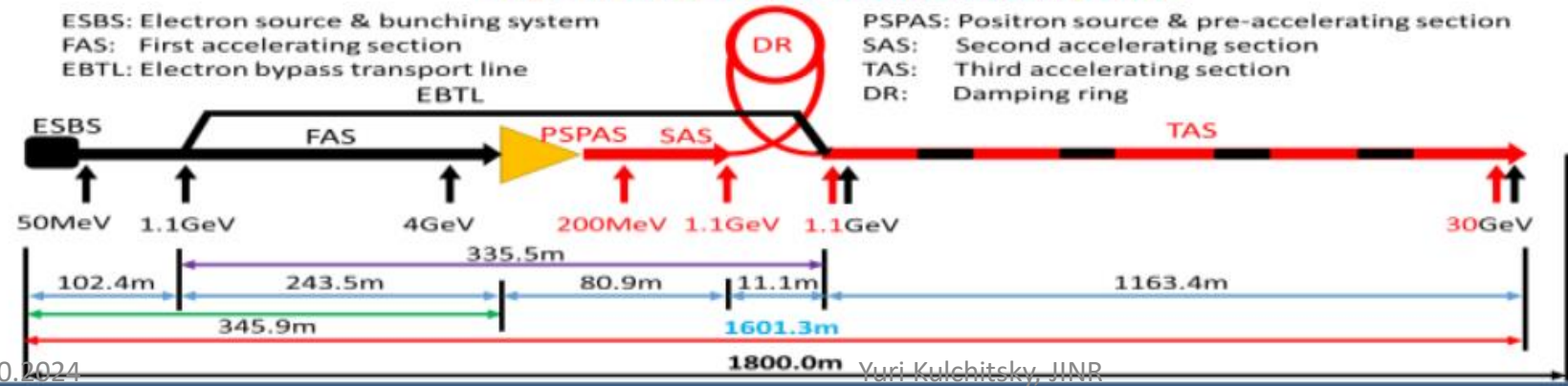


CEPC collider ring (100km)

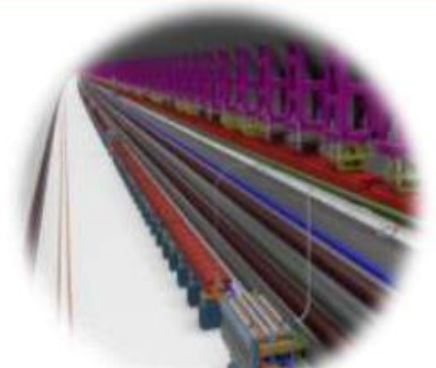


CEPC booster ring (100km)

CEPC TDR S+C-band 30GeV linac injector



CEPC/SppC in the same tunnel





CEPC ACCELERATOR SYSTEM PARAMETERS



Linac

Booster

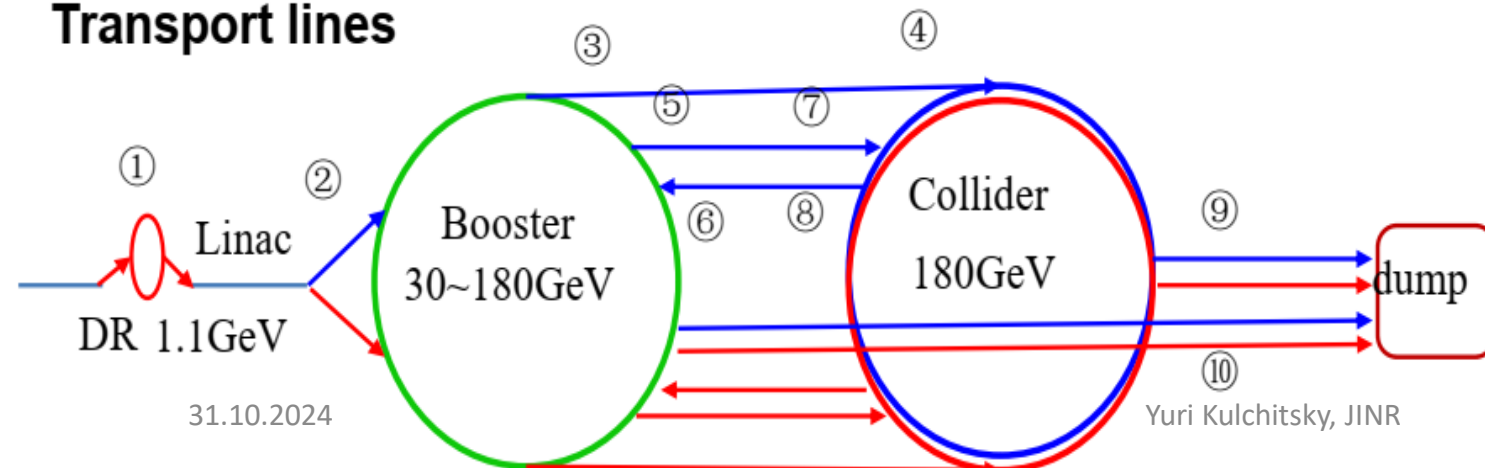
Collider

Parameter	Symbol	Unit	Baseline
Energy	E_e/E_{e^+}	GeV	30
Repetition rate	f_{rep}	Hz	100
Bunch number per pulse			1 or 2
Bunch charge		nC	1.5 (3)
Energy spread	σ_E		1.5×10^{-3}
Emittance	ϵ_r	nm	6.5

		$t\bar{t}$		H		W		Z	
		Off axis injection	Off axis injection	On axis injection	Off axis injection	Off axis injection	Off axis injection	Off axis injection	Off axis injection
Circumfer.	km	100							
Injection energy	GeV	30							
Extraction energy	GeV	180	120		80	45.5			
Bunch number		35	268	261+7	1297	3978	5967		
Maximum bunch charge	nC	0.99	0.7	20.3	0.73	0.8	0.81		
Beam current	mA	0.11	0.94	0.98	2.85	9.5	14.4		
SR power	MW	0.93	0.94	1.66	0.94	0.323	0.49		
Emittance	nm	2.83	1.26		0.56	0.19			
RF frequency	GHz	1.3							
RF voltage	GV	9.7	2.17		0.87	0.46			
Full injection from empty	h	0.1	0.14	0.16	0.27	1.8	0.8		

	Higgs	Z	W	$t\bar{t}$
Number of IPs	2			
Circumference (km)	100.0			
SR power per beam (MW)	30			
Energy (GeV)	120	45.5	80	180
Bunch number	268	11934	1297	35
Emittance ϵ_x/ϵ_y (nm/pm)	0.64/1.3	0.27/1.4	0.87/1.7	1.4/4.7
Beam size at IP σ_x/σ_y (um/nm)	14/36	6/35	13/42	39/113
Bunch length (natural/total) (mm)	2.3/4.1	2.5/8.7	2.5/4.9	2.2/2.9
Beam-beam parameters ξ_x/ξ_y	0.015/0.11	0.004/0.127	0.012/0.113	0.071/0.1
RF frequency (MHz)	650			
Luminosity per IP ($10^{34} \text{ cm}^{-2} \text{ s}^{-1}$)	5.0	115	16	0.5

Transport lines



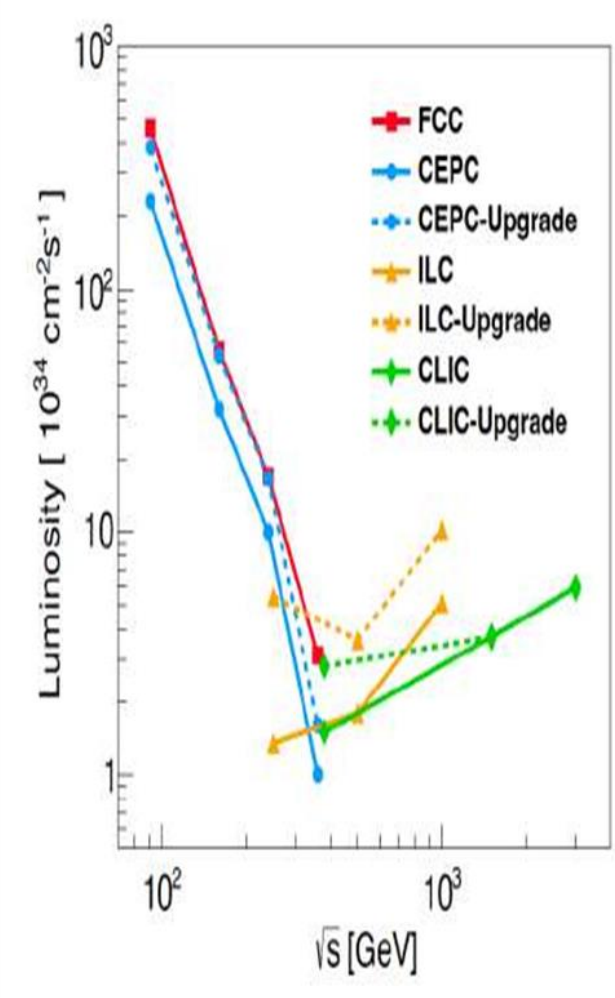
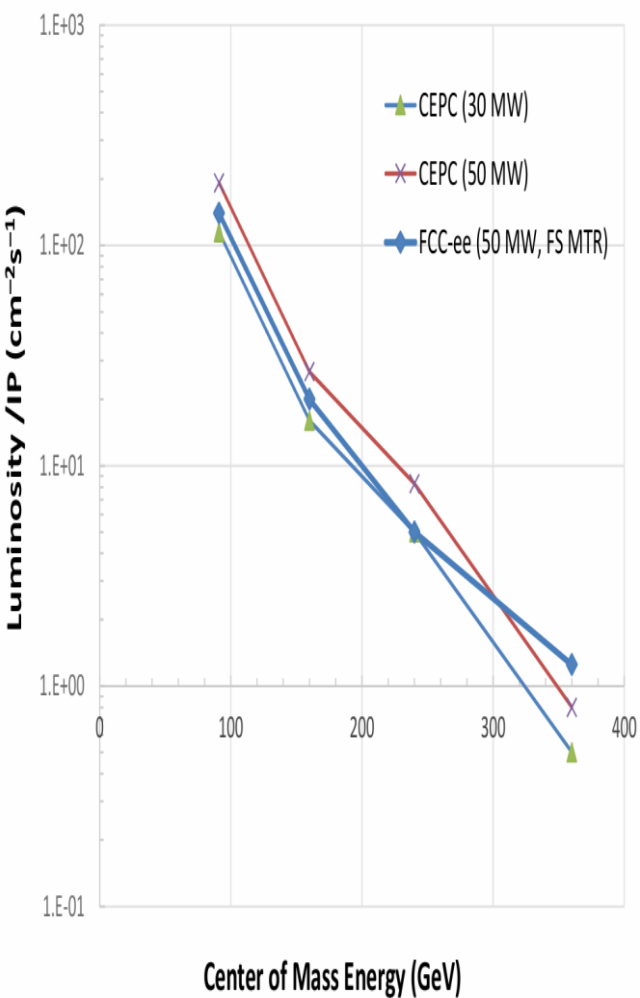
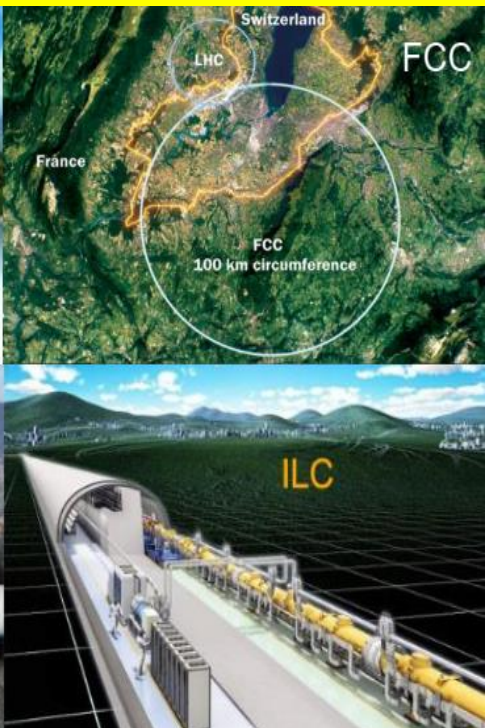
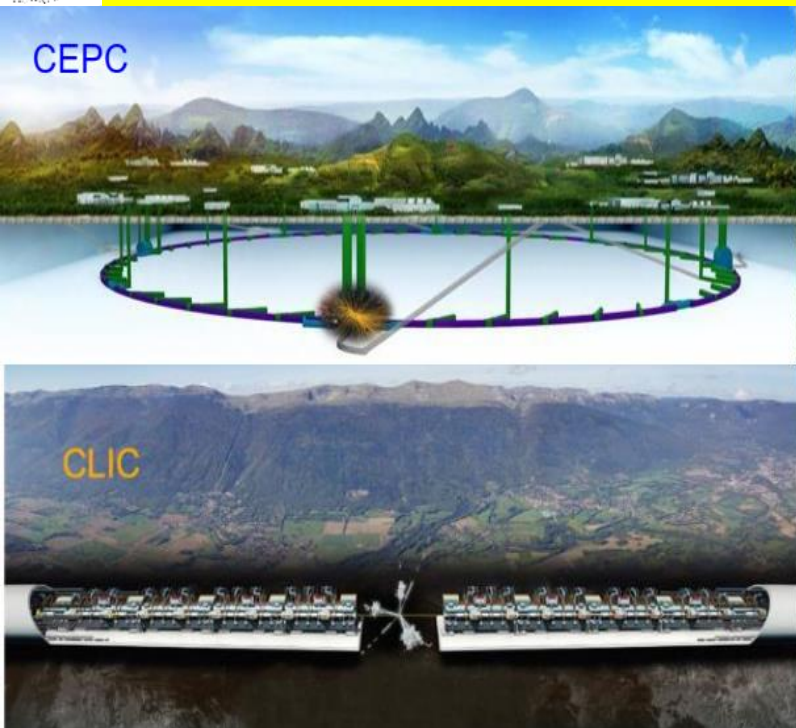
31.10.2024

Yuri Kulchitsky, JINR

CEPC Technical Design Report (TDR) includes:
 1) CEPC Accelerator TDR
 2) CEPC Detector TDRrd (rd=reference design)
 will be released by June 2025



COMPARISON OF HIGGS FACTORIES: CIRCULAR VS LINEAR



CEPC versus FCC-ee

- Earlier data: collisions in 2035 (vs. ~2045)
- Large tunnel size (ee & pp coexistence)
- Lower construction cost

CEPC versus Linear Colliders

- Higher luminosity: precision for H&Z
- Upgrade for pp collider

The **synchrotron radiation (SR)** power of **30 MW** per beam it can achieve a luminosity of **$5 \text{ e}^{34} / \text{cm}^2/\text{s}$** (Intg. Lum. of **$13 \text{ ab}^{-1}$** for **2** interaction points over a **decade**) producing **2.6×10^6 H-bosons**. Increasing the **SR power to 50 MW** per beam expands the CEPC's capability to generate **4.3×10^6 H-bosons**,



CEPC OPERATION PLAN & GOALS



Particle	$E_{c.m.}$ (GeV)	Years	SR Power (MW)	Lumi. per IP ($10^{34}cm^{-2}s^{-1}$)	Integrated Lumi. per year (ab^{-1} , 2 IPs)	Total Integrated L (ab^{-1} , 2 IPs)	Total no. of events
H^*	240	10	50	8.3	2.2	21.6	4.3×10^6
			30	5	1.3	13	2.6×10^6
Z	91	2	50	192**	50	100	4.1×10^{12}
			30	115**	30	60	2.5×10^{12}
W	160	1	50	26.7	6.9	6.9	2.1×10^8
			30	16	4.2	4.2	1.3×10^8
$t\bar{t}$	360	5	50	0.8	0.2	1.0	0.6×10^6
			30	0.5	0.13	0.65	0.4×10^6

Higgs - top priority!

* Higgs is the top priority. The CEPC will commence its operation with a focus on Higgs.

** Detector solenoid field is 2 Tesla during Z operation, 3Tesla for all other energies.

*** Calculated using 3,600 hours per year for data collection.



Circular Electron-Positron Collider

□ 91 (Z), 160 (WW), 240 (ZH), 360 (tt) GeV

□ Higgs Factor ($>10^6$ Higgs bosons):

- Precision study of Higgs (m_H , main quantum numbers JPC, couplings),
- Complementary to Linear colliders,
- Looking for hints of BSM physics:
 - ❖ Dark Matter,
 - ❖ ElectroWeak phase transition (EWPT),
 - ❖ Long-Lived Particles (LLP), ...

□ Z & W factory ($>10^{12} Z_0$):

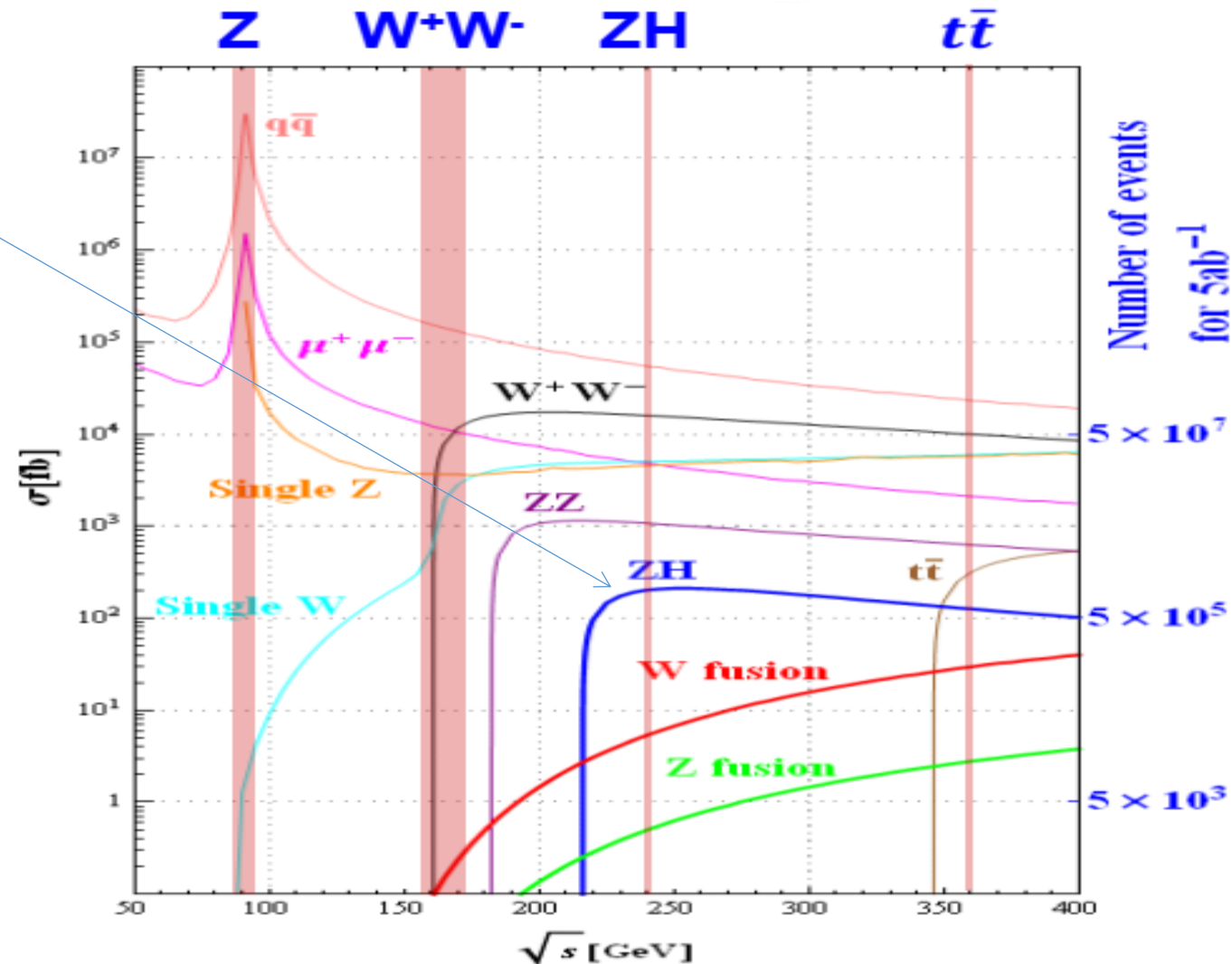
- Precision test of SM,
- Rare decays, ...

□ Flavor factory: b, c, t and QCD studies

Super proton-proton Collider

- ~125 TeV + Complementary to CEPC;
- Directly search for new physics BSM
- Precision test of SM

CEPC-SppC was proposed by Chinese scientists in September 2012, after H-Boson was discovered at CERN



X-sections for SM physics processes
Yuri Kulchitsky, JINR



The Higgs boson has a special role in the quest to answer some of the most profound questions

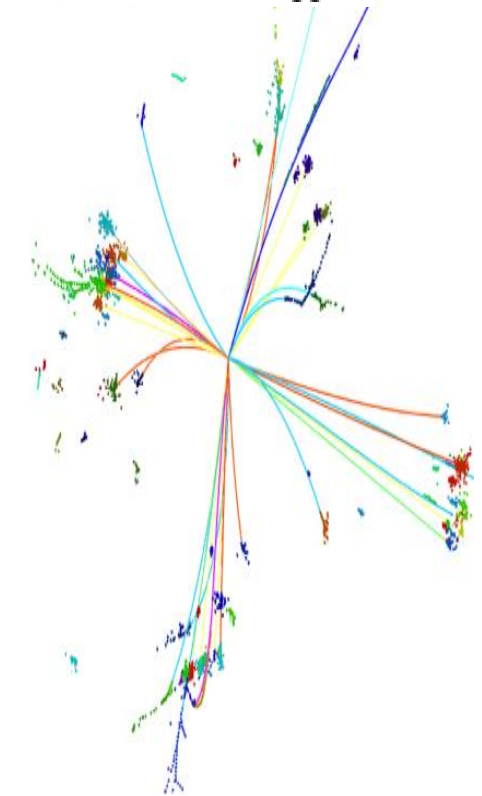
- ❖ These questions include the
 - nature of **the EW phase transition** that governed the *evolution of the early Universe*
 - **why the gravitational force is so weak compared** with other forces in nature.
 - It is possible that the **EW phase transition** could have caused the **observed baryon asymmetry of the Universe** and therefore provide an explanation for the baryon asymmetry problem. It could also have generated **observable gravitational waves**
- The **Higgs boson in e^+e^- collisions** is *practically free of systematic uncertainties* that limit the measurements at the **HL-LHC**
- *Precise measurements of the Higgs boson properties*, along with those of the mediators of the weak interaction will provide critical tests of the underlying fundamental physics principles of the SM and are *vital in the exploration of new physics BSM*
- The Experiments at **CEPC** will
 - ❖ measure the Higgs boson properties in *greater detail* and in *a model-independent way*
 - ❖ reach a new level of precision for the *measurements of the W, Z bosons properties*
 - ❖ allow *the search for potential unknown decay modes*
 - ❖ Also, could uncover deviations from the SM predictions and *reveal the existence of new particles that are beyond the reaches of direct searches at the current experiments.*



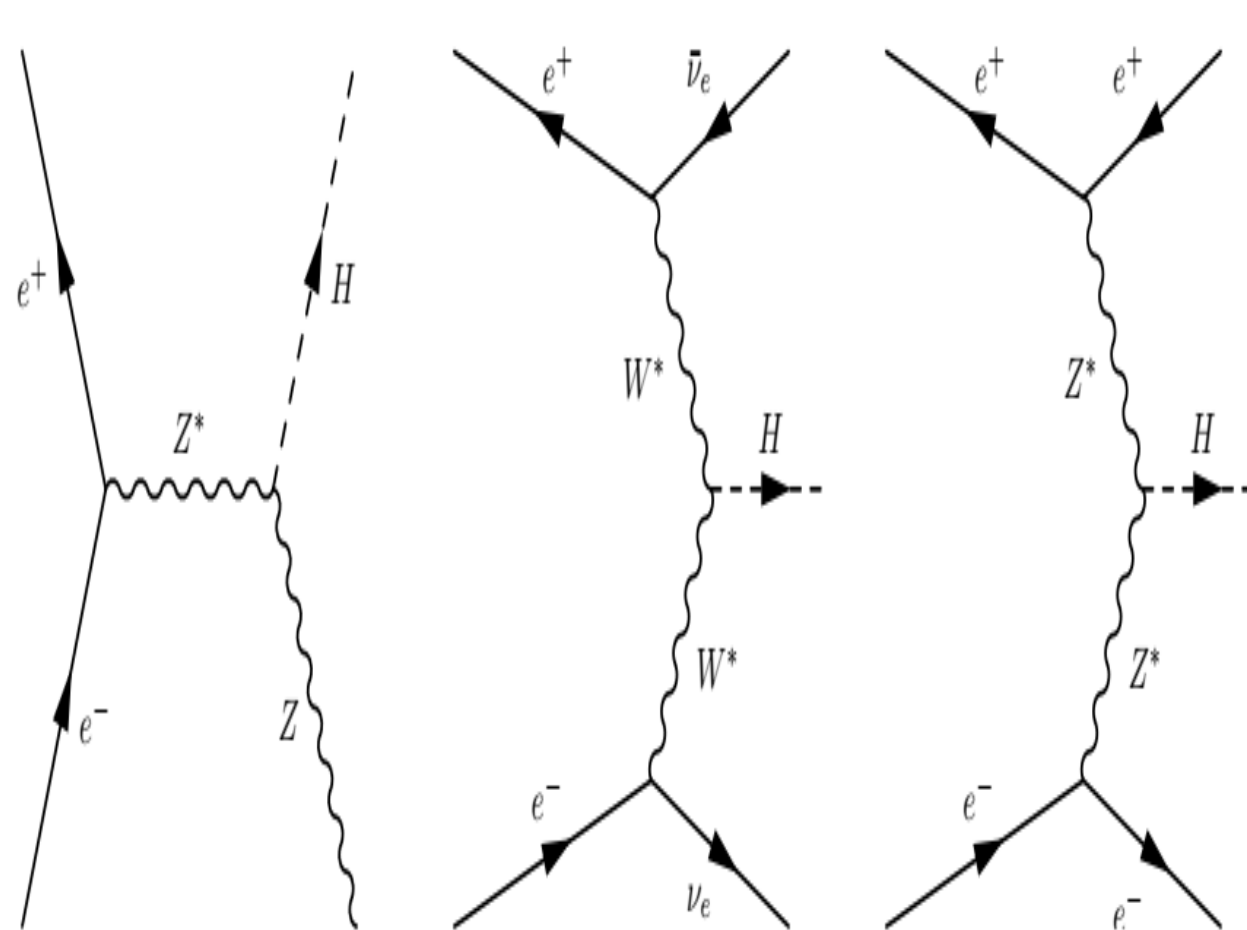
- ❑ The *precision Higgs boson measurements* could potentially *reveal crucial physics mechanism* that determines *the nature of the EW phase transition*.
 - It will be *another milestone* in our *understanding of the early history of our Universe*, &
 - could hold the key to unlock the *origin of the matter and antimatter asymmetry* in the Universe
 - These results could test the ideas that explain *the vast difference between the energy scales associated with the EW and gravitational interaction*.
- ❑ The CEPC will also search for a *variety of new particles*.
- ❑ Running as both a **Higgs factory** and a **Z factory**, the *exotic decays of Higgs and Z bosons are sensitive vehicles the search of new physics*, such as those with *light new particles*.
- ❑ *The dark matter* can be searched for through *its direct production and its indirect effects on the precision measurements*.
- ❑ The CEPC, as *B and τ -charm factories*, can perform studies that help to understand **the origin of different species of matter and their properties**.
- ❑ The CEPC is also an excellent facility to perform *precise tests of the theory of the strong interaction*



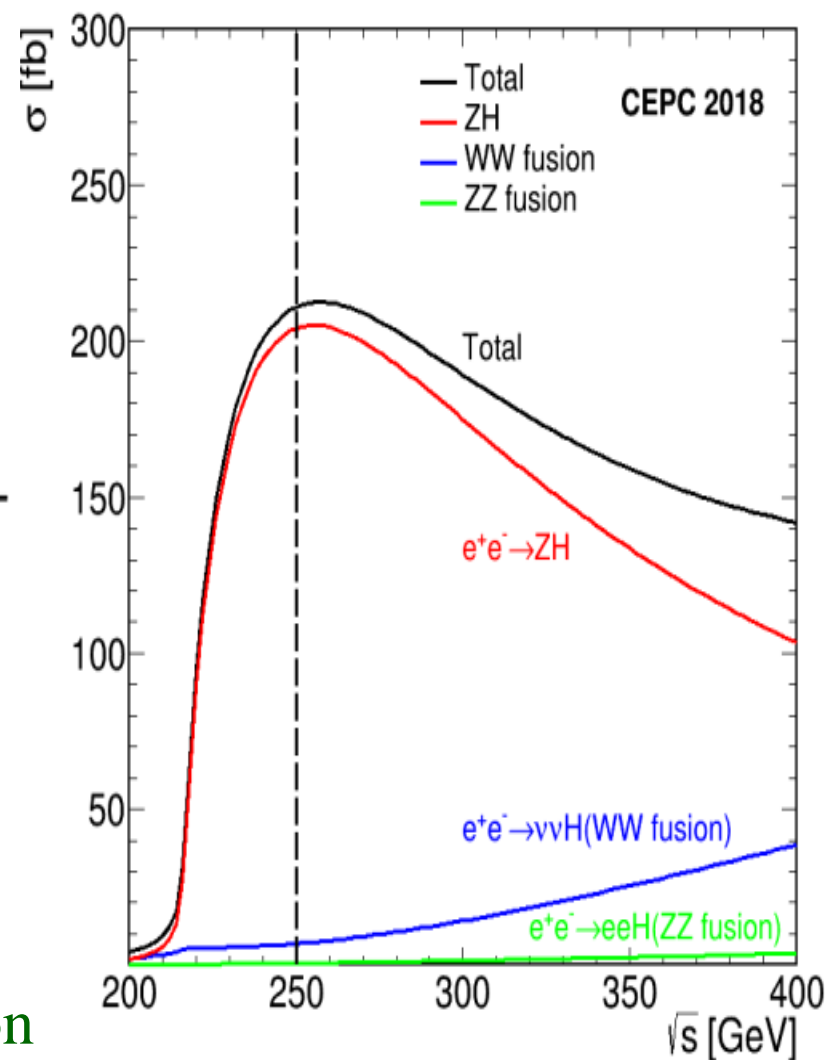
$$e^+e^- \rightarrow ZH \rightarrow q\bar{q} b\bar{b}$$



A simulated $e^+e^- \rightarrow ZH \rightarrow q\bar{q} b\bar{b}$ event reconstructed with the Arbor algorithm



Feynman diagrams of the Higgs boson production processes: $e^+e^- \rightarrow ZH$ (ZH associate production or Higgsstrahlung) and VBF $e^+e^- \rightarrow \nu\bar{\nu}H$ (WW fusion), $e^+e^- \rightarrow e^+e^-H$ (ZZ fusion)



Production cross sections of $e^+e^- \rightarrow ZH$ and $e^+e^- \rightarrow \nu\bar{\nu}H$ as functions of energy



$$\Gamma_H = \frac{\Gamma(H \rightarrow ZZ^*)}{\text{BR}(H \rightarrow ZZ^*)} \propto \frac{\sigma(ZH)}{\text{BR}(H \rightarrow ZZ^*)}$$

Decay mode	Branching ratio	Relative uncertainty
$H \rightarrow b\bar{b}$	57.7%	+3.2%, -3.3%
$H \rightarrow c\bar{c}$	2.91%	+12%, -12%
$H \rightarrow \tau^+\tau^-$	6.32%	+5.7%, -5.7%
$H \rightarrow \mu^+\mu^-$	2.19×10^{-4}	+6.0%, -5.9%
$H \rightarrow WW^*$	21.5%	+4.3%, -4.2%
$H \rightarrow ZZ^*$	2.64%	+4.3%, -4.2%
$H \rightarrow \gamma\gamma$	2.28×10^{-3}	+5.0%, -4.9%
$H \rightarrow Z\gamma$	1.53×10^{-3}	+9.0%, -8.8%
$H \rightarrow gg$	8.57%	+10%, -10%
Γ_H	4.07 MeV	+4.0%, -4.0%

Process	Cross section	Events in 5.6 ab^{-1}
Higgs boson production, cross section in fb		
$e^+e^- \rightarrow ZH$	204.7	1.15×10^6
$e^+e^- \rightarrow \nu_e \bar{\nu}_e H$	6.85	3.84×10^4
$e^+e^- \rightarrow e^+e^- H$	0.63	3.53×10^3
Total	212.1	1.19×10^6
Background processes, cross section in pb		
$e^+e^- \rightarrow e^+e^- (\gamma)$ (Bhabha)	850	4.5×10^9
$e^+e^- \rightarrow q\bar{q} (\gamma)$	50.2	2.8×10^8
$e^+e^- \rightarrow \mu^+\mu^- (\gamma)$ [or $\tau^+\tau^- (\gamma)$]	4.40	2.5×10^7
$e^+e^- \rightarrow WW$	15.4	8.6×10^7
$e^+e^- \rightarrow ZZ$	1.03	5.8×10^6
$e^+e^- \rightarrow e^+e^- Z$	4.73	2.7×10^7
$e^+e^- \rightarrow e^+\nu W^- / e^-\bar{\nu} W^+$	5.14	2.9×10^7

❖ Even with 10^6 H-boson events, **statistical uncertainties** are expected to be **dominant** and thus **systematic uncertainties**

- **In contrast to hadron collisions, e^+e^- collisions are unaffected by underlying events and pile-up effects.**
- **Theoretical calculations are less dependent on higher order QCD radiative corrections.**
- **More precise tests of theoretical predictions can be performed and will provide sensitive probes to BSM.**



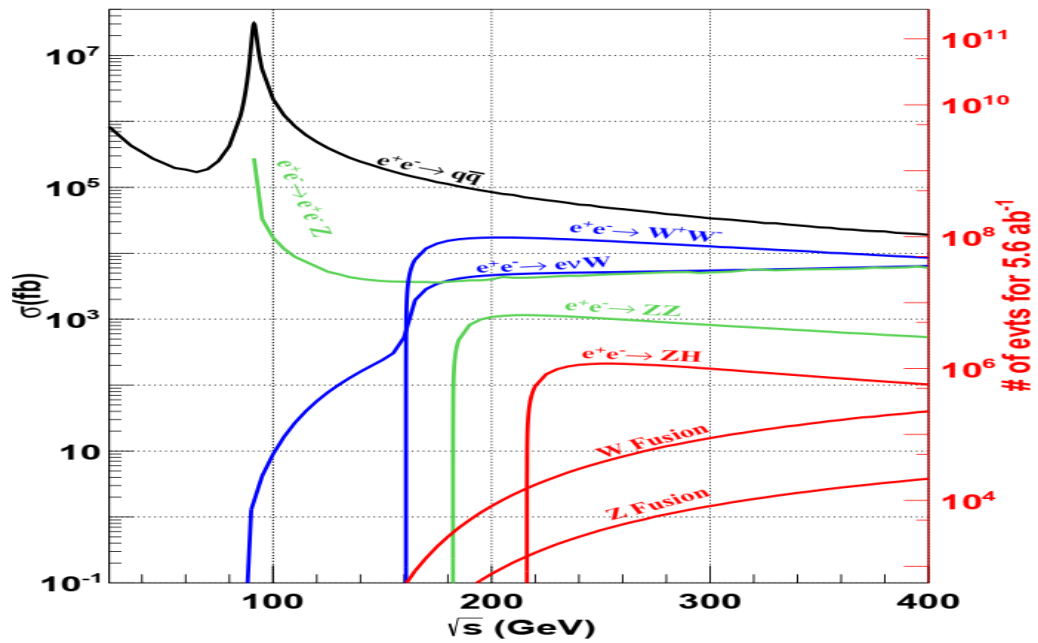
HIGGS PHYSICS: BACKGROUND PROCESSES



Apart from the Higgs boson production, other SM processes include $e^+e^- \rightarrow e^+e^-$ (Bhabha scattering), $e^+e^- \rightarrow Z\gamma$ (initial-state radiation return), $e^+e^- \rightarrow WW/ZZ$ (diboson), $e^+e^- \rightarrow e^+e^-Z$ & $e^+e^- \rightarrow e^+\nu W^-/e^-\nu^+W^+$ (single boson).

Cross sections of main SM processes of e^+e^- collisions vs energy.
 The calculations include initial-state radiation.
 The W and Z fusion processes refer to $e^+e^- \rightarrow \nu\nu H$, $e^+e^- \rightarrow e^+e^- H$ production.

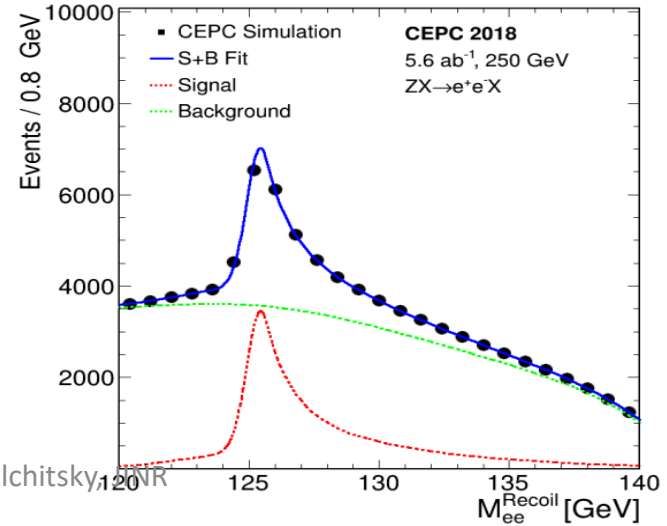
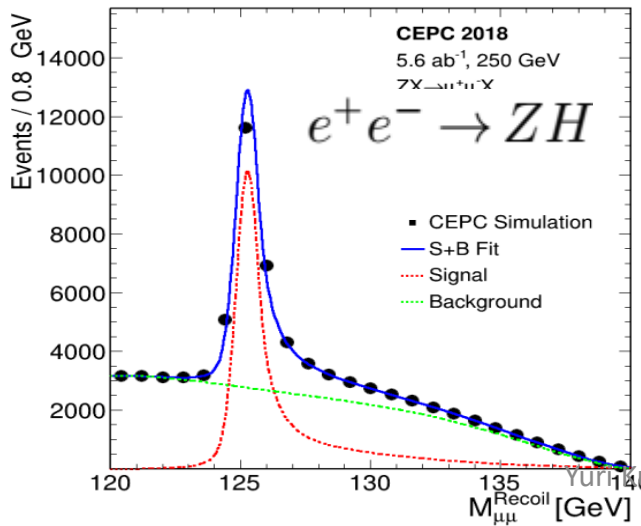
Many of these processes can lead to *identical final states* & interfere:
 $e^+e^- \rightarrow e^+\nu W^- \rightarrow e^+\nu_e e^-\nu_e^-$
 $e^+e^- \rightarrow e^+e^- Z \rightarrow e^+e^- \nu_e \nu_e^-$
 have the same final state after the decays of the W or Z bosons.



Higgsstrahlung event where the Z boson decays to a pair of visible fermions (ff), the mass of the system recoiling against the Z boson, commonly known as the **recoil mass**, can be calculated assuming the event has a total energy and zero total momentum:

$$M_{\text{recoil}}^2 = (\sqrt{s} - E_{ff})^2 - p_{ff}^2 = s - 2E_{ff}\sqrt{s} + m_{ff}^2$$

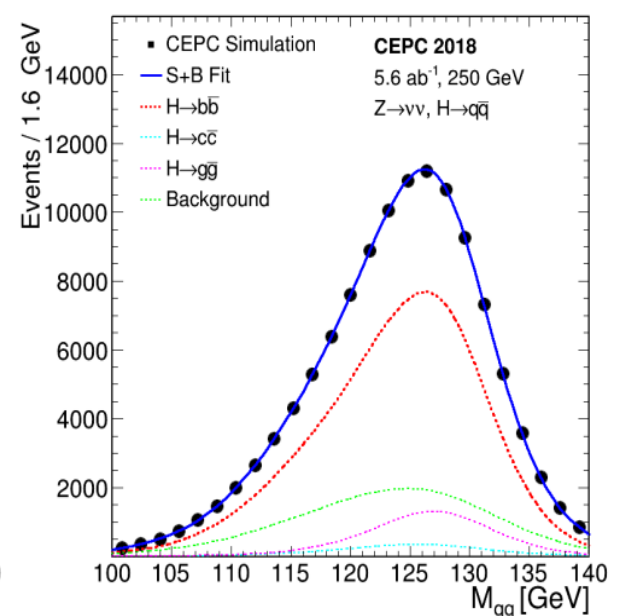
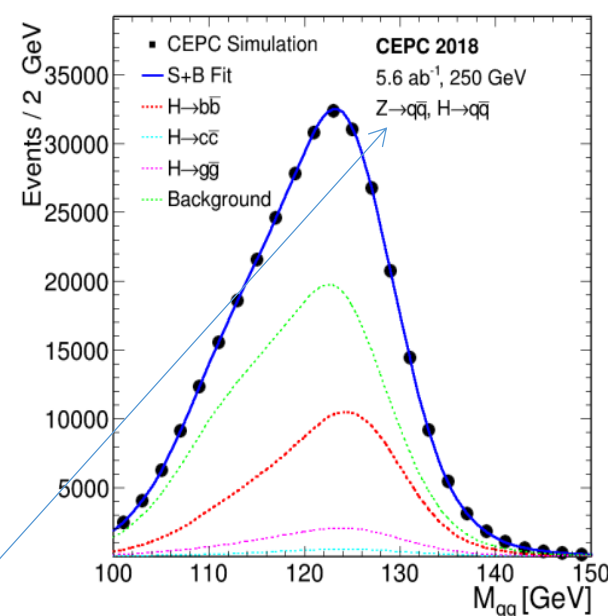
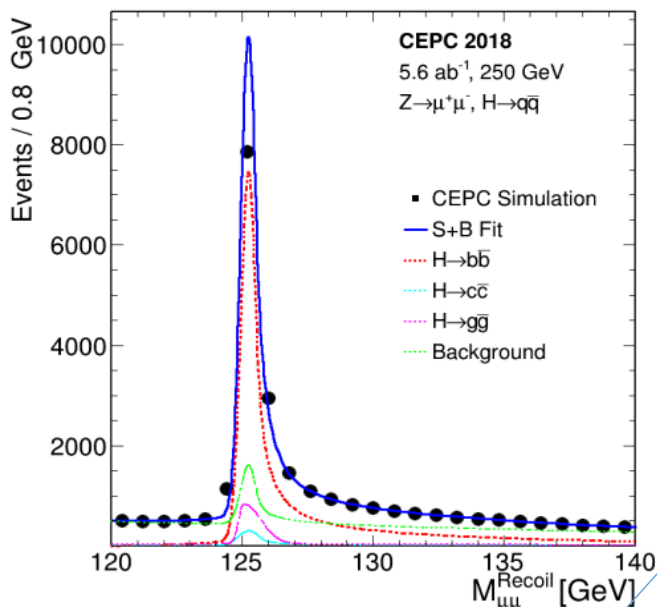
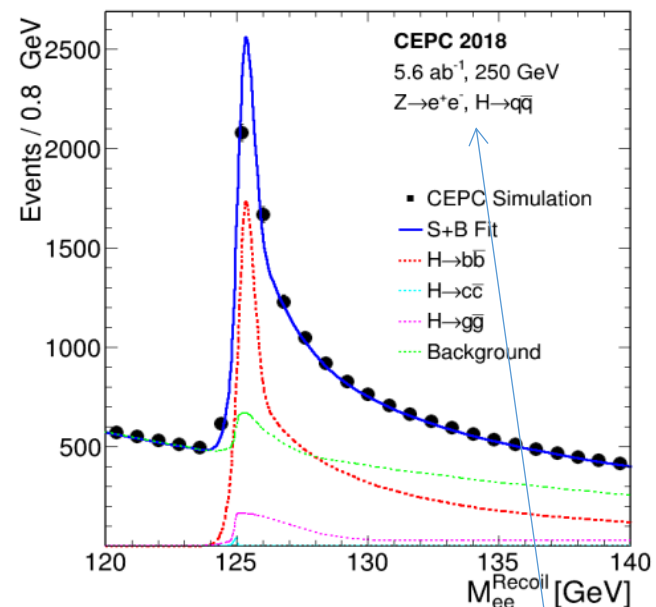
Here, E_{ff} , p_{ff} and m_{ff} are the total energy, momentum and invariant mass of the fermion pair. The M_{recoil} distribution should show a peak at the Higgs boson mass m_H for $e^+e^- \rightarrow ZH$ and $e^+e^- \rightarrow e^+e^- H$ processes.



The inclusive recoil mass spectra of $e^+e^- \rightarrow ZX$ candidates for $Z \rightarrow \mu+\mu^-$ and $Z \rightarrow e+e^-$. No attempt to identify X is made. The markers and their uncertainties (too small to be visible) represent expectations from a CEPC dataset of 5.6 ab^{-1} , whereas the solid blue curves are the fit results. The dashed curves are the signal and background components.



HIGGS PHYSICS: ZH PRODUCTION WITH $H \rightarrow BB^-/CC^-/GG$



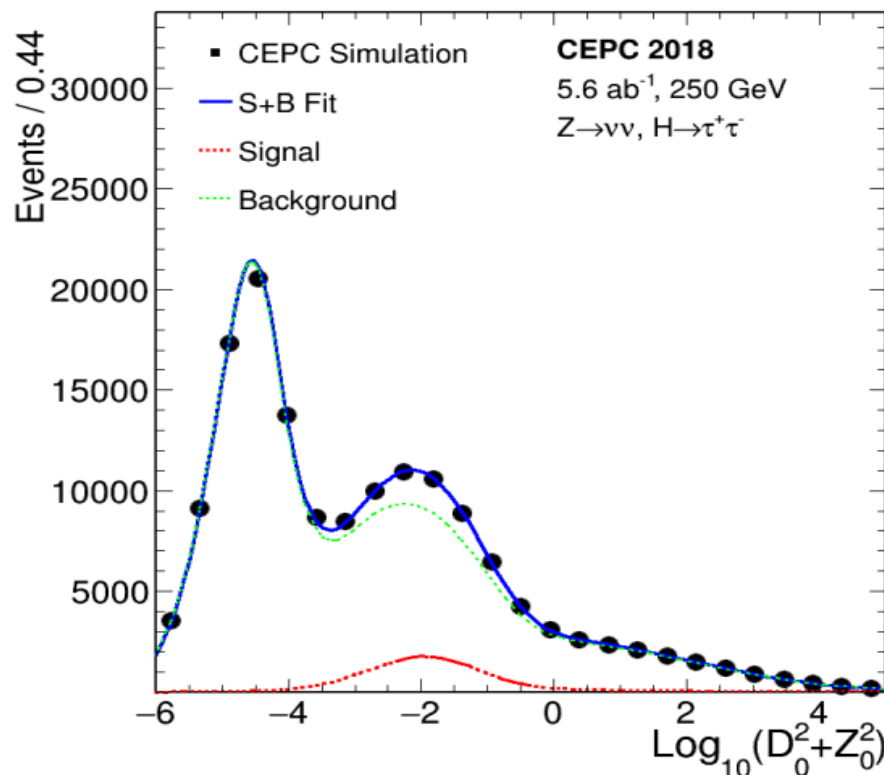
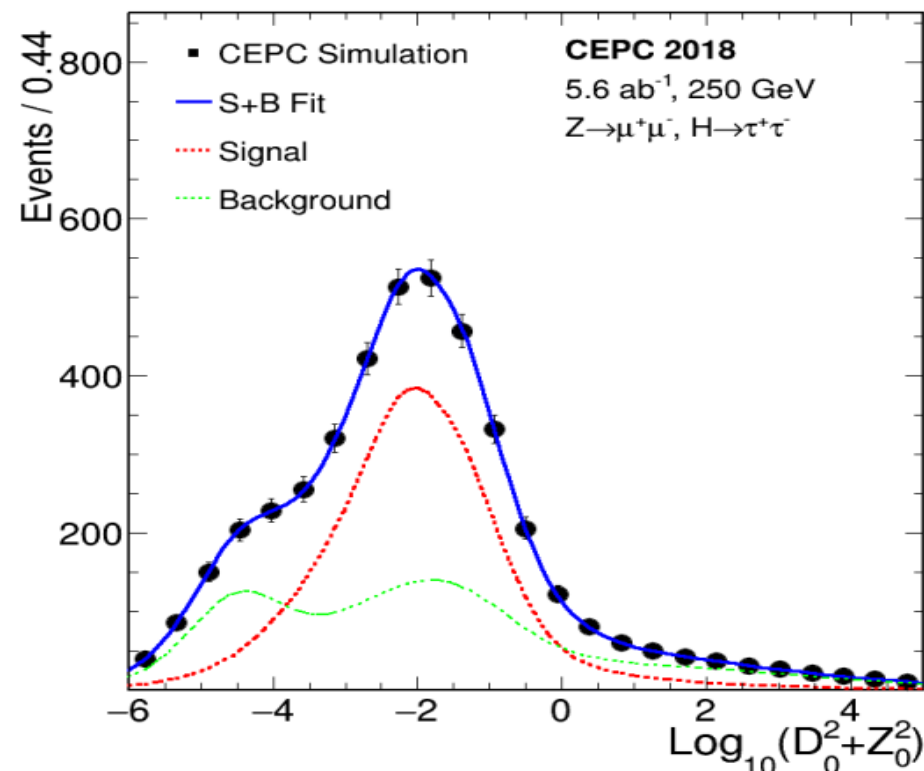
ZH production with $H \rightarrow bb^-/cc^-/gg$: the recoil mass distributions of $Z \rightarrow e^+e^-$ & $Z \rightarrow \mu^+\mu^-$; the dijet mass distributions of Higgs boson candidates for $Z \rightarrow qq^-$ & $Z \rightarrow \nu\nu^-$. The markers and their uncertainties represent expectations from a CEPC dataset of 5.6 ab^{-1} whereas the solid blue curves are the fit results. The dashed curves are the signal and background components. Contributions from other decays of the Higgs boson are included in the background.

Z decay mode	$H \rightarrow b\bar{b}$	$H \rightarrow c\bar{c}$	$H \rightarrow gg$
$Z \rightarrow e^+e^-$	1.3%	12.8%	6.8%
$Z \rightarrow \mu^+\mu^-$	1.0%	9.4%	4.9%
$Z \rightarrow q\bar{q}$	0.5%	10.6%	3.5%
$Z \rightarrow \nu\bar{\nu}$	0.4%	3.7%	1.4%
Combination	0.3%	3.1%	1.2%

- Expected **relative precision** on $\sigma(\text{ZH}) \times \text{BR}$ for the $H \rightarrow bb^-/cc^-/gg$ decays from a CEPC dataset of 5.6 ab^{-1} .
- Combining all Z boson decay modes studied, a relative statistical precision for $\sigma(\text{ZH}) \times \text{BR}$ of **0.3%, 3.3% and 1.3%** can be achieved for the $H \rightarrow bb^-/cc^-/gg$ decays, respectively



HIGGS PHYSICS: THE INVISIBLE DECAY OF THE HIGGS BOSON: $H \rightarrow \text{inv}$



Distributions of the impact parameter variable of the leading tracks from 2-tau candidates in the Z-decay mode: $Z \rightarrow \mu^+ \mu^-$ & $Z \rightarrow \nu \nu$. Here D_0 and Z_0 are the transverse & longitudinal impact parameters.

ZH final state studied	Relative precision on $\sigma \times \text{BR}$	Upper limit on BR(H → inv)
$Z \rightarrow e^+ e^-$ $H \rightarrow \text{inv}$	339%	0.82%
$Z \rightarrow \mu^+ \mu^-$ $H \rightarrow \text{inv}$	232%	0.60%
$Z \rightarrow q \bar{q}$ $H \rightarrow \text{inv}$	217%	0.57%
Combination	143%	0.41%

□ The sensitivity of the $\text{BR}(H \rightarrow \text{inv})$ measurement is studied for the $Z \rightarrow t^+ t^-$ and $Z \rightarrow q \bar{q}$ decay modes.

➤ The $H \rightarrow ZZ^* \rightarrow \nu \nu \bar{\nu} \bar{\nu}$ decay ($\text{Br} = 1.06 \times 10^{-3}$) is used to model the $H \rightarrow \text{inv}$ decay both in the context of the SM and BSM. This is made possible by the fact that the Higgs boson is narrow scalar so that its production and the decay can be treated separately.

➤ The main background is SM ZZ production with one of the Z bosons decay invisibly and the other decays visibly.

Expected relative precision on $\sigma(\text{ZH}) \times \text{BR}(H \rightarrow \text{inv})$ and 95% CL upper limit on $\text{BR}(H \rightarrow \text{inv})$ from a CEPC dataset of 5.6 ab⁻¹. Subtracting the SM $H \rightarrow ZZ^* \rightarrow \nu \nu \bar{\nu} \bar{\nu}$ contribution, a 95% CL upper limit of 0.30% on $\text{BR}_{\text{inv}}^{\text{BSM}}$, the BSM contribution to the $H \rightarrow \text{inv}$ decay can be obtained.

31.10.2024

Yuri Kulchitsky, JINR



The SM makes specific predictions for the H-boson couplings to the SM fermions, $\mathbf{g}_{\text{SM}}(\text{Hff})$, and to the SM gauge bosons, $\mathbf{g}_{\text{SM}}(\text{HVV})$. The potential deviations from the SM are parameterized as:

$$\kappa_f = \frac{g(\text{Hff})}{g_{\text{SM}}(\text{Hff})}, \quad \kappa_V = \frac{g(\text{HVV})}{g_{\text{SM}}(\text{HVV})},$$

with $\kappa_i = 1$ being the SM prediction. The rates of the H production and decays are modified accordingly.

$$\sigma(\text{ZH}) = \kappa_Z^2 \cdot \sigma_{\text{SM}}(\text{ZH})$$

$$\sigma(\text{ZH}) \times \text{BR}(\text{H} \rightarrow \text{ff}) = \frac{\kappa_Z^2 \kappa_f^2}{\kappa_\Gamma^2} \cdot \sigma_{\text{SM}}(\text{ZH}) \times \text{BR}_{\text{SM}}(\text{H} \rightarrow \text{ff}) \quad \kappa_\Gamma^2 (\equiv \Gamma_H / \Gamma_H^{\text{SM}})$$

κ_Γ^2 parameterizes the change in the Higgs width due to both the coupling modifications and the presence of BSM decays

□ It is possible that the Higgs boson can decay directly into new particles or have BSM decays to SM particles.

➤ In this case, two types of new decay channels should be distinguished:

I. **Invisible decay.** This is a specific channel in which H decay into new physics particles which are invisible in the detector. The CEPC sensitivity to this decay channel is quantified by the upper limit on $\text{BR}^{\text{BSM}}_{\text{inv}}$.

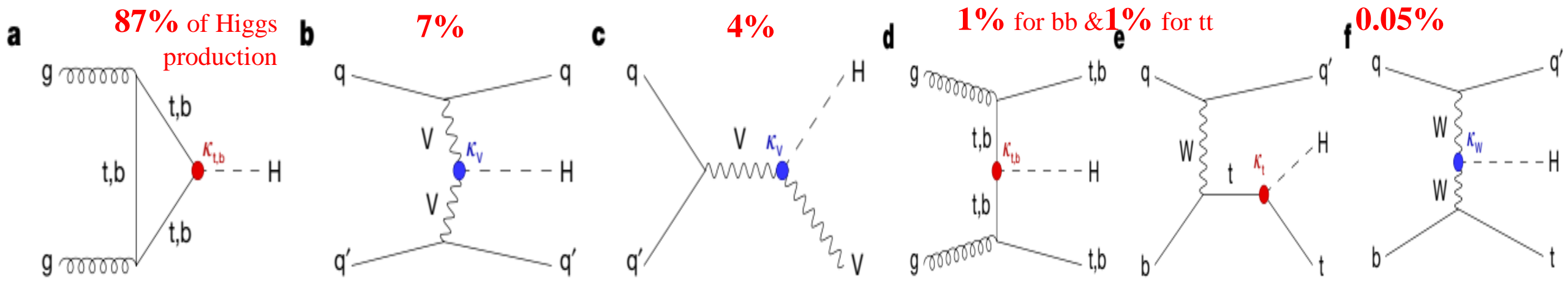
II. **Exotic decays.** These include all the other new physics channels. Whether they can be observed, what precision? In one extreme, the final states can be very distinct, and the rate can be well measured. In the another extreme, they can be completely swamped by the background. Without the knowledge of the final states and the corresponding expected CEPC sensitivity, the exotic decays are accounted for by treating the Higgs boson width Γ_H as an independent free parameter in the interpretation.

$$\kappa_b, \kappa_c, \kappa_g, \kappa_W, \kappa_\tau, \kappa_Z, \kappa_\gamma, \kappa_\mu, \text{BR}_{\text{inv}}^{\text{BSM}}, \Gamma_H$$

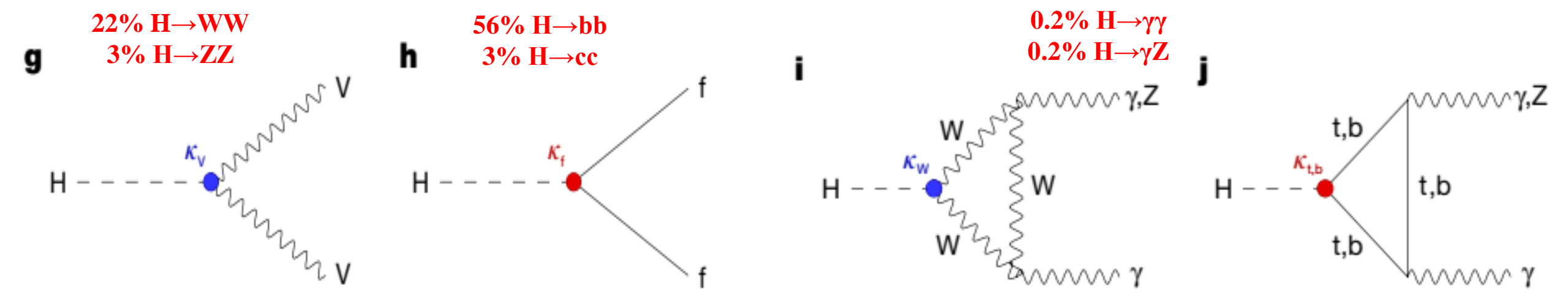
These 10 & 7 parameters are useful for studies at hadron colliders as the Higgs boson total width cannot be measured with good precision. The interpretation of the CEPC results is also performed using this reduced set to allow for direct comparisons with the expected HL-LHC sensitivity.

$$\kappa_b, \kappa_c, \kappa_g, {}^3\kappa_W, {}^2\kappa_Z, \kappa_\gamma, \kappa_\tau = \kappa_\mu$$

The κ_i parameters do not include all possible effects of new physics either.

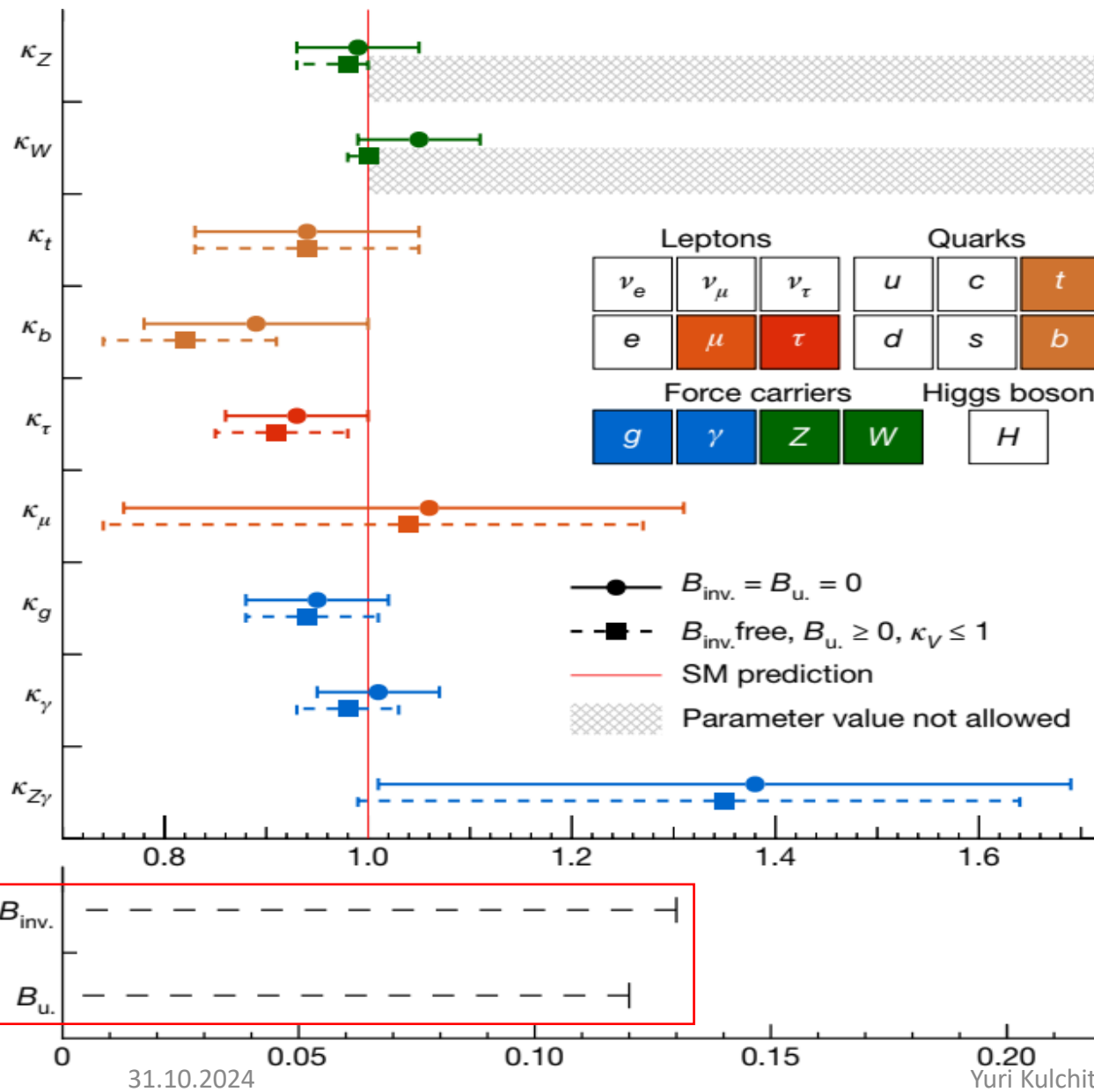


Higgs boson production in **ggH (a)** and **VBF (b)**, associated production with a W or Z (V) boson (**VH; c**), associated production with a top or bottom quark pair (**ttH or bbH; d**); associated production with a top quark (**tH; e, f**)



Higgs boson decays into **heavy vector boson pairs (g)**, **fermion–antifermion pairs (h)** and **photon pairs or Zγ (i,j)**.

COUPLING STRENGTH MODIFIERS



Reduced coupling strength modifiers and their uncertainties per particle type with effective photon, $Z\gamma$ and gluon couplings.

➤ The scenario in which $B_{inv.} = B_u = 0$ is assumed is shown as solid lines with circle markers. The p value for compatibility with the SM prediction is 61% in this case.

➤ The scenario in which $B_{inv.}$ and B_u are allowed to contribute to the total Higgs boson decay width while assuming that $\kappa_V \leq 1$ and $B_u \geq 0$ is shown as dashed lines with square markers.

➤ **The lower panel shows the 95% CL upper limits on $B_{inv.}$ and B_u .**



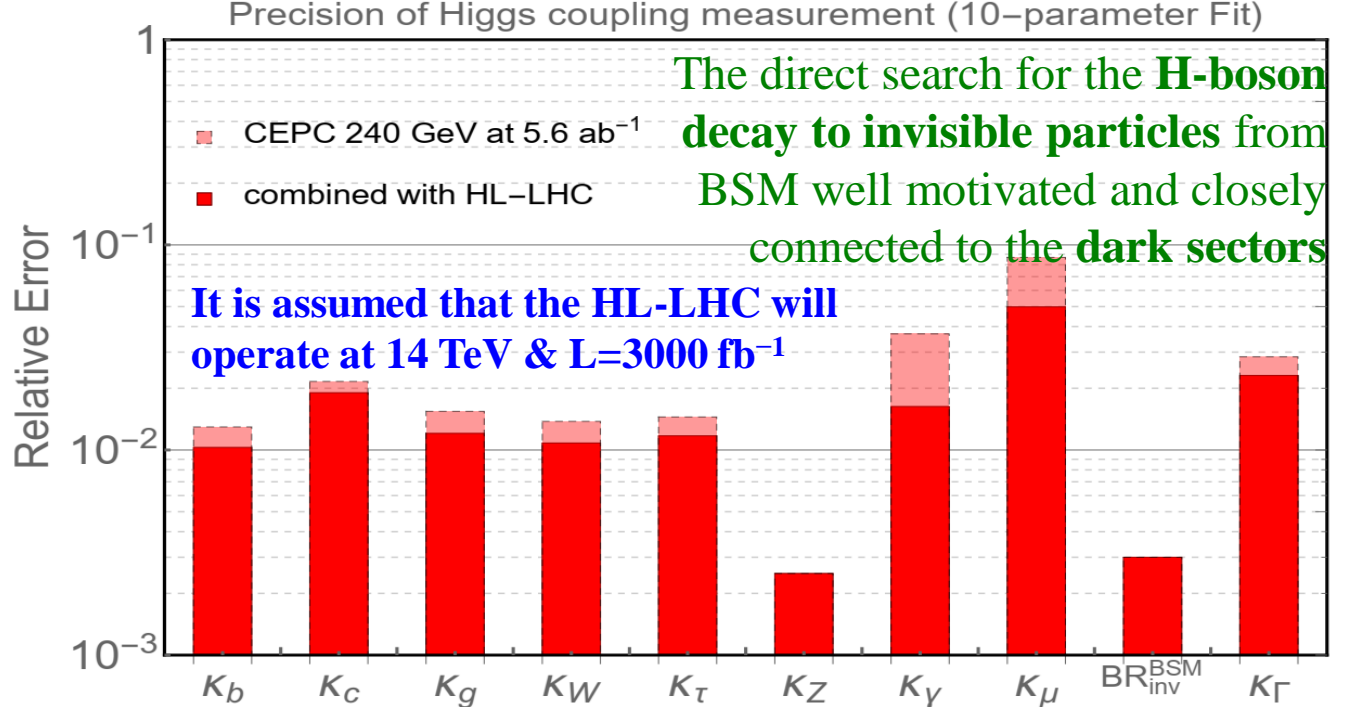
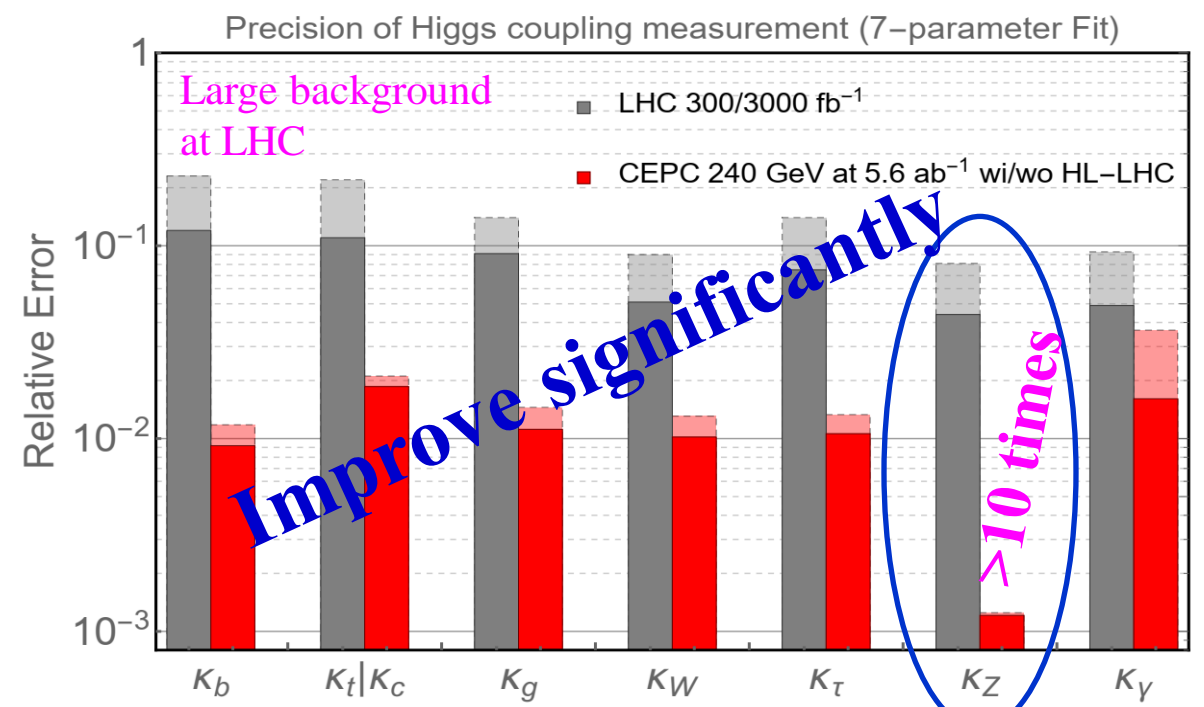
HIGGS PHYSICS: COUPLING FITS IN THE κ -FRAMEWORK



Coupling measurement precision from the 10-parameter fit and 7-parameter fit for the CEPC, and corresponding results after combination with the HL-LHC. All the numbers refer to are relative precision except for BR_{inv}^{BSM} for which the 95% CL upper limit are quoted respectively. Some entries are left vacant for the 7-parameter fit as they are not dependent parameters under the fitting assumptions.

Quantity	10-parameter fit		7-parameter fit	
	CEPC	CEPC+HL-LHC	CEPC	CEPC+HL-LHC
κ_b	1.3%	1.0%	1.2%	0.9%
κ_c	2.2%	1.9%	2.1%	1.9%
κ_g	1.5%	1.2%	1.5%	1.1%
κ_W	1.4%	1.1%	1.3%	1.0%
κ_τ	1.5%	1.2%	1.3%	1.1%
κ_Z	0.25%	0.25%	0.13%	0.12%
κ_γ	3.7%	1.6%	3.7%	1.6%
κ_μ	8.7%	5.0%		
BR_{inv}^{BSM}	< 0.30%	< 0.30%		
Γ_H	2.8%	2.3%		

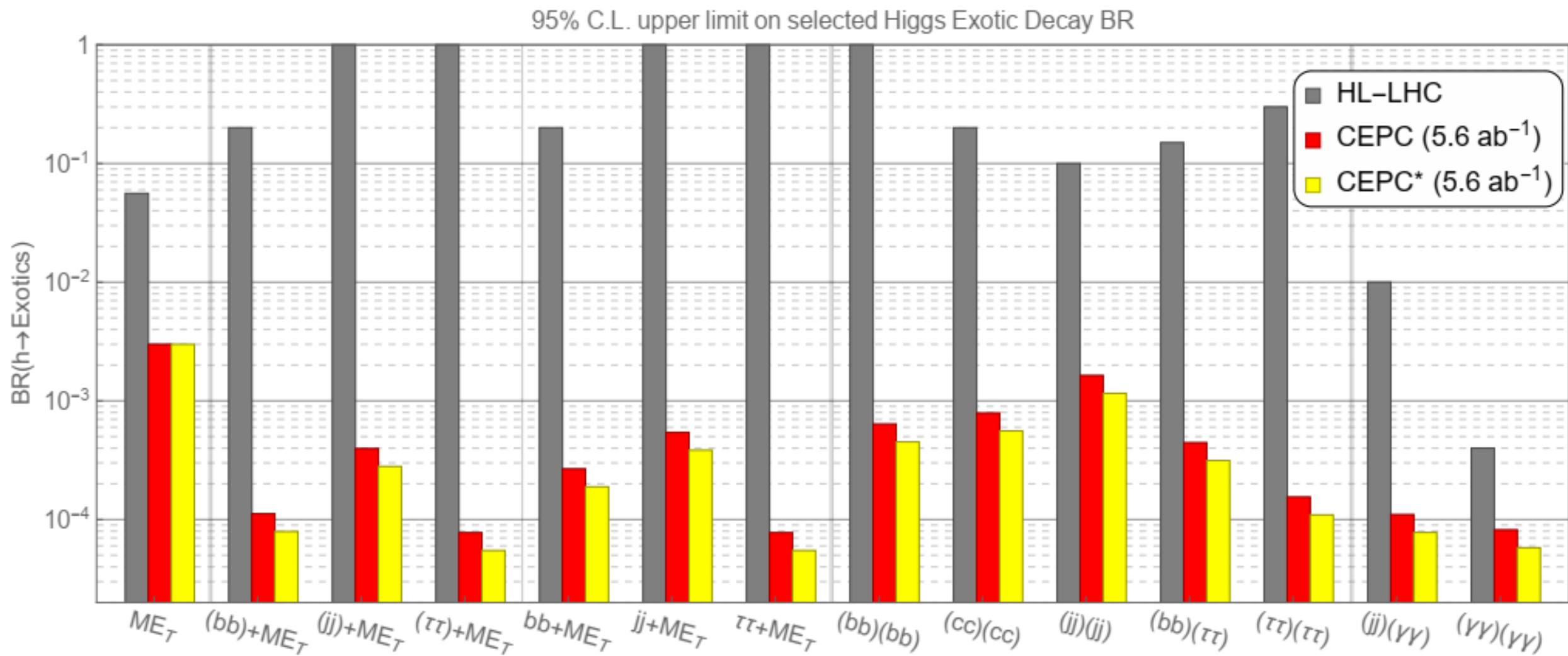
Systematic uncertainties are under much better control at CEPC



The results of the 7 and 10 parameter fits and comparison with the HL-LHC.



BRANCHING OF SELECTED HIGGS BOSON DECAYS



- ❑ The 95% CL upper limit on selected Higgs exotic decay branching fractions at **HL-LHC and CEPC**.
- ❑ **The red bars correspond to the results using only leptonic decays of the spectator Z-boson.**
- ❑ **The yellow bars further include extrapolation with the inclusion of the hadronic decays of the spectator Z-boson**
- ❑ Several vertical lines are drawn in this figure to **divide different types of Higgs boson exotic decays.**

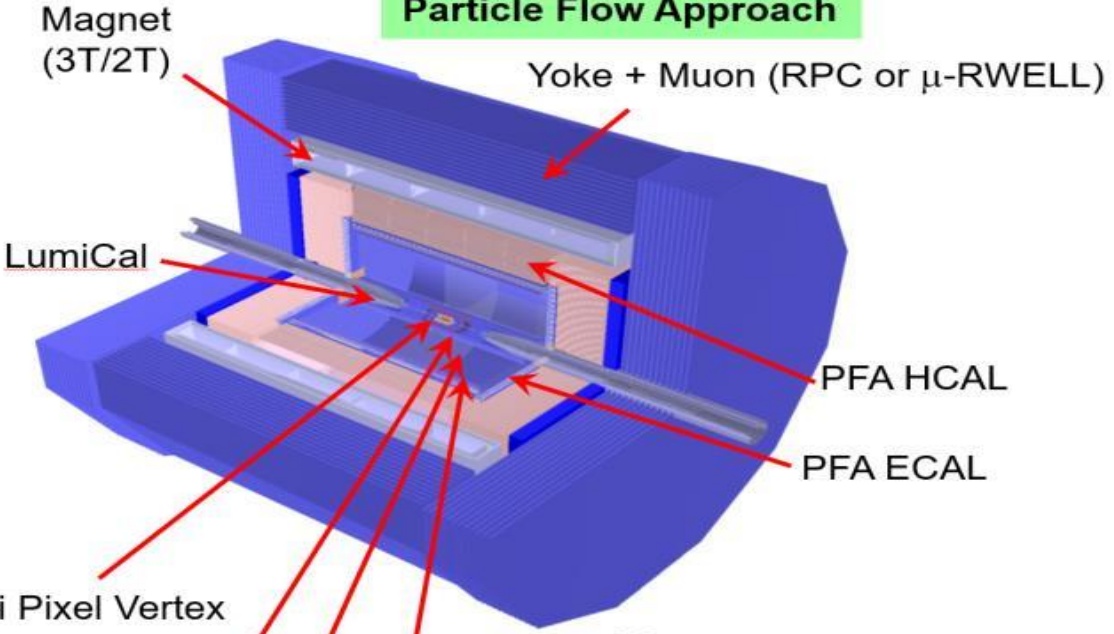


CEPC DETECTORS DESIGNS



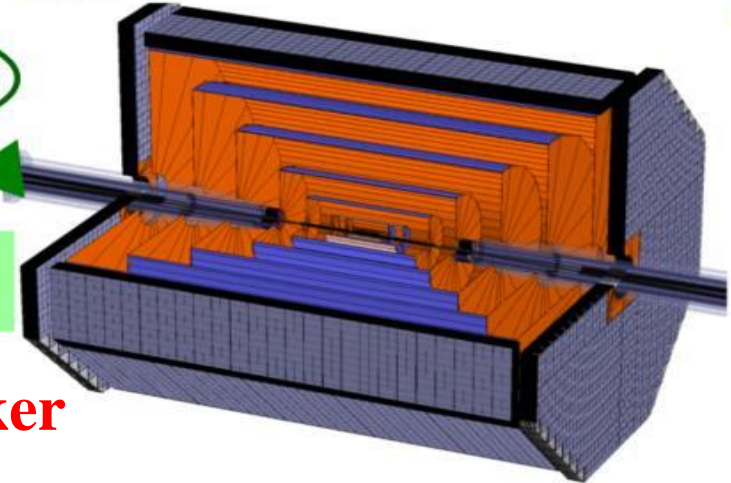
Innovative Detector for Electron-positron Accelerator

(Baseline Design)
Particle Flow Approach

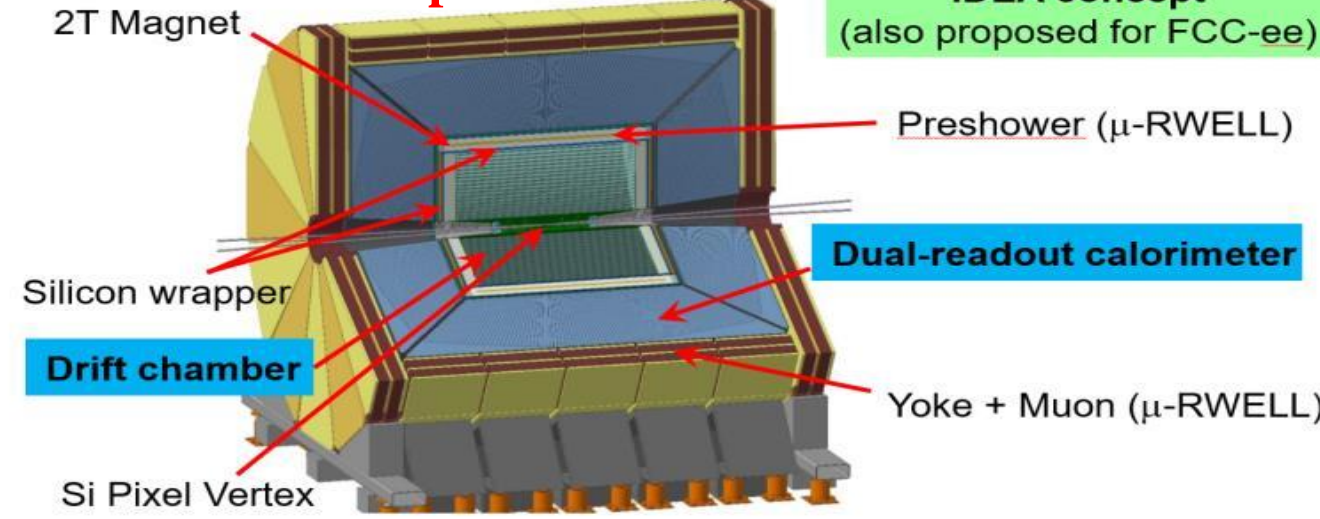


- SIT
- TPC
- SET
- FTD
- ETD

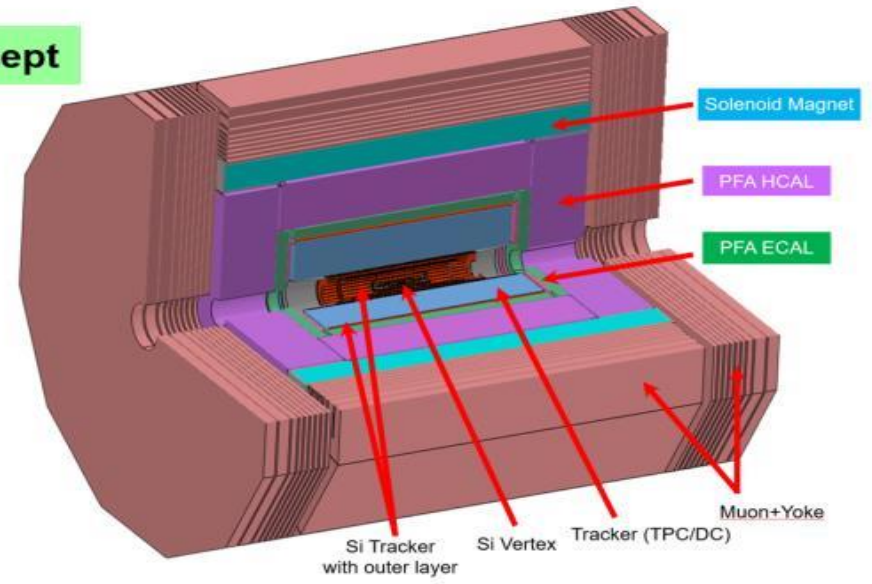
FST concept
(Full Silicon Tracker)



IDEA concept
(also proposed for FCC-ee)



The 4th Concept



Full Silicon Tracker

Large number of detector technology options and R&D projects on-going. Need to converge technology options towards a CEPC reference detector TDR: Start preparation in January 2024; Release of ref-TDR in June 2025. International detector collaborative efforts: HL-LHC detector R&D efforts help to prepare teams for CEPC detectors. **Detector Research & Development (DRD) collaboration (DRD: 1-8).**



1. Gaseous

e.g.
time/spatial
resolution;

environment
friendly gases

2. Liquid

e.g.
Light/charge
readout;

low background
materials

3. Semiconductor

e.g.
CMOS pixel
sensors;

High time
resolution
(10s ps)

4. PID & Photon

e.g.
spectral range
of photon
sensors;

Time
resolution

5. Quantum

quantum
sensors
- R&D, incl.
beyond QFTP
in conventional
detectors

6. Calorimetry

e.g.
Sandwich;
noble liquid;
optical

7. Electronics

e.g.
ASICs;
FPGAs;
DAQ

8. Integration

tracking
detector
mechanics



DETECTORS CONCEPTS



Parameters of the *International Large Detector (ILD)* [1,2] & the *CEPC detector concepts*

Concept	ILD	CEPC baseline	IDEA	An alternative detector
Tracker	TPC/Silicon Time Projection Chamber (TPC)	TPC/Silicon or FST	Drift Chamber/Silicon	
Solenoid B-Field (T)	3.5	3	2	
Solenoid Inner Radius (m)	3.4	<i>The baseline concept was developed from the ILD concept, optimized for the CEPC collision environment</i>	3.2	<i>It employs an ultra high granular calorimetry system to efficiently separate the final state particle showers, a low material tracking system to minimize the interaction of the final state particles in the tracking material, and a large volume 3T solenoid that encloses the entire calorimetry system</i>
Solenoid Length (m)	8.0		7.8	
L* (m)	3.5		2.2	
VTX Inner Radius (mm)	16		16	
Tracker Outer Radius (m)	1.81		1.81	
Calorimeter	PFA		PFA	Dual readout
Calorimeter λ_I	6.6		5.6	7.5
ECAL Cell Size (mm)	5		10	-
ECAL Time resolution (ps)	-		200	-
ECAL X_0	24		24	-
HCAL Layer Number	48		40	-
HCAL Absorber	Fe		Fe	-
HCAL λ_I	5.9		4.9	-
DRCAL Cell Size (mm)	-		-	6.0
DRCAL Time resolution (ps)	-		-	100
DRCAL Absorber	-		-	Pb or Cu or Fe
Overall Height (m)	14.0		14.5	11.0
Overall Length (m)	13.2		14.0	13.0

L* is the distance between the IP and the final focusing quadrupole magnet

A Dual Readout calorimeter to achieve the excellent energy resolution for both the electromagnetic and hadronic showers

1. Linear Collider ILD Concept Group - Collaboration, T. Abe et al., The International Large Detector: Letter of Intent, arXiv:1006.3396 [hep-ex]
 2. H. Abramowicz et al., The International Linear Collider Technical Design Report, Volume 4: Detectors, arXiv:1306.6329 [physics.ins-det].



To deliver the physics program **CEPC detector concepts** must meet the **stringent performance requirements**

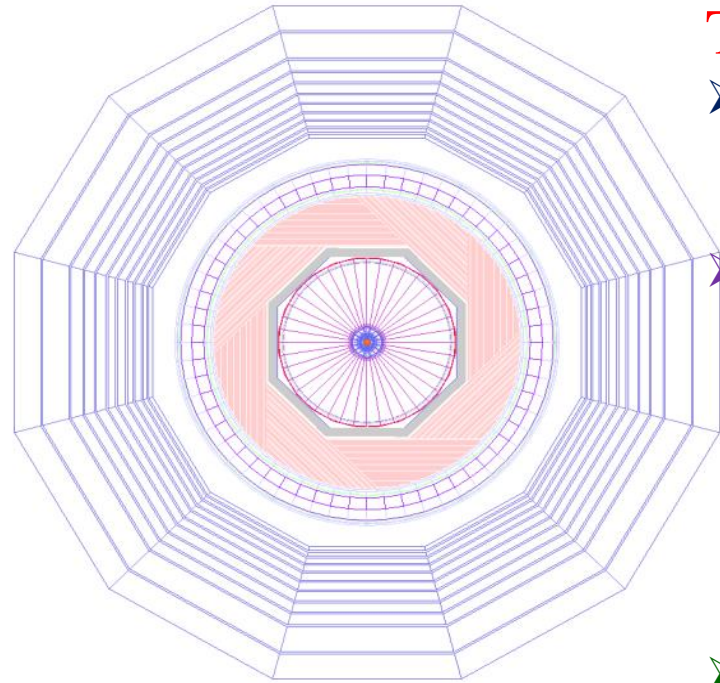
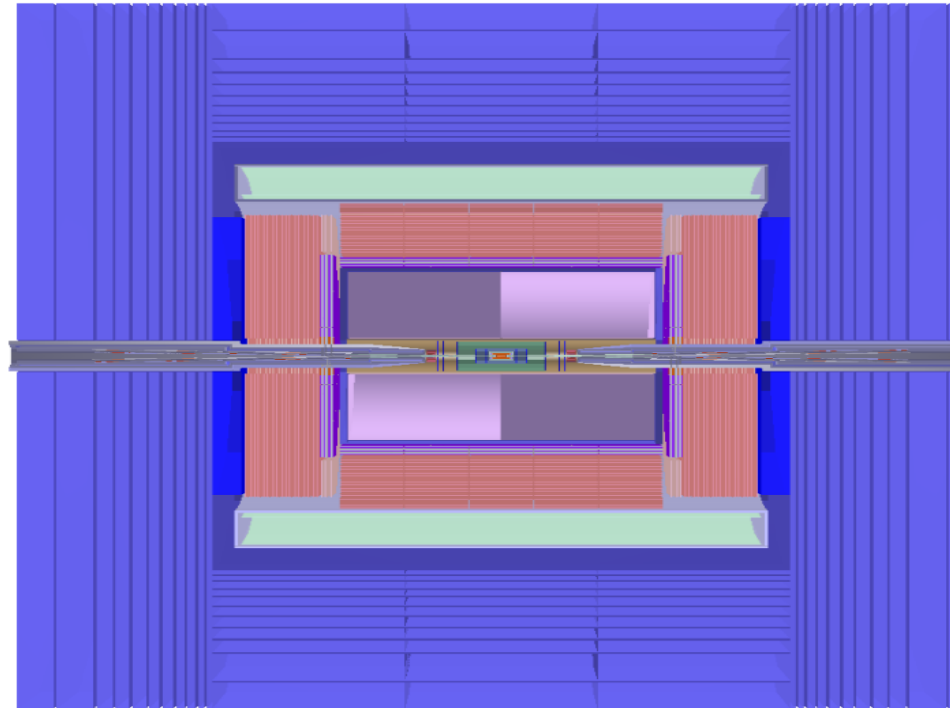
- ❖ The detector designs are guided by the principles of
 - large and precisely defined solid angle coverage, excellent particle identification, precise particle energy/momentum measurement, efficient vertex reconstruction, **superb jet reconstruction** and measurement as well as **the flavor tagging**.
- ✓ Two primary detector concepts are described, a **baseline with two approaches to the tracking systems**, and an *alternative* with a **different strategy for meeting the jet resolution requirements**.
- ❖ The **baseline detector concept incorporates the particle flow principle** with
 - a **precision vertex detector**, a *Time Projection Chamber (TPC)*, a *silicon tracker*, a *high granularity calorimetry system*, a **3 Tesla** superconducting solenoid followed by, a *muon detector embedded in a flux return yoke*.
- ❖ **The alternative concept is based on**
 - a **precision vertex detector**, a drift chamber tracker, a **dual readout calorimetry**, a **2 Tesla** solenoid, and a *muon detector*.
- ❖ The **baseline detector concept** has been studied in detail through **realistic simulation** and the **results demonstrate** that it can **deliver the performance necessary to achieve the physics goals of the CEPC**



- ❑ To develop the detector concepts into **full-scale technical designs** for the planned detectors, a set of **critical R&D tasks** has been identified.
 - Prototypes of key detector components will be built and tested.
 - Mechanical integration, thermal control and data acquisition schemes must be developed.
 - Industrialization of the detector component fabrication will be pursued.
- ❑ **International collaborations** will need to be formed *before the detector designs can be finalized* and the *technical design reports can be developed*.
- ❑ The CEPC will be a world-class multifaceted scientific facility for research, education, and international collaboration.
 - CEPC will be a center for discoveries and innovation and a magnet for attracting top scientists from all over the world to work together to understand the fundamental nature of our Universe.
 - ❖ The CEPC will also provide **leading educational opportunities for universities and research institutions** in China and around the world.
 - The CEPC together with its possible upgrade, the **Super proton-proton Collider**, will firmly place China at the forefront of the cutting-edge research and exploration in fundamental physics for the **next half century**.
 - ✓ CEPC will have profound impacts on **science, economy and society** that will reverberate across the world.



CEPC: BASELINE DETECTOR CONCEPT



The **baseline concept** employs

- **high granular sampling ECAL and HCAL, providing 3-dimensional spatial and the energy information.**
- The ECAL is composed of **30 longitudinal layers of alternating silicon sensors and tungsten absorbers**, splitting into **two** sections of different absorber thickness. The total absorber length at $\theta=90^\circ$ is 8.4 cm, or equivalently 24 radiation lengths (X_0).
- Transversely, each sensor layer is segmented into **10x10 mm²** cells.
- The **HCAL** uses **steel as absorbers and scintillator tiles or gaseous detectors such as RPCs as sensors**. It has **40** longitudinal layers, each consists of a **2.5** cm steel absorber. The total steel thickness is about 100 cm at $\theta=90^\circ$, corresponding to 5.6 interaction lengths. Like the **ECAL**, the **HCAL** is segmented into **10x10 mm²** cells transversely.

The Baseline detector concept:

- ❑ **Barrel:** The detector is composed of *a silicon pixel vertex detector, a silicon inner tracker, a TPC, a silicon external tracker, an ECAL, an HCAL, a solenoid of 3 Tesla and a return yoke with embedded a muon detector.*
- ❑ **Forward:** *Five pairs of silicon tracking disks* are installed to enlarge the tracking acceptance $0.99 < |\cos(\theta)| < 0.996$

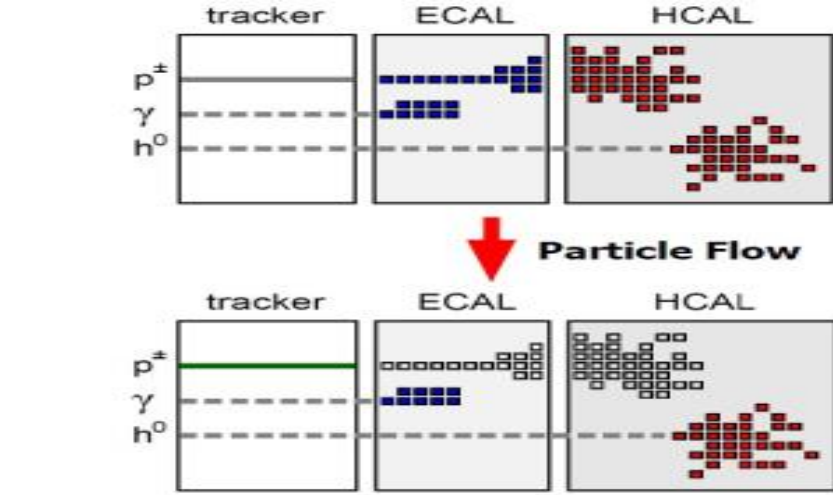
The **calorimetry system** provides good energy measurements for **neutral particles**: $\sim 16\%/\sqrt{E/\text{GeV}}$ for **photons** and $60\%/\sqrt{E/\text{GeV}}$ for **neutral hadrons**. A jet energy resolution of **3–5%** are expected for jet energies **20 – 100 GeV**.



HIGH GRANULARITY CALORIMETRY: PARTICLE-FLOW ALGORITHM



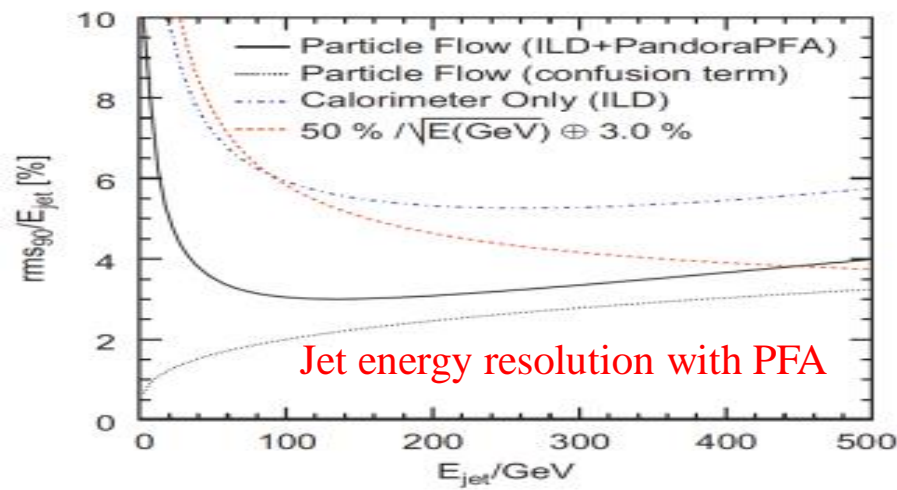
Components in jets	Sub-Detectors	Energy fraction (average) within a jet*	(Typical) Sub-detector Resolution
charged particles (X^\pm)	Tracker	$\sim 62\% E_j$	$10^{-4} E^2_X$
photons (γ)	ECAL	$\sim 27\% E_j$	$0.15 \sqrt{E_\gamma}$
neutral hadrons (h)	ECAL+HCAL	$\sim 10\% E_j$	$0.55 \sqrt{E_h}$



Particle Flow Algorithm (PFA) *Measurements of jet fragmentation at LEP (and $\sim 1\%$ by neutrinos)

- To achieve unprecedented jet energy resolution of $\sim 30\%/\sqrt{E_{jet}}$
- Choose a sub-detector best suited for each particle in a jet
- Charged particles measured in tracker
- Photons in ECAL and neutral hadrons in HCAL
- Separation of close-by particles in the calorimeters
- **PFA-oriented calorimeters: high granularity (1~10 million channels)**

$$\sigma_{jet}^2 = \sigma_{h^\pm}^2 + \sigma_\gamma^2 + \sigma_{h^0}^2 + \sigma_{confusion}^2 + \sigma_{threshold}^2 + \sigma_{losses}^2$$

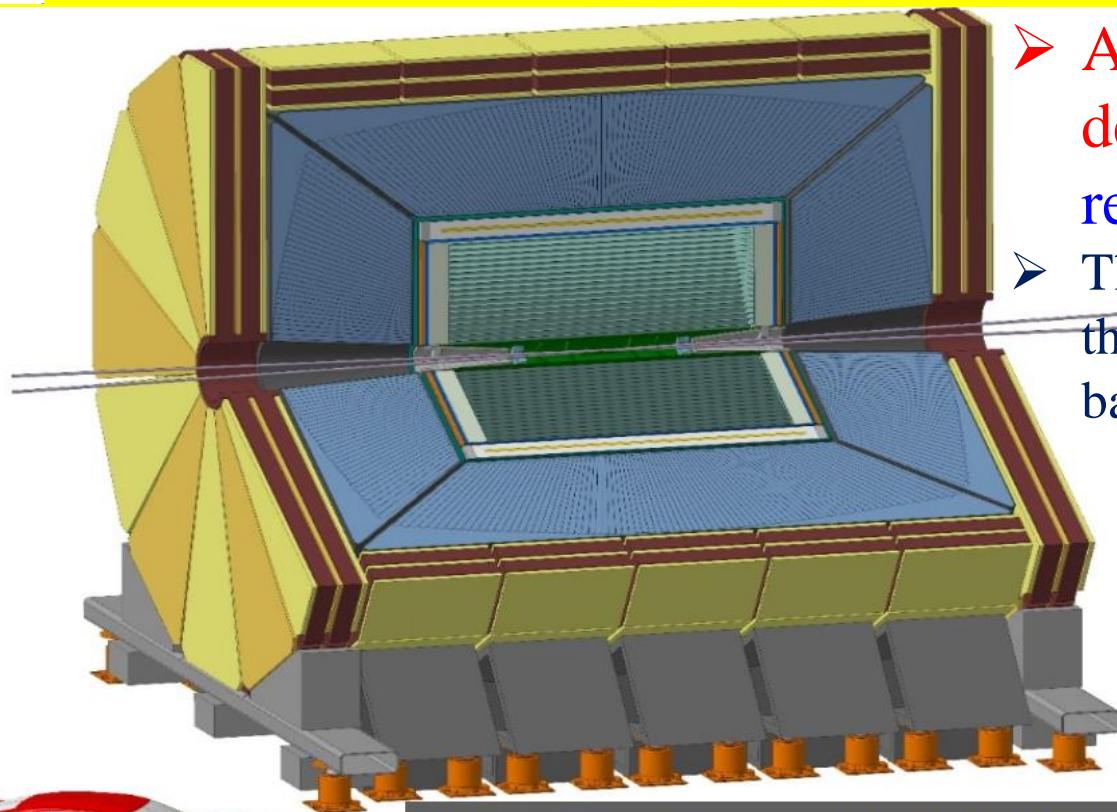


Particles in jets	Fraction of energy	Measured with	Resolution [σ^2]
Charged	65 %	Tracker	Negligible
Photons	25 %	ECAL with $15\%/\sqrt{E}$	$0.07^2 E_{jet}$
Neutral Hadrons	10 %	ECAL + HCAL with $50\%/\sqrt{E}$	$0.16^2 E_{jet}$
Confusion			$\leq 0.24^2 E_{jet}$

} 18%/√E

Required for 30%/√E

- Jet energy resolution will be dominated by the intrinsic resolution at low jet energies
- Jet energy resolution of 3-4% required to separate W/Z peak not suitable for CEPC: worse resolution should be still tolerable



IDEA concept (proposed in FCC CDR)
Innovative Detector for e⁺e⁻ Accelerator



- An alternative detector concept, **IDEA**, has been designed for a **CEPC**. It is being adopted as a reference detector for FCC-ee
- The concept design attempts to **economize** on the overall cost of the detector and proposes **different technologies** than the baseline concept for some of the detector subsystems

Innovative, more cost-effective concept:

- ❖ Silicon vertex detector
- ❖ Short-drift, ultra-light wire chamber
- ❖ **Dual-readout calorimeter**
- ❖ Thin and light solenoid coil inside calorimeter system: Small magnet ⇒ small yoke
- ❖ Muon system made of 3 layers of μ -RWELL detectors in the return yoke

□ The **IDEA detector** concept could be an excellent choice for one of the **IPs**:: Very good momentum measurement; Outstanding PID with cluster counting from the drift chamber; **Excellent calorimetry**; Precise and efficient muon detector; Very appealing upgrade options! (DR EM crystal calorimeter, LGADs for the Si wrapper)

□ **Need for significant R&D in the next 4-5 years**: A lot of ongoing activities on all IDEA sub-detectors; Profiting from several national funding schemes, EU projects, etc.; **Several international colleagues have joined**



PHYSICS PROCESSES USED AS BENCHMARKS



Physics processes and key observables used as benchmarks for setting the requirements and the optimization of the CEPC detectors

□ $\Delta(1/p_T)$

➤ high precision measurement at the end of tracker

□ $\sigma_{r\phi}$

➤ finely segmented vertex detector

□ σ_E^{jet}/E

➤ excellent Jet energy resolution

□ $\sigma_E^{e/\gamma}/E$

➤ Good em energy resolution

□ Challenging requirements for detector materials

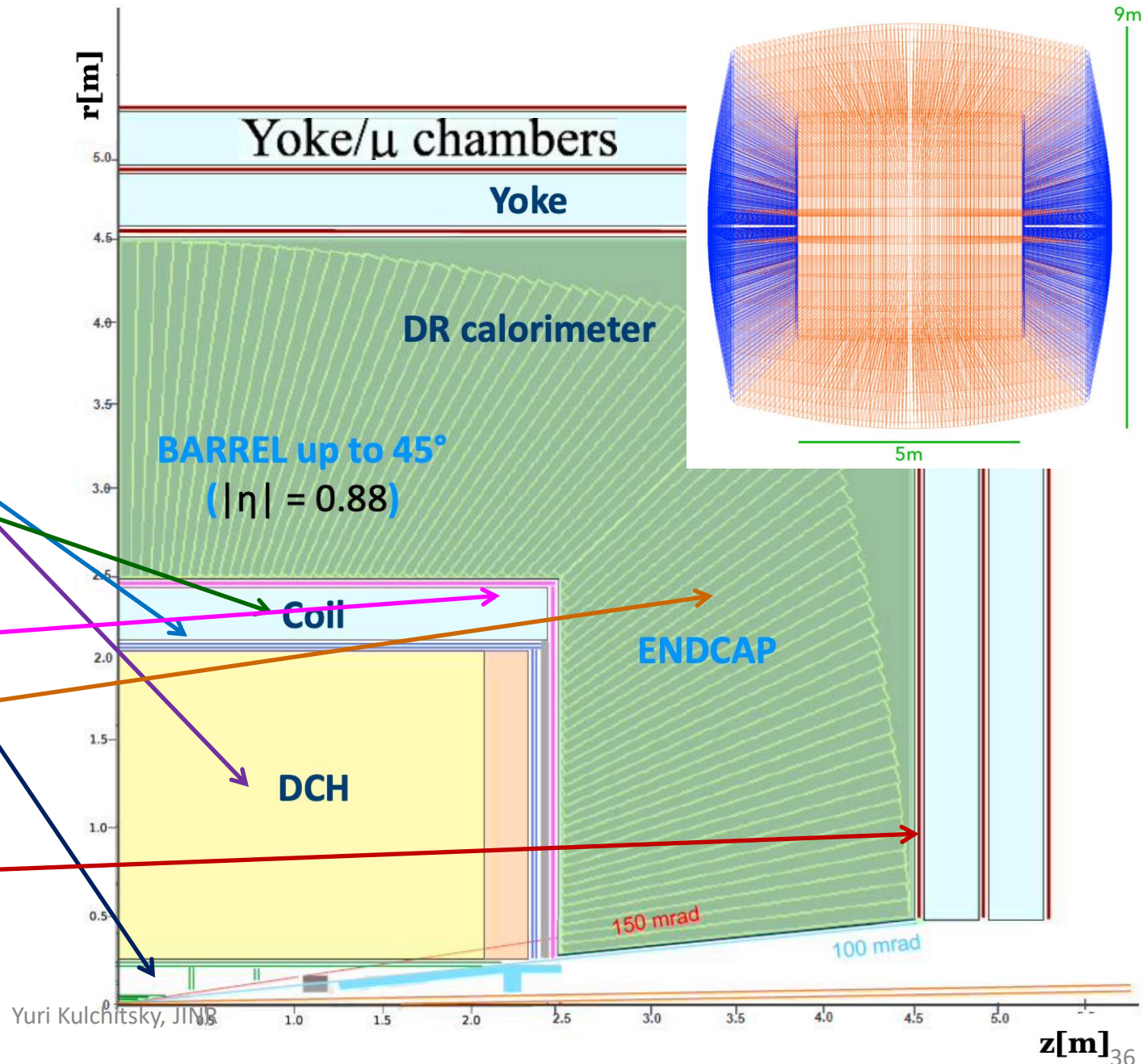
Physics process	Measurands	Detector subsystem	Performance requirement
$ZH, Z \rightarrow e^+e^-, \mu^+\mu^-$ $H \rightarrow \mu^+\mu^-$	$m_H, \sigma(ZH)$ $\text{BR}(H \rightarrow \mu^+\mu^-)$	Tracker	$\Delta(1/p_T) = 2 \times 10^{-5} \oplus \frac{0.001}{p(\text{GeV}) \sin^{3/2} \theta}$
$H \rightarrow b\bar{b}/c\bar{c}/gg$	$\text{BR}(H \rightarrow b\bar{b}/c\bar{c}/gg)$	Vertex	$\sigma_{r\phi} = 5 \oplus \frac{10}{p(\text{GeV}) \times \sin^{3/2} \theta} (\mu\text{m})$
$H \rightarrow q\bar{q}, WW^*, ZZ^*$	$\text{BR}(H \rightarrow q\bar{q}, WW^*, ZZ^*)$	ECAL HCAL	$\sigma_E^{\text{jet}}/E = 3 \sim 4\% \text{ at } 100 \text{ GeV}$
$H \rightarrow \gamma\gamma$	$\text{BR}(H \rightarrow \gamma\gamma)$	ECAL	$\Delta E/E = \frac{0.20}{\sqrt{E(\text{GeV})}} \oplus 0.01$



THE IDEA DETECTOR LAYOUT

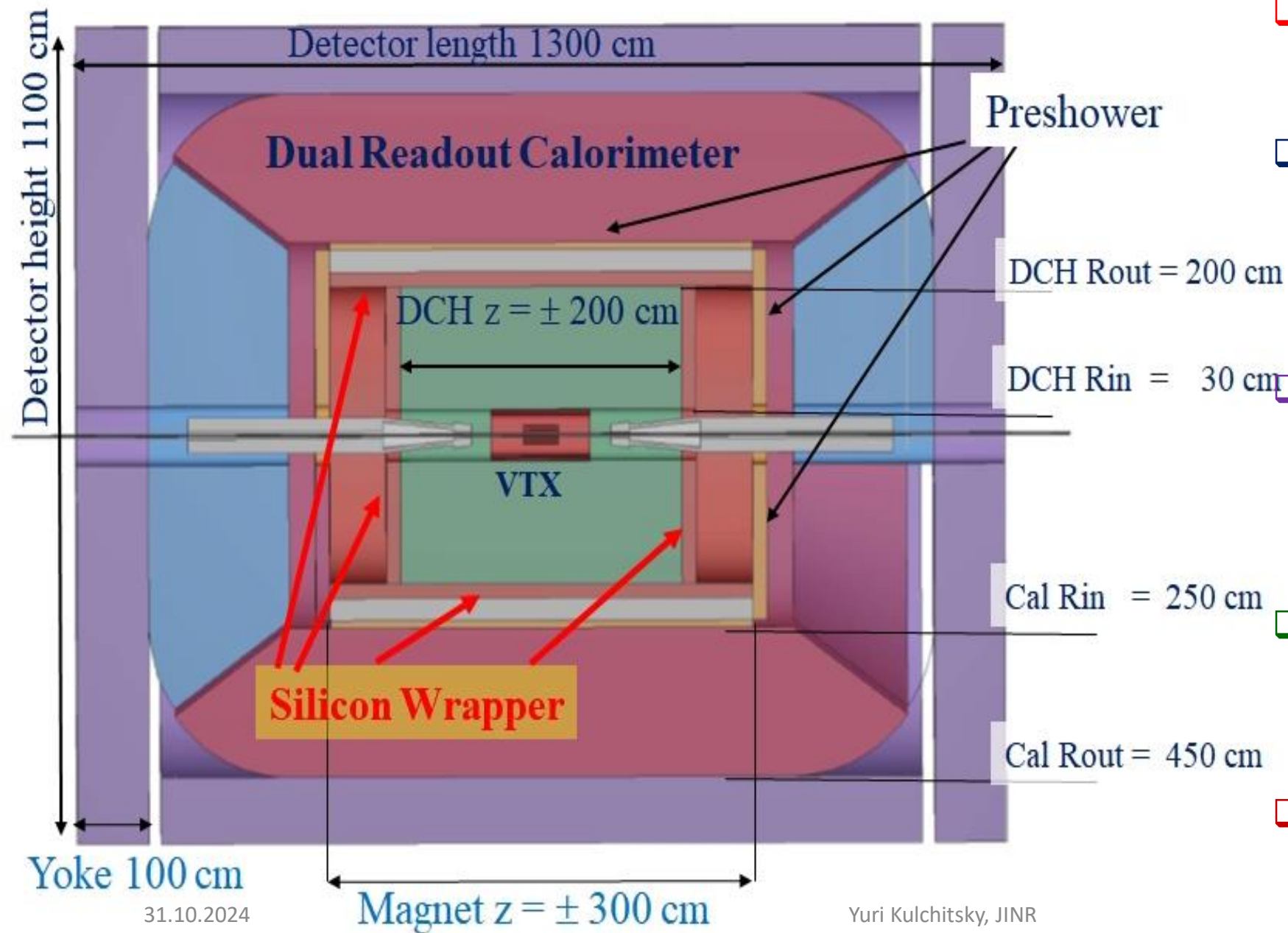


- **Beam pipe:** $R \sim 1.0$ cm
- **Vertex:** 5 MAPS layers, $R = 1.37 - 31.5$ cm
- **Drift Chamber:** 112 layers, 4 m long, $R = 35 - 200$ cm
- **Outer Silicon wrapper:** Si strips
- **Superconducting solenoid coil:** 2 T, $R \sim 2.1 - 2.4$ m
0.74 X_0 , 0.16 λ @ 90°
- **Preshower:** $\sim 1 X_0$
- **Dual-Readout Calorimetry:** $2m / 7\lambda_{int}$; Preshower μ -Rwell
- **Yoke +**
- **Muon chambers**





THE IDEA DETECTOR LAYOUT



- ❑ A key element of **IDEA** is a **thin, 30 cm, and low mass, $0.8 X_0$, solenoid with a magnetic field 2T**
- ❑ The low mass and thickness of the solenoid allows it to be located between the tracking volume and the calorimeter without a significant performance loss
- ❑ The low-magnetic field is optimal as it minimizes the impact on emittance growth and allows for manageable fields in the compensating solenoids
- ❑ It puts stringents constraints on the tracker design required to achieve the necessary momentum resolution
- ❑ **IDEA** has consequently adopted a large low-mass cylindrical drift chamber has its main tracker



□ *The following R&D program is being pursued in order to address and clarify several issues:*

- **Absorber material choice**, current candidates: *lead, brass and iron*;
- **Machining and assembly procedure** for modules of **10x10 cm²** cross section;
- **Development of a modular, projective solution** for a **4π calorimeter** concerning both the construction of *single modules* and the *design and construction of a full detector*;
- **Identification of adequate solid-state photo-sensors** in order to *independently optimize both Cerenkov and scintillation light detection*
- **Readout granularity** (i.e. identify the *optimal fiber grouping* into a *single readout channel*);

1. **DREAM Collaboration**, R.Wigmans, The DREAM project: Towards the ultimate in calorimetry, NIM A617 (2010) 129–133.
2. N.Akchurin et al., The electromagnetic performance of the **RD52** fiber calorimeter, NIM A735 (2014) 130–144.
3. **RD52 (DREAM) Collaboration**, R.Wigmans, New results from the **RD52** project, NIM A824 (2016) 721–725.
4. N.Akchurin et al., Particle identification in the longitudinally unsegmented **RD52** calorimeter, NIM A735 (2014) 120–129

5.5: Dual-readout calorimeter

Franco Bedeschi bed@fnal.gov,
Roberto Ferrari roberto.ferrari@cern.ch,

INFN - Sezione di Pisa, Università' di Pisa and Scuola Normale Superiore
INFN - Sezione di Pavia and University of Pavia



- ❑ *The following R&D program is being pursued in order to address and clarify several issues:*
- *Identification of a tailored front-end electronics, likely composed by an ASIC and an FPGA chip, in order to extract in real time both charge and time information (a time resolution of 100 ps allow to identify the shower starting point inside the calorimeter with a precision of 6 cm);*
- *Particle ID performance with PFA, with and without a longitudinal segmentation;*
- *Development and validation of full and fast simulations of both test beam modules and an integrated 4π detector;*
- *Assessment of the performance for the most relevant physics channels (W, Z, H decays).*

5.5: Dual-readout calorimeter

Franco Bedeschi bed@fnal.gov,

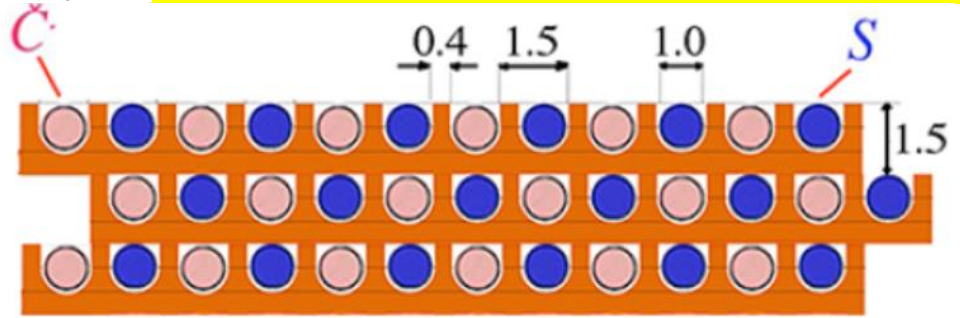
Roberto Ferrari roberto.ferrari@cern.ch,

INFN - Sezione di Pisa, Universita' di Pisa and Scuola Normale Superiore

INFN - Sezione di Pavia and University of Pavia

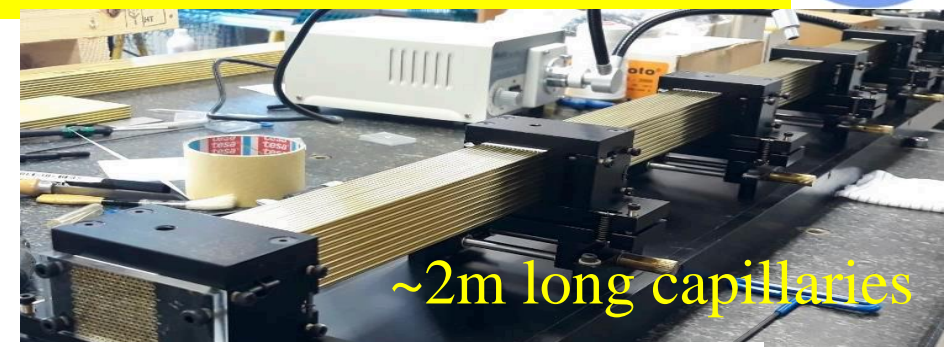


IDEA DETECTOR: DUAL READOUT CALORIMETRY



Alternate

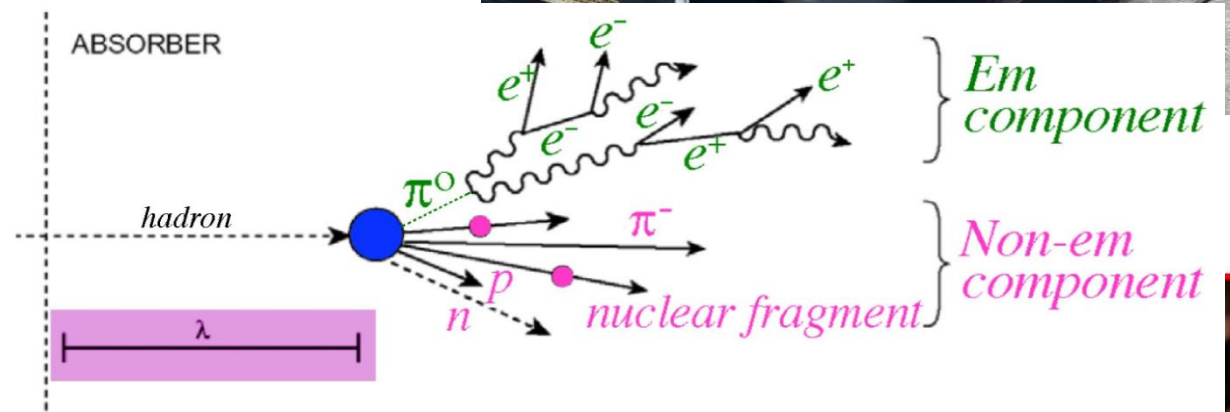
- ✓ Cherenkov fibers
- ✓ Scintillating fibers



~2m long capillaries

Dual-Readout calorimetry **allows to remove** fluctuations by correcting for f_{em} event-by-event using two readout channels with different h/e

- ☐ Measure simultaneously:
 - Scintillation signal (S)
 - Cherenkov signal (C)
- ☐ Calibrate both signals with e^-
- ☐ Unfold event by event f_{em} to obtain corrected energy

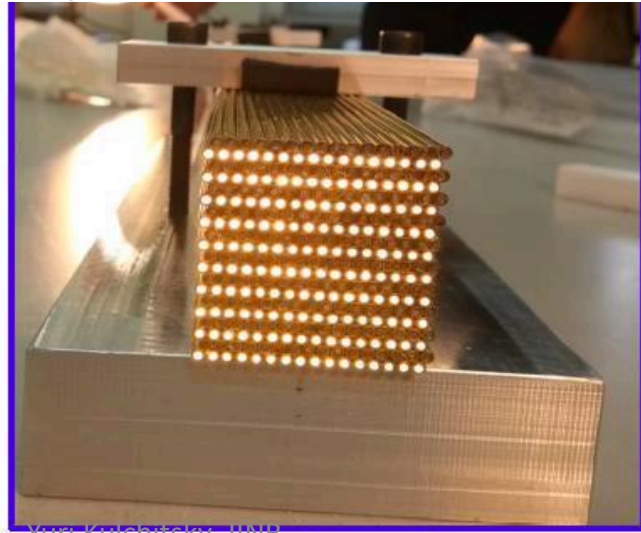


$$S = E [f_{em} + (h/e)_S (1 - f_{em})]$$

$$C = E [f_{em} + (h/e)_C (1 - f_{em})]$$

$$E = \frac{S - \chi C}{1 - \chi} \quad \text{with: } \chi = \frac{1 - (h/e)_S}{1 - (h/e)_C}$$

31.10.2024



Scintillation fibers



Newer DR calorimeter (bucatini calorimeter)

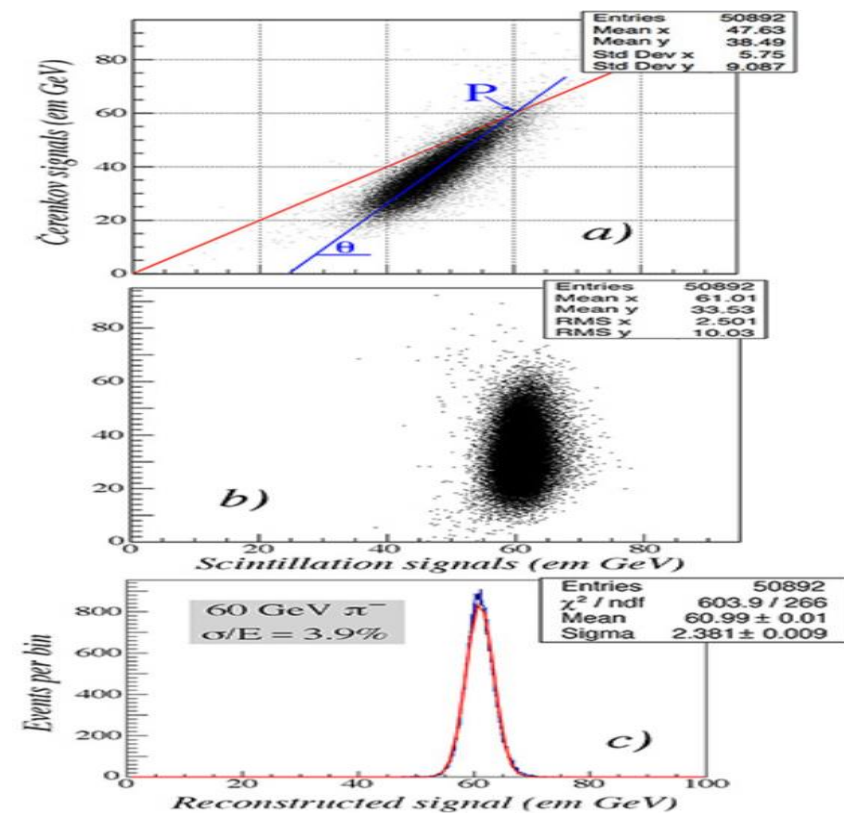
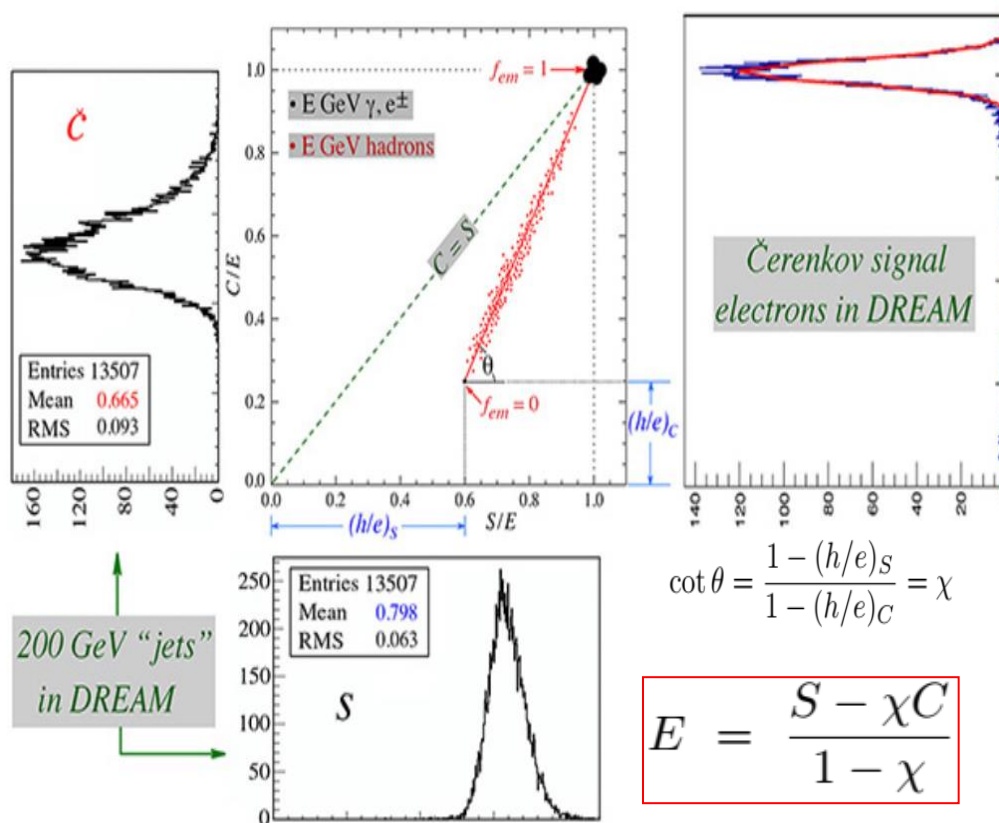
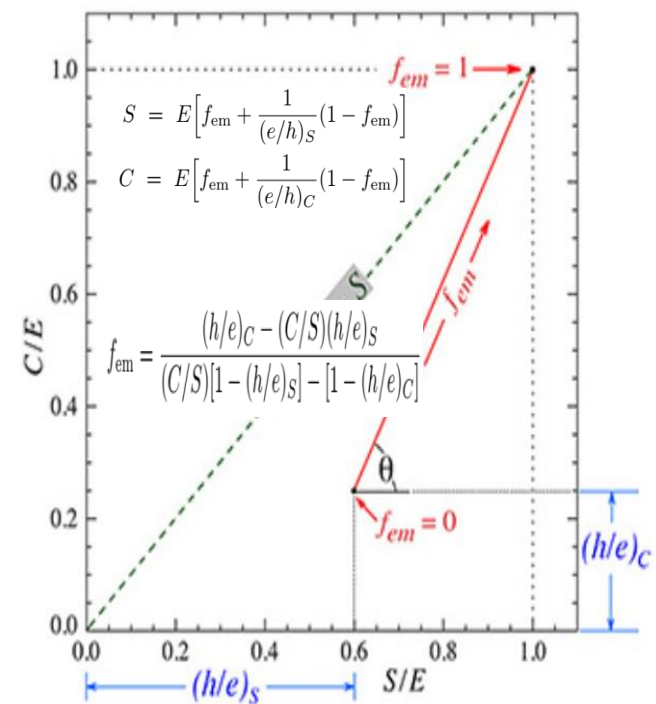
Cherenkov fibers



DUAL READOUT CALORIMETRY



The DR calorimetry has emerged as a technique for measuring the properties of high-energy hadrons and hadron jets



The data points for hadron showers detected with a dual-readout calorimeter are located around the straight (red) line in this diagram. The data points for em showers in this calorimeter are clustered around the point where this line intersects the C=S line.

The hadron events are clustered around the straight (red) line, the electron events around the point (1,1). Experimental signal distributions measured in the scintillation and Čerenkov channels for **200 GeV jets** with the **DREAM** fiber calorimeter. Also shown is a typical (Čerenkov) response function measured for electrons in **DREAM**.

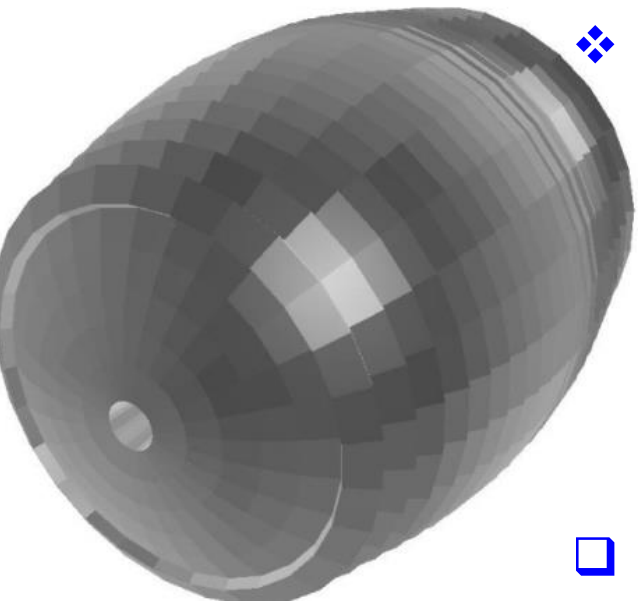
Signal distributions of the Dual-Readout lead fiber calorimeter for 60 GeV pions. Scatter plot of the 2 types of signals as recorded for these particles and rotated over an $\theta=30^\circ$ around the point where the 2 lines from diagram a intersect. Projection of the latter scatter plot on the x-axis.



IDEA DETECTOR: DUAL READOUT CALORIMETRY

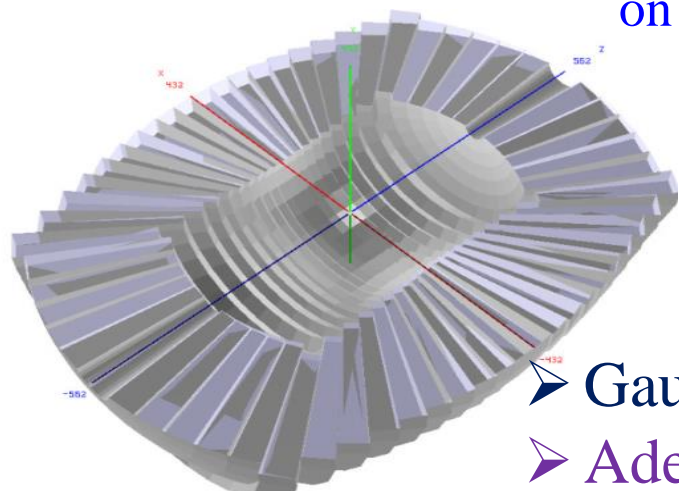


Full GEANT4 implementation of the DR calorimeter



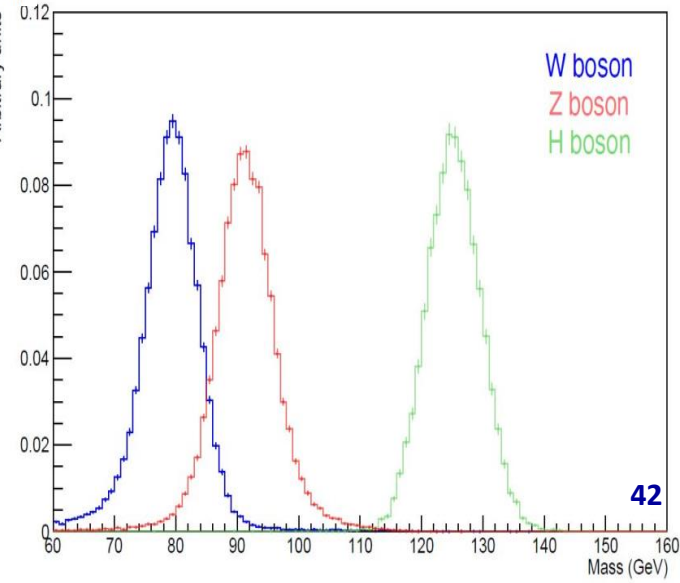
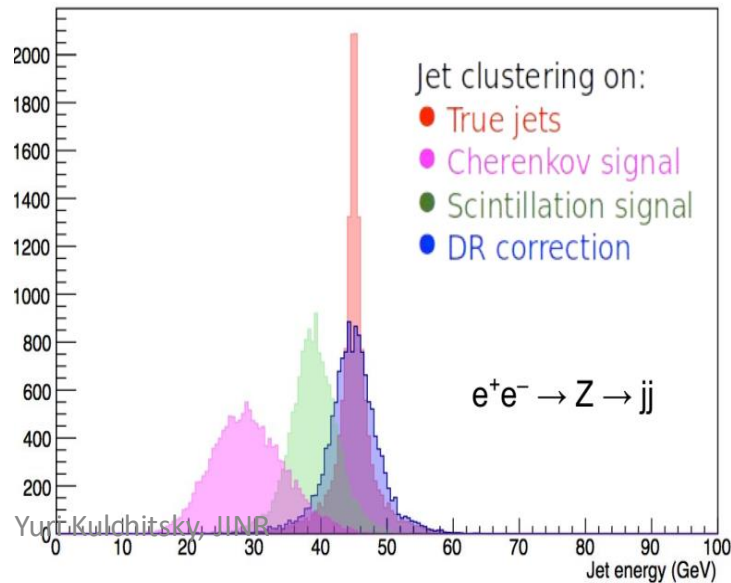
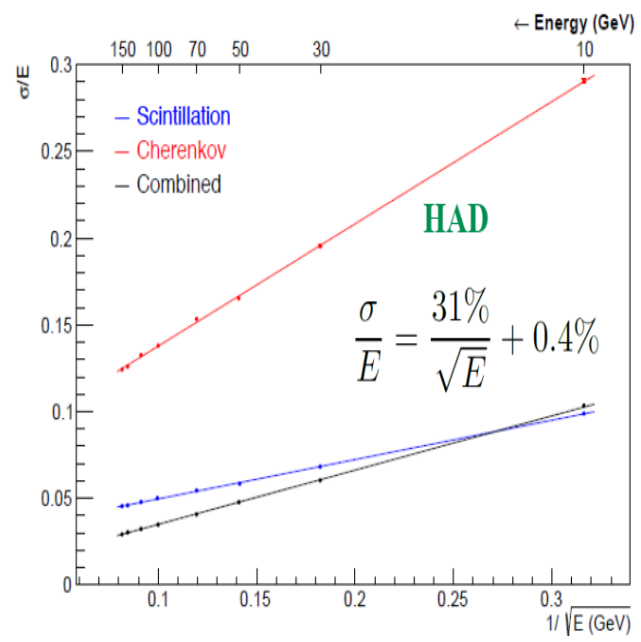
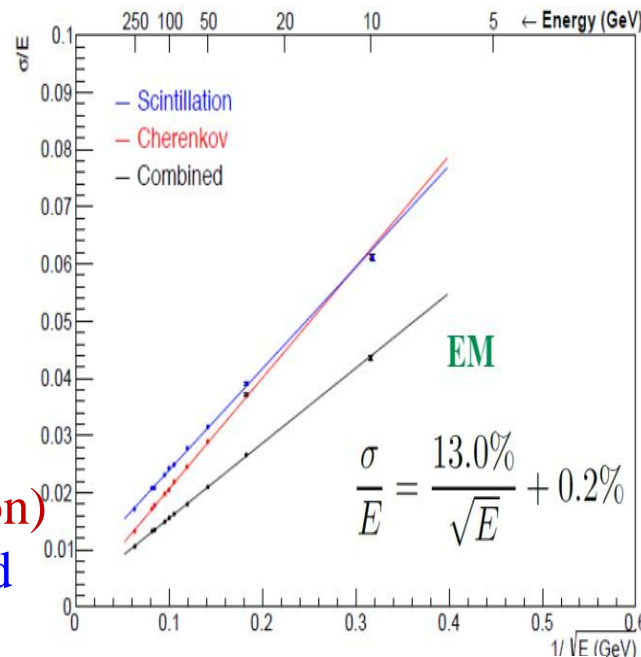
- ❖ International collaboration:
 1. TTU (USA),
 2. Sussex (UK),
 3. Universities (Korea),
 4. Chile,
 5. Princeton,
 6. Maryland (USA),
 7. CERN (crystal extension)

☐ EM prototype built and tested on beams (DESY/CERN)



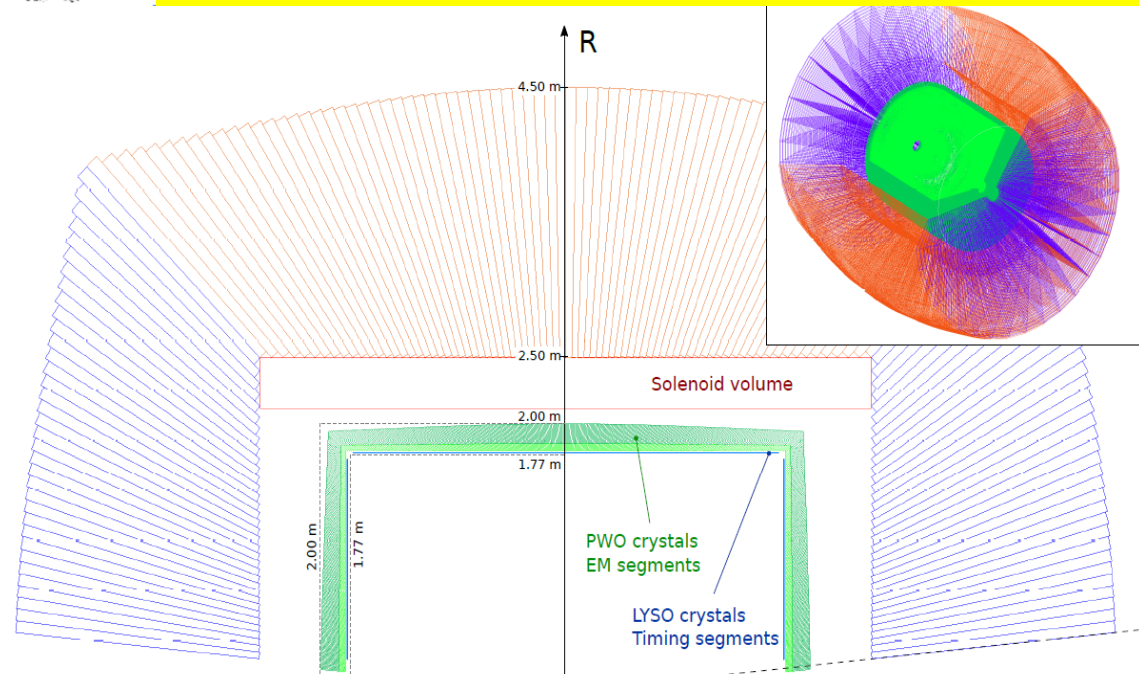
- Gaussian resolution
- Adequate separation of W/Z/H

Geant 4: good resolutions averaged over η and ϕ

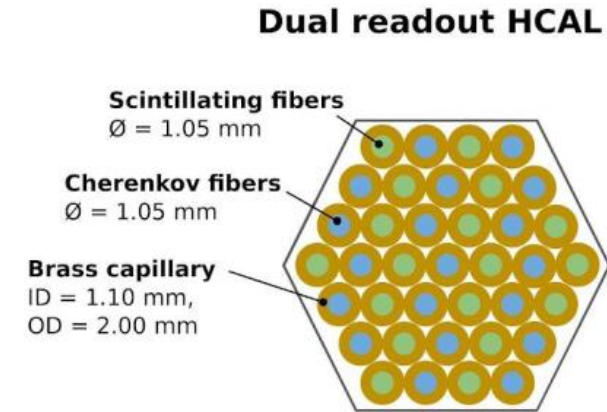




IDEA DETECTOR: CRYSTAL ECAL OPTION

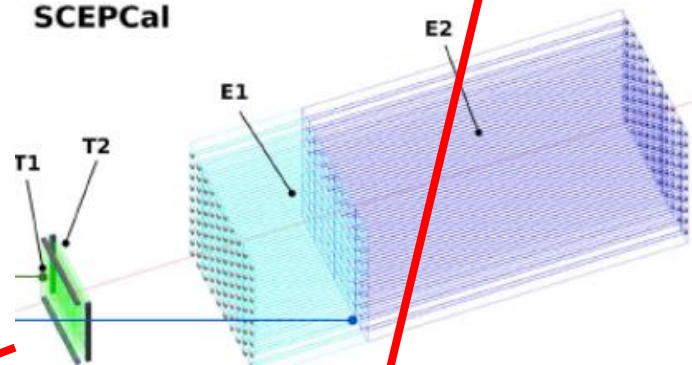


- ❑ **ECAL ~20 cm PbWO4**
 - 2 layers: 6+16 X0
 - $\sigma_{EM} \approx 3\%/\sqrt{E}$
 - Dual readout (DR) with filters
- ❑ **Timing layer**
 - ❖ LYSO 20 – 30 ps
 - ❖ 3x3x60 mm³ active cell
 - ❖ 3x3 mm² SiPMs (10-15 um)



❑ **Particle flow (PF) for jets** $\sigma_{EM}^E/E \sim 3\%/\sqrt{E}$

- ❑ **ECAL layer:**
 - PbWO crystals
 - front segment 5 cm (~5.4 X₀)
 - rear segment for core shower (15 cm ~16.3 X₀)
 - 10x10x200 mm³ of crystal
 - 5x5 mm² SiPMs (10-15 um)



Geometry built from projective towers

- O(100M) fibres embedded in absorber in longitudinal direction
- Absorber material being investigated (copper, brass, steel)
- Tower geometries, based on chessboard or honeycomb layout of fibres, available
- High transverse granularity:: Excellent angular resolution, Lateral shape sensitivity
- No longitudinal segmentation out of the box
- For both EM and HAD calorimetry:: Option with dedicated crystal ECAL in front



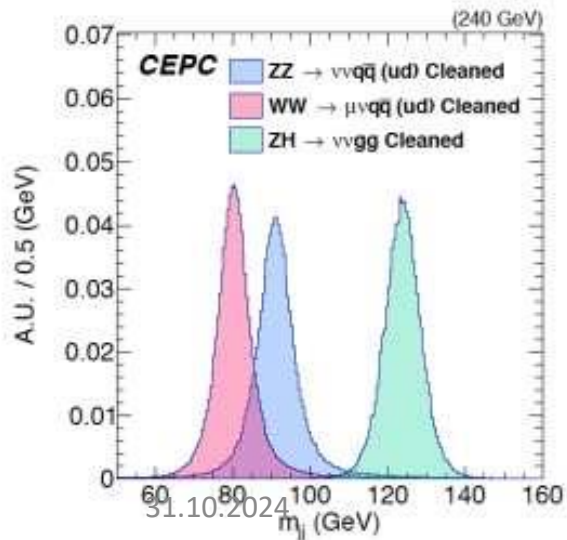
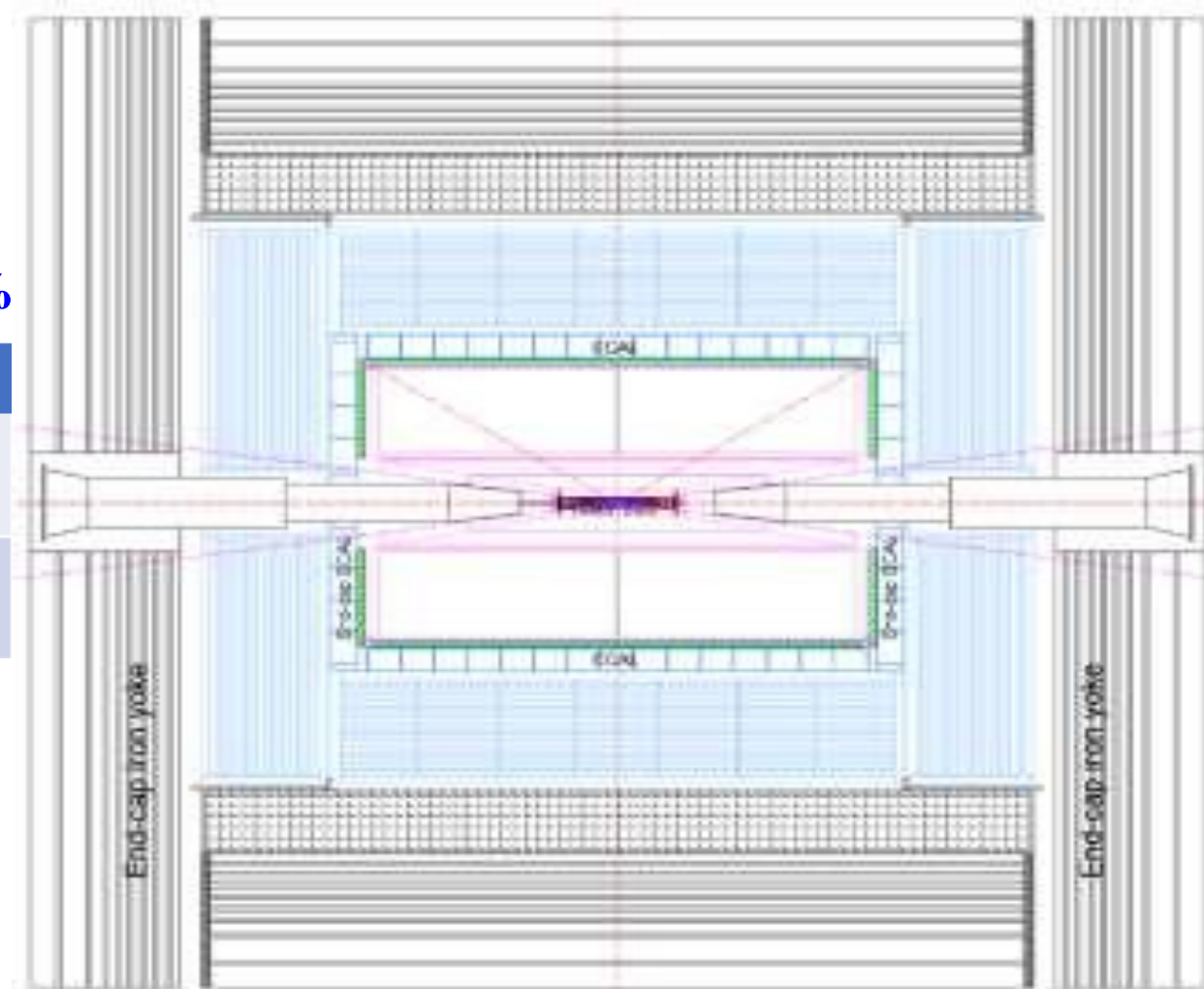


CEPC DETECTOR: IDEA OF THE "4TH CONCEPT"



- ❑ **Requirements:** boson mass resolution (**BMR ~3%**)
- ❑ **Challenges:** Support Particle flow with = High granularity & High precision
- ❑ Novel detector design based on Particle Flow Algorithm (PFA) calorimeter to improve the BMR from **4% to 3%**

Detector	Key parameter	World level	4 th concept
PFA based EM calorimeter	EM shower E resolution	~ 15-20%/√E	<3%/√E
PFA based Hadron calorimeter	Single hadron E resolution	~ 50-60%/√E	~40%/√E



- ❖ Silicon combined with gaseous chamber as the tracker and PID
- ❖ **ECAL** based on crystals with timing for 3D shower profile for PFA and EM energy
- ❖ Scintillation glass **HCAL** for better hadron sampling and energy resolution



CEPC DETECTOR: IDEA OF THE "4TH CONCEPT"



Scint Glass
PFA HCAL

Advantage: Cost efficient, high density
Challenges: Light yield, transparency, massive production.

Solenoid Magnet (3T / 2T)
Between HCAL & ECAL

Advantage: the HCAL absorbers act as part of the magnet return yoke.
Challenges: thin enough not to affect the jet resolution (e.g. BMR); stability.

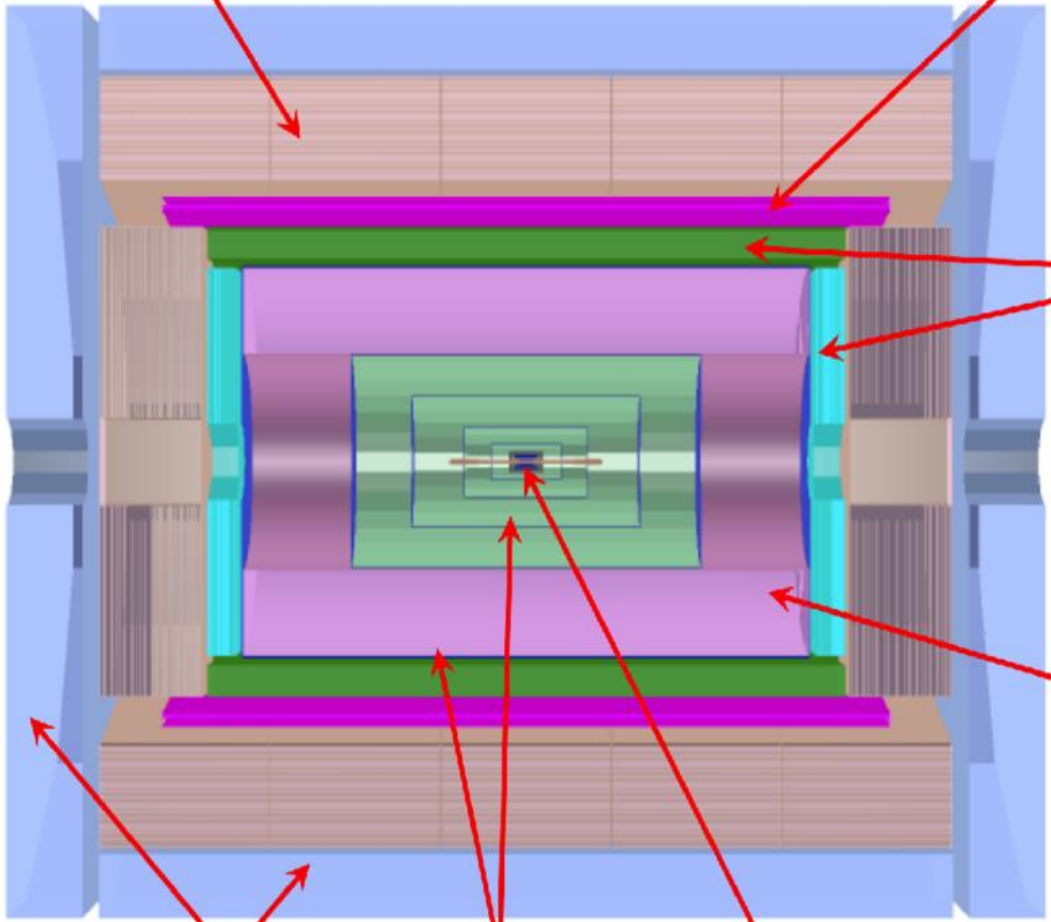
Crystal ECAL

Advantage: better π^0/γ reconstruction.
Challenges: minimum number of readout channels; compatible with PFA calorimeter; maintain good jet resolution.

A Drift chamber
that is optimized for PID

Advantage: Work at high luminosity Z runs
Challenges: sufficient PID power; thin enough not to affect the moment resolution.

- Excellent e/gamma energy resolution
- PID capability
- Better hadronic energy resolution
- Magnet in much reduced size



31.10.2024
Mu+Yoke Si Tracker w/TOF outer layer Si Vertex

Yuri Kulchitsky, JINR

JINR Participation in Experiments at CEPS (preferable in the IDEA experiment)

- Hardware contribution** to experiments (MHPD have good experience in experiments: ATLAS, CDF, mu2e, Comet, ...): MHPD team
 1. Double Readout Hadronic calorimeter
 2. Crystal Electromagnetic calorimeter
 3. Forward calorimeter for Luminosity measurement
 4. Micro-Resistive WELL (μ -RWELL) muon system
 5. Monte Carlo simulations for detector development
- The physics program preparation:** G.Lykasov, V.Lyubushkin, I.Boyko, Y.Kulchitsky, ...
 1. Precision Higgs boson physics (based on $5 \times 10^6 e^+e^- \rightarrow ZH$ at 240-250 GeV),
 2. New physics BSM,
 3. Flavor Physics (B physics, C physics)
- Theoretical support** of the CEPC Physics program: A. Arbuzov, ...
- Development** of event generators (SANC, ...): L.Kalinovskaya + SANC team
- Precision calculations** of experimental observables: L.Kalinovskaya, I.Boyko, ...
- Participation** in a code development for data preparation and analysis

JINR group has developed the computer codes

□ e+e- initial state:

- MC generator *ReneSANCe*
- MC integrator *MCSANCe*

□ $\gamma\gamma$ initial state: MC integrator *SANCphot*

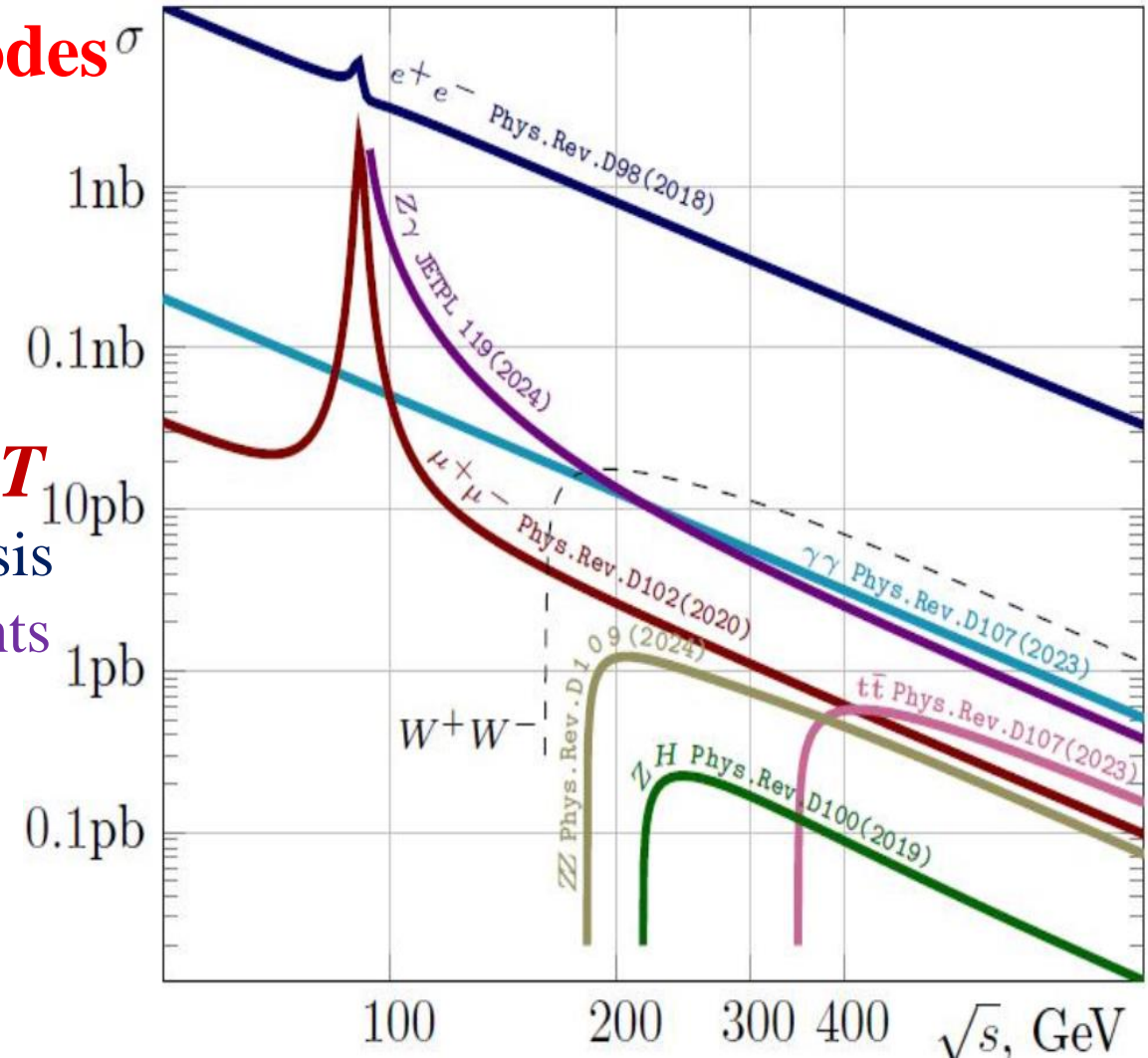
□ semi-analytic programs *Zfitter* and *DIZET*

- were the main tools for LEP1/LEP2 data analysis
- new versions prepared for the future experiments

SANC advanced features

- full one-loop electroweak corrections,
- higher order corrections,
- fully massive case,
- accounting for polarization effects,
- full phase space operation.

31.10.2024



JINR calculations of e^+e^- SM annihilation processes. The cross sections are given for polar angles 10° - 170° in the final state.

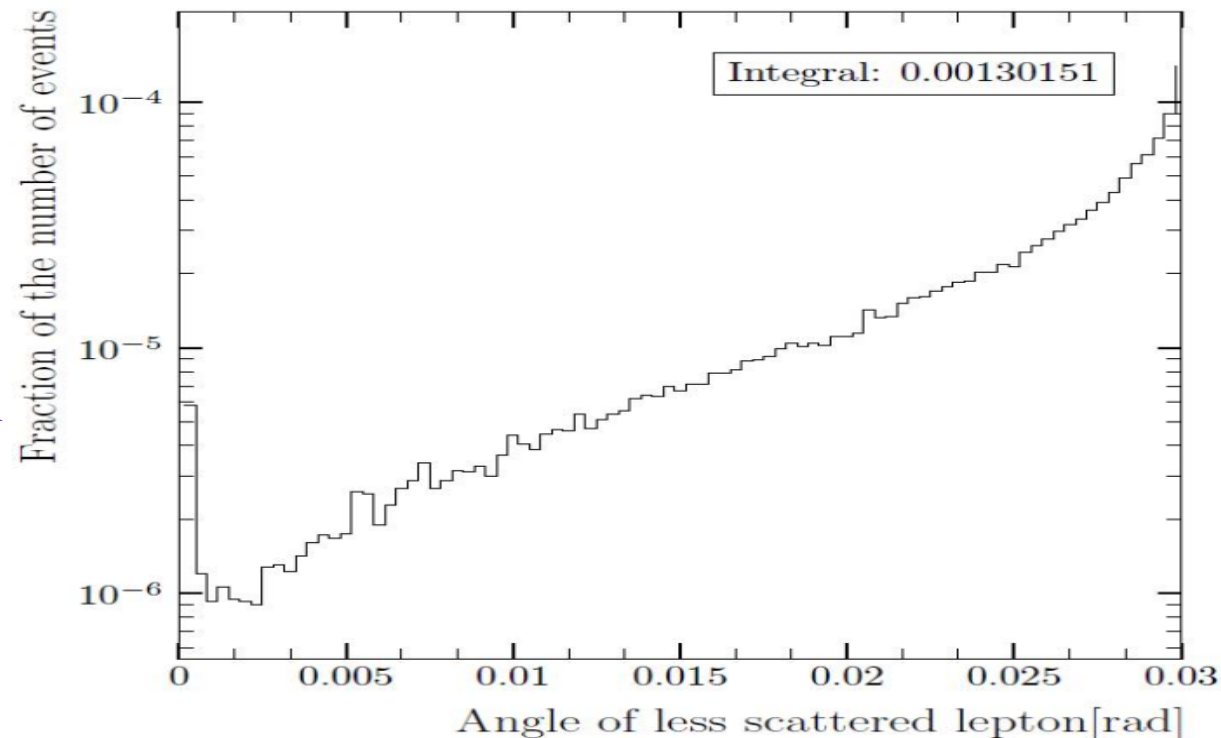
Luminosity measurement with precision $<10^{-4}$ is necessary for e^+e^- experiments

- ❑ Traditionally, **BabaYaga** and **BHLUMI** have been used for theoretical estimation of luminosity,
- ❑ **ReneSANCe**: Simulation of **Bhabha** and other processes used for luminosity monitoring, taking into account initial and final state polarization in the full phase space.
- ❑ $e^+e^- \rightarrow e^+e^-$ **SABS** (Small Angle Bhabha Scattering)
- ❑ $e^+e^- \rightarrow e^+e^-$ (all angles)
- ❑ $e^+e^- \rightarrow \mu^+\mu^-$
- ❑ $e^+e^- \rightarrow \gamma\gamma$

Luminosity in ReneSANCe

- ❑ **DONE**: 1-loop for all processes,
- ❑ **DONE**: leading 2-loop contributions. They include EW corrections at $O(G_\mu^2)$ and the mixed EWxQCD at $O(G_\mu\alpha_s)$
- ❑ **UNDER DEVELOPMENT**: complete 2-loop for all lumi processes

31.10.2024



The Luminosity determination for LEP experiments was re-analyzed in Chin.Phys.C48, 4, 043002 (2024)

- Beam scattering down to zero angle has been considered, thank to SANC feature of the full phase space.
- The conclusion is that by neglecting very small scattering angles, LEP experiments have underestimated their luminosity by 1.3 ppm
- The effect is comparable to the overall LEP experimental precision.



SUMMARY



- ❖ **CEPC addressed most pressing & critical science problems in particle physics**
 - Accelerator design & technology R&D are reaching maturity.
 - Accelerator ready for construction 3-5 years
 - Reference detector **TDR** under preparation, to be completed by **2025**
 - **A strong and experienced team, backed by IHEP and international teams**
 - ✓ **Call for collaboration** and proposals once **CEPC** is approved
 - **Work with government and funding agencies** to get support
- ❖ **Desirable areas of DLNP at JINR participation in CEPS experiments:**
 - **Hardware contribution to experiments**
 - Double Readout Hadronic calorimeter
 - Crystal Electromagnetic calorimeter
 - Forward calorimeter for Luminosity measurement
 - Micro-Resistive WELL (μ -RWELL) muon system
 - Monte Carlo simulations for detector development
 - Theoretical support of the CEPC Physics program
 - The physics program preparation for CEPC experiments
 - Development of event generators
 - Precision calculations of experimental observables
 - Participation in a code development for data preparation and analysis

The background of the slide is a scenic landscape featuring a body of water in the foreground, a line of green trees and buildings in the middle ground, and a range of blue mountains under a bright blue sky with light clouds. Overlaid on this scene is a large, bold, red 3D-style text message that reads "THANK YOU VERY MUCH FOR ATTENTION!". The text is arranged in three lines, with "THANK YOU" on the top line, "VERY MUCH" on the middle line, and "FOR ATTENTION!" on the bottom line. The letters have a white outline and a slight shadow, giving them a three-dimensional appearance.

**THANK YOU
VERY MUCH
FOR ATTENTION!**

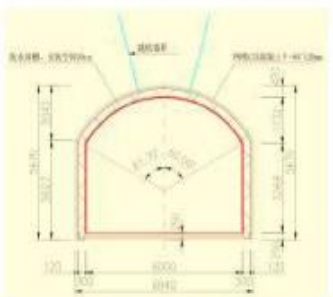
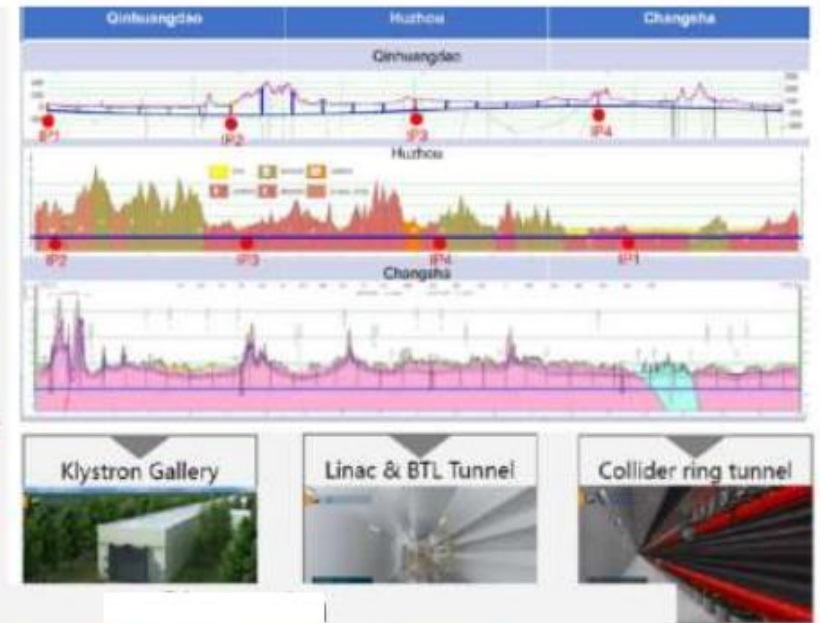


BACKUP SLIDES

Google earth



CEPC SITE PREPARATIONS (3 CANDIDATES IN TDR)



Drill-blast tunnel (6.0m×5.0m)



TBM tunnel (D6.5m)



2034

⑧

ject is

COOPERATION JINR WITH CHINA INSTITUTES

3.07.24 в Шанхае: 2 заседание **Совместного координационного комитета по сотрудничеству ОИЯИ и Китая**
ОИЯИ имеет партнерские отношения с >40 китайскими институтами и университетами

□ **Комитет принял решение о начале реализации в 2024 году 8 совместных проектов:**

1. теоретическую физику,
2. разработку технологий для сверхбольшого глубоководного нейтринного телескопа,
3. использование нейтронных пучков для решения фундаментальных и прикладных задач,
4. синтез и изучение свойств сверхтяжелых элементов,
5. разработку ускорительных технологий,
6. создание монолитных кремниевых детекторов,
7. сотрудничество в рамках подготавливаемого в КНР нейтринного эксперимента **JUNO**.

□ **Поддержка совместной программы академических обменов и проведения научных мероприятий.**

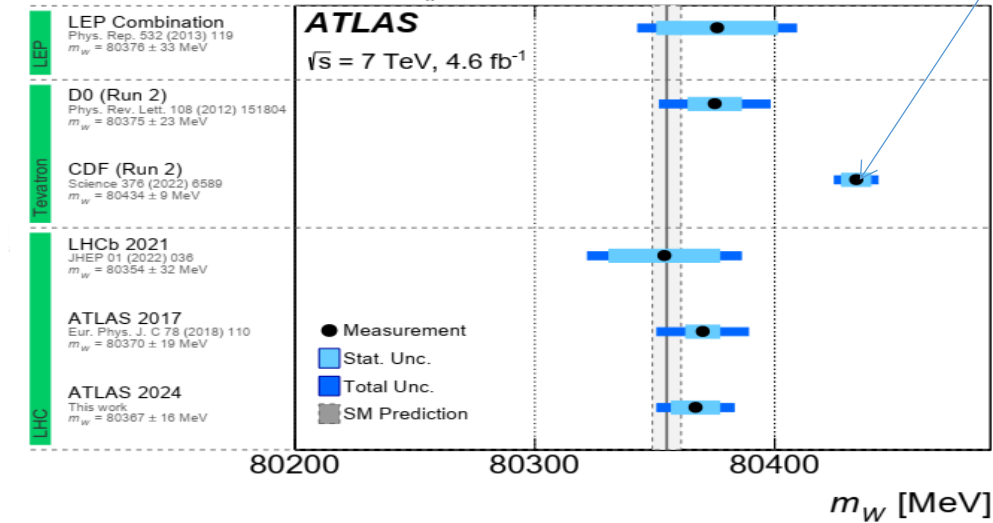
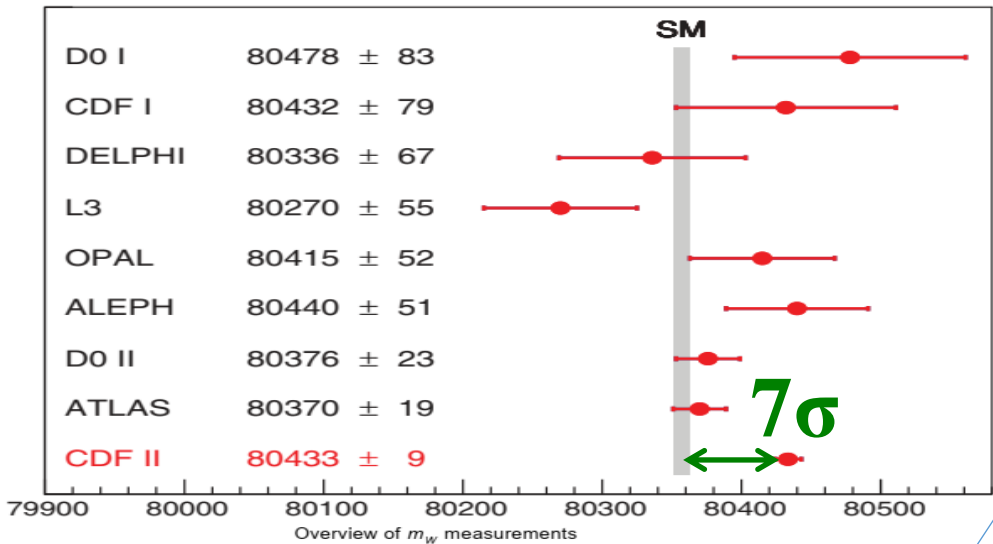
□ **Использование платформы DIRAC Interware для построения распределенных вычислительных систем, в том числе с применением облачных ресурсов, позволяет обрабатывать данные NICA, JUNO и BESIII.**

□ **Важным направлением сотрудничества ОИЯИ и КНР может стать радиобиология и медицина.**

□ **Подчеркнут прогресс в сотрудничестве: стороны ведут совместную подготовку экспериментов MPD и SPD на NICA, продолжают сотрудничество в проектах BESIII и JUNO, в области физики тяжелых ионов, нейтронной физики, разработки медицинских ускорителей, теоретических исследований и др.**

«Мы договорились о том, что в перспективе перечень направлений для совместных проектов может быть расширен, а число проектов может быть увеличено по мере развития сотрудничества и оценки реализации уже одобренных проектов», Директор ОИЯИ.

CDF II Collaboration, High-precision measurement of the W boson mass with the CDF detector. *PoS ICHEP2022 (2022) 898*



The ATLAS Collaboration has reported a measurement
 $M_W = 80370 \pm 7$ (stat) ± 11 (syst) ± 1 (mod. syst) $= 80370 \pm 19$ MeV
 $M_W = 80366.5 \pm 9.8$ (stat) ± 12.5 (syst) $= 80366.5 \pm 15.9$ MeV

□ **CDF II** measure the W boson mass, M_W , using data corresponding to 8.8 fb^{-1} collected in proton-antiproton collisions at a **1.96 TeV** with the CDF II detector at the Fermilab Tevatron collider. A sample of approximately 4×10^6 W boson is used to obtain $M_W = 80433.5 \pm 6.4$ (stat) ± 6.9 (syst) $= 80433.5 \pm 9.4$ MeV. The W bosons are identified using their decays to ev & $\mu\nu$ and the mass is measured by fitting template distributions of transverse momentum and mass: $m_T = \sqrt{2p_T^x p_T^y (1 - \cos \Delta\phi)}$

□ A comparison with the **SM expectation** of $M_W = 80357 \pm 6$ MeV, treating the quoted uncertainties as independent, yields a difference with a significance of **7σ**. The suggests are:

- the improvements to the SM calculation or
- of extensions to the SM

□ SM result includes the published estimates of the uncertainty (4 MeV) due to missing higher-order quantum corrections and the uncertainty (4 MeV) from other global measurements used as input to the calculation

ATLAS Collaboration, Measurement of the WW-boson mass in pp collisions at $\sqrt{s} = 7$ TeV with the ATLAS detector, *Eur. Phys. J. C 78 (2018) 2, 110, Eur. Phys. J. C 78 (2018) 11, 898 (erratum), arXiv:1701.07240; e-Print: 2403.15085 [hep-ex]*
 A measurement of the mass of the W boson is presented based on proton-proton collision data recorded in 2011 at a **7 TeV** with the **ATLAS** detector at the LHC, and corresponding to **4.6 fb⁻¹** of integrated luminosity. The selected data sample consists $\sim 7.8 \times 10^6$ candidates in the $W \rightarrow \mu\nu$ channel and 5.9×10^6 candidates in the $W \rightarrow ev$ channel.

ATLAS/CMS: Run-2 at 13 TeV is 139/137 fb⁻¹

FCC-EE MAIN MACHINE PARAMETERS

Parameter	4 years 5×10^{12} Z LEP $\times 10^5$	Z	2 years $> 10^8$ WW LEP $\times 10^4$	WW	3 years 2×10^6 H	H (ZH)	5 years 2×10^6 tt pairs	ttbar
beam energy [GeV]		45.6		80		120		182.5
beam current [mA]		1270		137		26.7		4.9
number bunches/beam		11200		1780		440		60
bunch intensity [10^{11}]		2.14		1.45		1.15		1.55
SR energy loss / turn [GeV]		0.0394		0.374		1.89		10.4
total RF voltage 400/800 MHz [GV]		0.120/0		1.0/0		2.1/0		2.1/9.4
long. damping time [turns]		1158		215		64		18
horizontal beta* [m]		0.11		0.2		0.24		1.0
vertical beta* [mm]		0.7		1.0		1.0		1.6
horizontal geometric emittance [nm]		0.71		2.17		0.71		1.59
vertical geom. emittance [pm]		1.9		2.2		1.4		1.6
vertical rms IP spot size [nm]		36		47		40		51
beam-beam parameter x_x / x_y		0.002/0.0973		0.013/0.128		0.010/0.088		0.073/0.134
rms bunch length with SR / BS [mm]		5.6 / 15.5		3.5 / 5.4		3.4 / 4.7		1.8 / 2.2
luminosity per IP [10^{34} cm ⁻² s ⁻¹]		140		20		≥5.0		1.25
total integrated luminosity / IP / year [ab ⁻¹ /yr]		17		2.4		0.6		0.15
beam lifetime rad Bhabha + BS [min]		15		12		12		11



CEPC AND OTHER ACCELERATOR PROJECTS IN CHINA



Project name	Machine type	Location	Cost (B RMB)	Completion time
CEPC	Higgs factory Upto 100 GeV energy	Led by IHEP, China	36.4 (where accelerator 19)	Around 2035 (starting time around 2027)
BEPCII-U	e+e-collider 2.8GeV/beam	IHEP (Beijing)	0.15	2025
HEPS	4 th generation light source of 6GeV	IHEP (Huanrou)	5	2025
SAPS	4th generation light source of 3.5GeV	IHEP (Dongguan)	3	2031 (in R&D, to be approved)
HALF	4th generation light source of 2.2GeV	USTC (Hefei)	2.8	2028
SHINE	Hard XFEL of 8GeV	Shanghai-Tech Univ., SARI and SIOM of CAS (Shanghai)	10	2027
S3XFEL	S3XFEL of 2.5GeV	Shenzhen IASF	11.4	2031
DALS	FEL of 1GeV	Dalian DICP	-	(in R&D, to be approved,)
HIAF	High Intensity heavy ion Accelerator Facility	IMP, Huizhou	2.8	2025
CIADS	Nuclear waste transmutation	IMP, Huizhou	4	2027
CSNS-II	Spallation Neutron source proton injector of 300MeV	IHEP, Dongguan	2.9	2029

The total cost of the *accelerator projects under construction* is 39B RMB (5.5 M\$);

CEPC cost is 36.4B RMB (5.1 M\$)

11.10.2024

Yuri Kulchitsky, JINR



LEPTON COLLIDERS



Location	Name (type ^[a])	Beam Energy ^[b] (GeV)	Luminosity ^[b] (cm ⁻² s ⁻¹)	Operation Period
Stanford/SLAC, USA	CBX ^[c] (e ⁻ e ⁻ DR)	0.5	2×10^{28}	1963-1968
	SPEAR (SR)	4	1.2×10^{31}	1972-1988
	PEP (SR)	15	6×10^{31}	1980-1990
	SLC (LC)	49	2.5×10^{30}	1989-1998
	PEP-II (DR)	9 (e ⁻) 3.1 (e ⁺)	1.2×10^{34}	1998-2008
Frascati, Italy	AdA (SR)	0.25	5×10^{25} [d]	1961-1964
	ADONE (SR)	1.5	6×10^{29}	1969-1993
	DAΦNE (SR)	0.51	2.4×10^{32} 4.5×10^{32} [e]	1999-present
BINP, Russia	VEP-1 (e ⁻ e ⁻ DR)	0.16	5×10^{27}	1964-1968
	VEPP-2 (SR)	0.67	4×10^{28}	1966-1970
	VEPP-2M (SR)	0.7	5×10^{30} (@0.511)	1974-2000
	VEPP-3 (SR)	1.55	2×10^{27}	1974-1975
	VEPP-4M (SR)	6	2×10^{31}	1984-present
	VEPP-2000 (SR)	1	5×10^{31}	2010-present
Cambridge, USA	CEA Bypass (SR)	3	8×10^{27}	1971-1973
Orsay, France	ACO (SR)	0.54	1×10^{29}	1965-1975
	DCI (DR)	1.8	1.7×10^{30}	1977-1985
DESY, Germany	DORIS (SR)	5.6	3.3×10^{31}	1973-1993
	PETRA (SR)	23.4	2.4×10^{31} (@17.5)	1978-1986
CERN, Europe	LEP (SR)	104.5	1×10^{32}	1989-2000
Cornell, USA	CESR (SR)	5.5	1.3×10^{33}	1979-2008
KEK, Japan	TRISTAN (SR)	32	4.1×10^{31}	1986-1995
	KEKB (DR)	8 (e ⁻) 3.5 (e ⁺)	2.1×10^{34}	1998-2010
	SuperKEKB (DR)	7 (e ⁻) 4 (e ⁺)	8×10^{35} [f]	2016-present
IHEP, China	BEPC (SR)	2.4	1×10^{31} (@1.84)	1988-2004
	BEPC II (DR)	2.47	1×10^{33} (@1.89)	2009-present



HADRON COLLIDERS



Location	Name (type ^[a])	Beam Energy ^[b] (GeV)	Luminosity ^[b] (cm ⁻² s ⁻¹)	Operation Period
CERN, Europe	ISR (pp DR)	31.4	1.4×10^{32}	1971-1984
	Sp \bar{p} S (p \bar{p} SR)	315	6×10^{30}	1981-1991
	LHC (pp, ii, pi DR)	6800 (p) 2510/n (Pb) ^[c] 6500 (p) 2560/n (Pb) ^[c]	2.1×10^{34} 6.1×10^{27} 9×10^{29}	2009-present
Fermilab, USA	Tevatron (p \bar{p} SR)	980	4.3×10^{32}	1987-2011
DESY, Germany	HERA (ep DR)	27.5 (e ⁻) 920 (p)	5.3×10^{31}	1992-2007
Brookhaven, USA	RHIC (pp, ii DR)	250 (p) 100/n (Au) ^[c]	2.5×10^{32} 1.6×10^{28}	2000-present
	EIC (ep, ei DR) ^[d]	18 (e ⁻) 275 (p) 18 (e ⁻) 110/n (Au) ^[c]	1×10^{34} 3×10^{30}	(under construction)



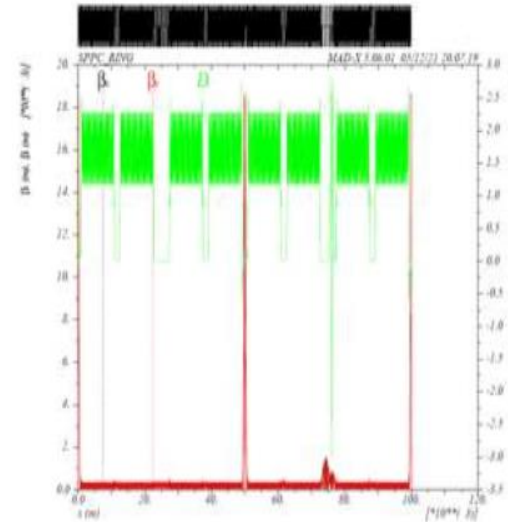
SPPC COLLIDER PARAMETERS



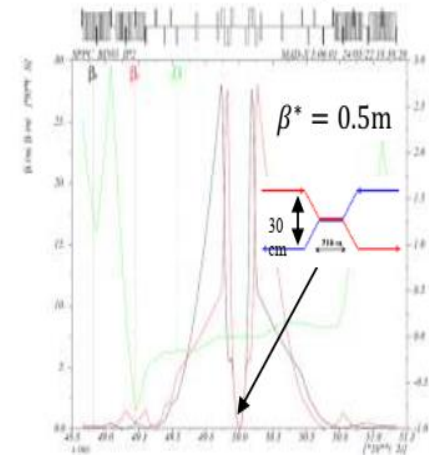
Main parameters

Circumference	100	km
Beam energy	62.5	TeV
Lorentz gamma	66631	
Dipole field	20.00	T
Dipole curvature radius	10415.4	m
Arc filling factor	0.780	
Total dipole magnet length	65442.0	m
Arc length	83900	m
Total straight section length	16100	m
Energy gain factor in collider rings	19.53	
Injection energy	3.20	TeV
Number of IPs	2	
Revolution frequency	3.00	kHz
Revolution period	333.3	μ s
Physics performance and beam parameters		
Initial luminosity per IP	4.3E+34	$\text{cm}^{-2}\text{s}^{-1}$
Beta function at initial collision	0.5	m
Circulating beam current	0.19	A
Nominal beam-beam tune shift limit per	0.015	
Bunch separation	25	ns
Bunch filling factor	0.756	
Number of bunches	10080	
Bunch population	4.0E+10	
Accumulated particles per beam	4.0E+14	

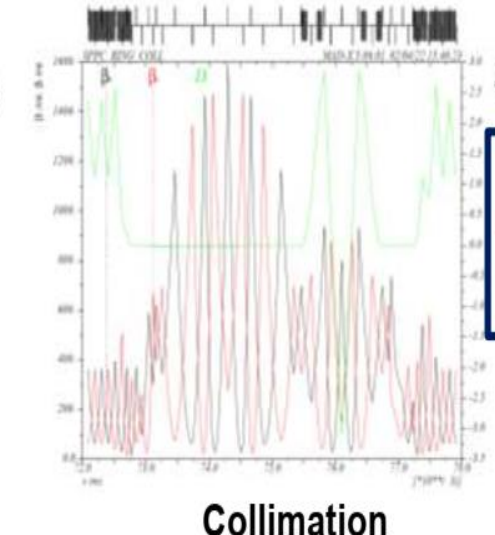
Lattice of SPPC



Whole ring

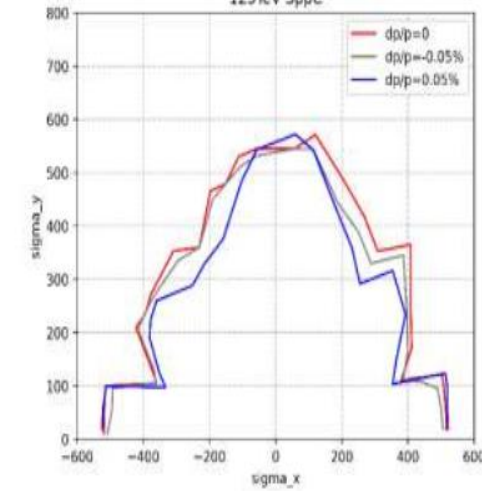


IP



Collimation

125TeV SppC

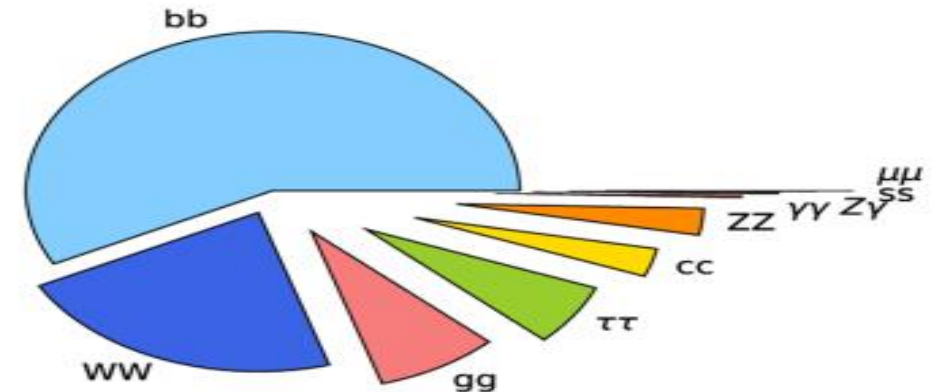
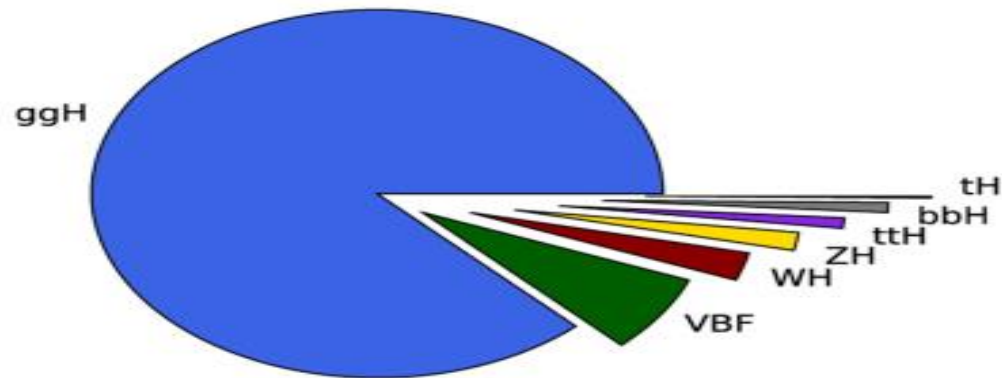


Dynamic Aperture

SppC is compatible with CEPC in the same tunnel

Ecm=125TeV with dipole field of 20T

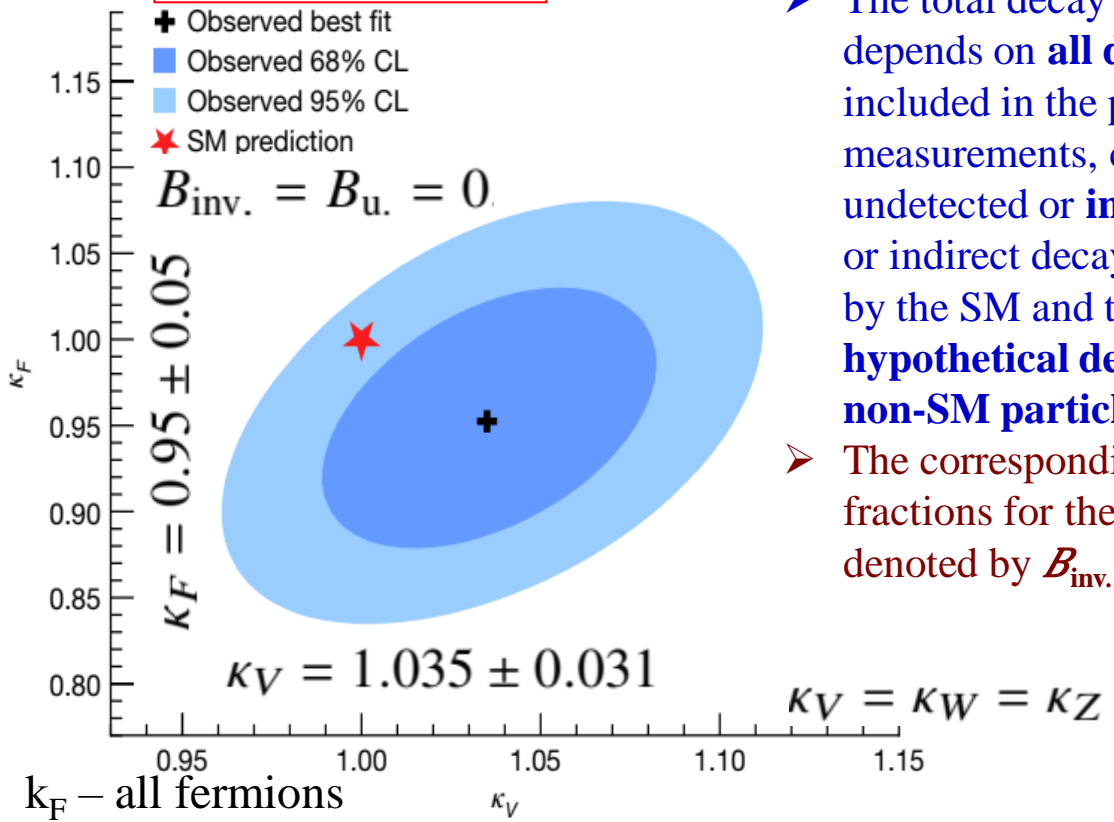
Production mode	Cross section (pb)	Decay channel	Branching fraction (%)
ggH	48.31 ± 2.44	bb	57.63 ± 0.70
VBF	3.771 ± 0.807	WW	22.00 ± 0.33
WH	1.359 ± 0.028	gg	8.15 ± 0.42
ZH	0.877 ± 0.036	ττ	6.21 ± 0.09
ttH	0.503 ± 0.035	cc	2.86 ± 0.09
bbH	0.482 ± 0.097	ZZ	2.71 ± 0.04
tH	0.092 ± 0.008	γγ	0.227 ± 0.005
		Zγ	0.157 ± 0.009
		ss	0.025 ± 0.001
		μμ	0.0216 ± 0.0004



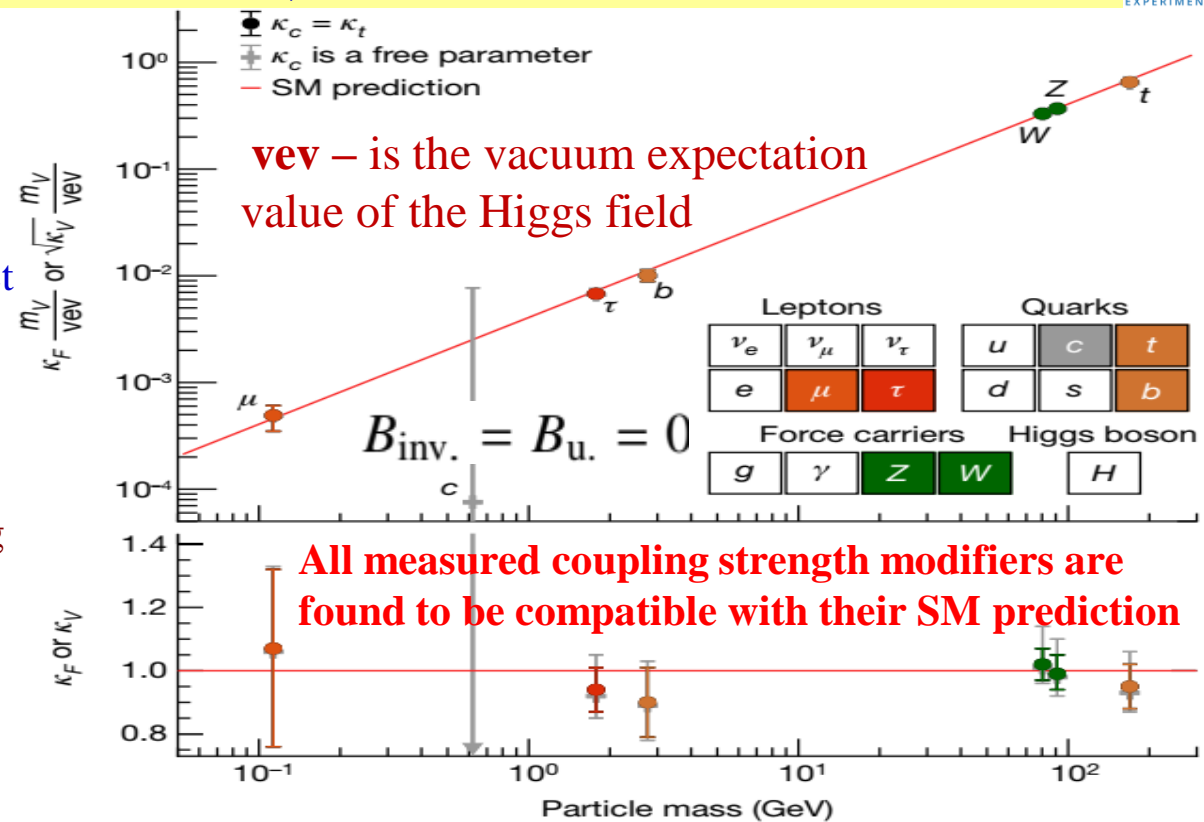
Theoretical cross-sections for each production mode and branching fractions for the decay channels, at 13 TeV for $m_H=125.38$ GeV

HIGGS BOSON COUPLING STRENGTH

the SM prediction of $\kappa_V = \kappa_F = 1$



- The total decay width depends on **all decay modes** included in the present measurements, currently undetected or **invisible**, direct or indirect decays predicted by the SM and the **hypothetical decays into non-SM particles**.
- The corresponding branching fractions for the two are denoted by $B_{inv.}$ and B_u



v_{ev} – is the vacuum expectation value of the Higgs field

All measured coupling strength modifiers are found to be compatible with their SM prediction

κ_F – all fermions
 Negative log-likelihood contours corresponding to 68% and 95% CL in the (κ_V, κ_F) plane. The p -value for compatibility of the combined measurement and the SM prediction is 14%

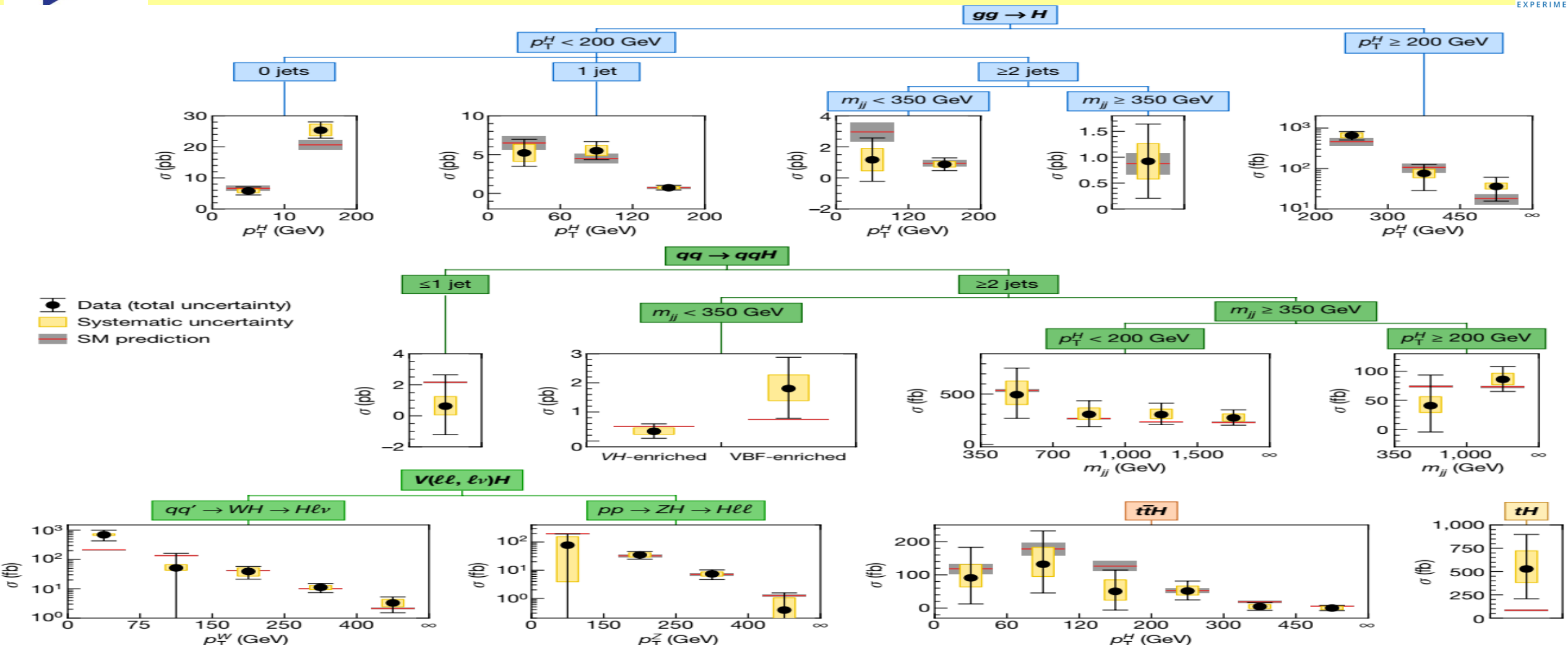
A coupling strength modifier κ_p for a production or decay process via the coupling to a given particle p is defined as

$$\kappa_p^2 = \sigma_p / \sigma_p^{SM} \quad \kappa_p^2 = \Gamma_p / \Gamma_p^{SM}$$

Γ_p is the partial decay width into a pair of particles p .

Reduced Higgs boson coupling strength modifiers and their uncertainties. They are defined as $\kappa_F m_F / v_{ev}$ for fermions ($F = t, b, \tau, \mu$) and $\sqrt{\kappa_V} m_V / v_{ev}$ for vector bosons as a function of their masses m_F and m_V . Two fit scenarios with $\kappa_c = \kappa_t$ (coloured circle markers), or κ_c left free-floating in the fit (grey cross markers) are shown. Loop-induced processes are assumed to have the SM structure, and Higgs boson decays to non-SM particles are not allowed. The lower panel shows the values of the coupling strength modifiers.

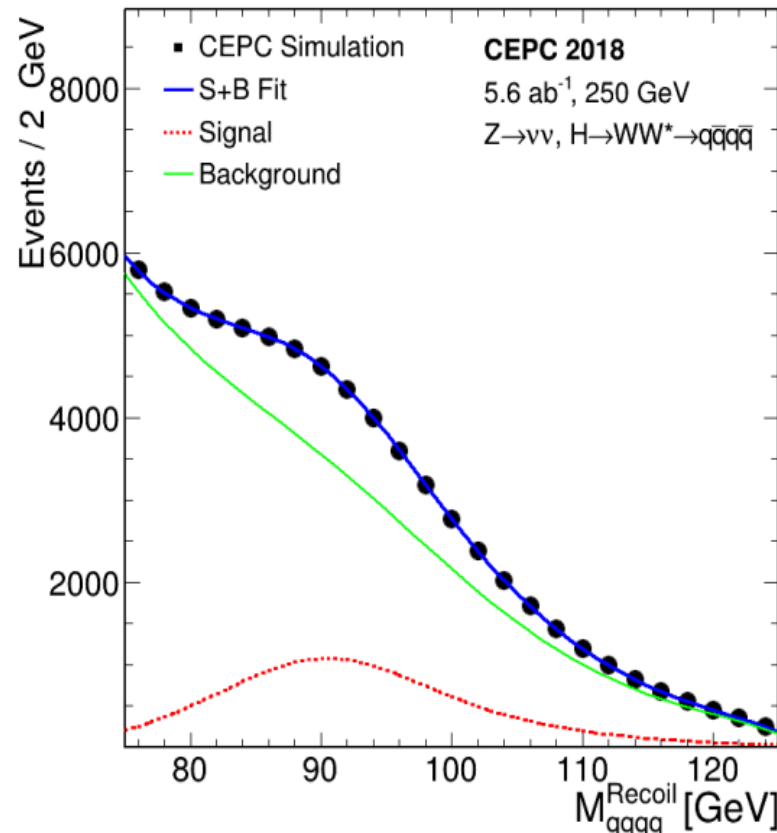
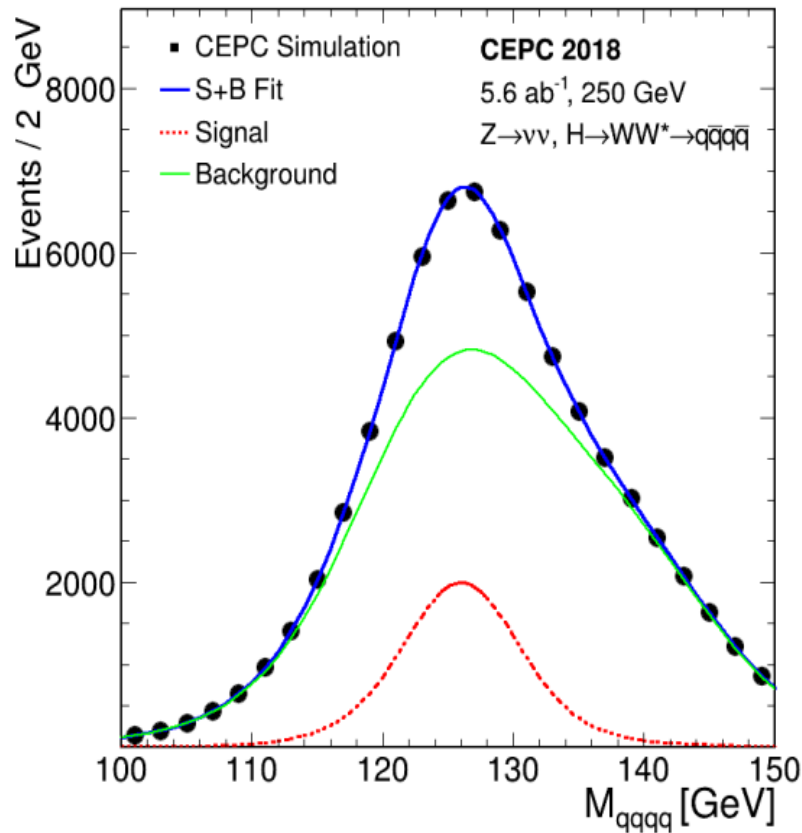
THE RESULTS OF THE SIMULTANEOUS MEASUREMENT IN 36 REGIONS



Observed and predicted Higgs boson production cross-sections in different kinematic regions. The p value for compatibility of the combined measurement and the SM prediction is 94%. Kinematic regions are defined separately for each production process, based on the jet multiplicity, the transverse momentum of the Higgs (p_T^H) and vector bosons (p_T^W and p_T^Z) and the two-jet invariant mass (m_{jj}). The ‘VH-enriched’ and ‘VBF-enriched’ regions with the respective requirements of $m_{jj} \in [60, 120)$ GeV and $m_{jj} \notin [60, 120)$ GeV are enhanced in signal events from VH and VBF productions.



- ❑ At least **two Cosmological phase transitions** are very probable to have happened since the beginning of the Universe, one of them being the **electroweak phase transition** responsible for the **breaking of the EW symmetry**.
- ❑ It is possible that the **EW phase transition** could have caused the **observed baryon asymmetry** of the Universe and therefore provide an **explanation for the baryon asymmetry problem**.
- ❑ **It could also have generated observable gravitational waves.**
- ❑ Both of these possibilities however hinge on the fact that the **EW phase transition** had been a **first-order phase transition**, which it is not according to the standard model.
- ❑ **The SM predicts a crossover transition.**



ZH final state		Precision
$Z \rightarrow e^+e^-$	$H \rightarrow WW^* \rightarrow \nu\nu', \nu\nu, \nu qq̄$	2.6%
$Z \rightarrow \mu^+\mu^-$	$H \rightarrow WW^* \rightarrow \nu\nu', \nu\nu, \nu qq̄$	2.4%
$Z \rightarrow \nu\bar{\nu}$	$H \rightarrow WW^* \rightarrow \nu\nu qq̄, qq̄qq̄$	1.5%
$Z \rightarrow qq̄$	$H \rightarrow WW^* \rightarrow qq̄qq̄$	1.7%
Combination		0.9%

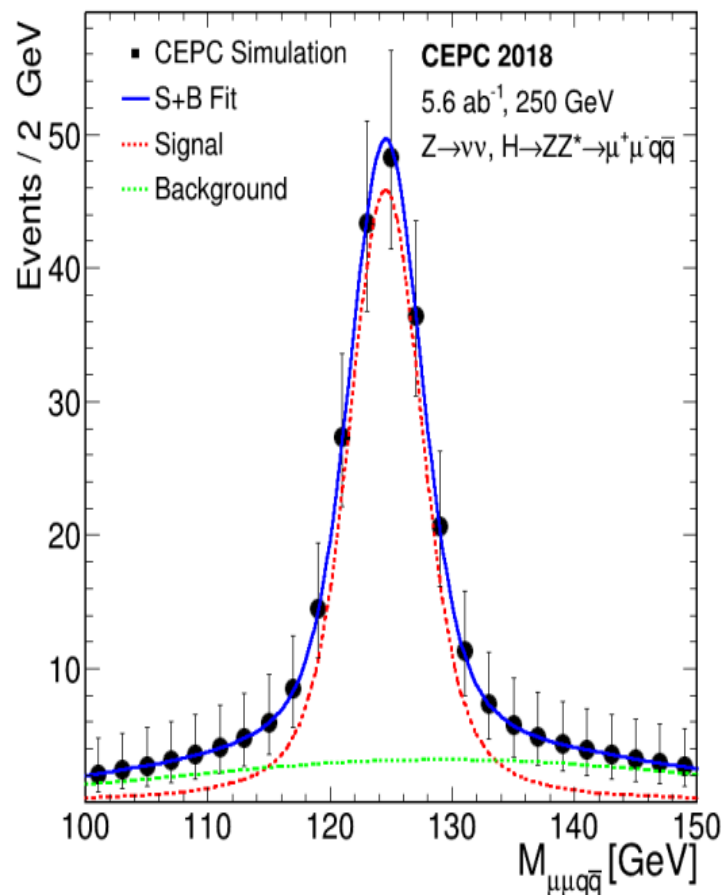
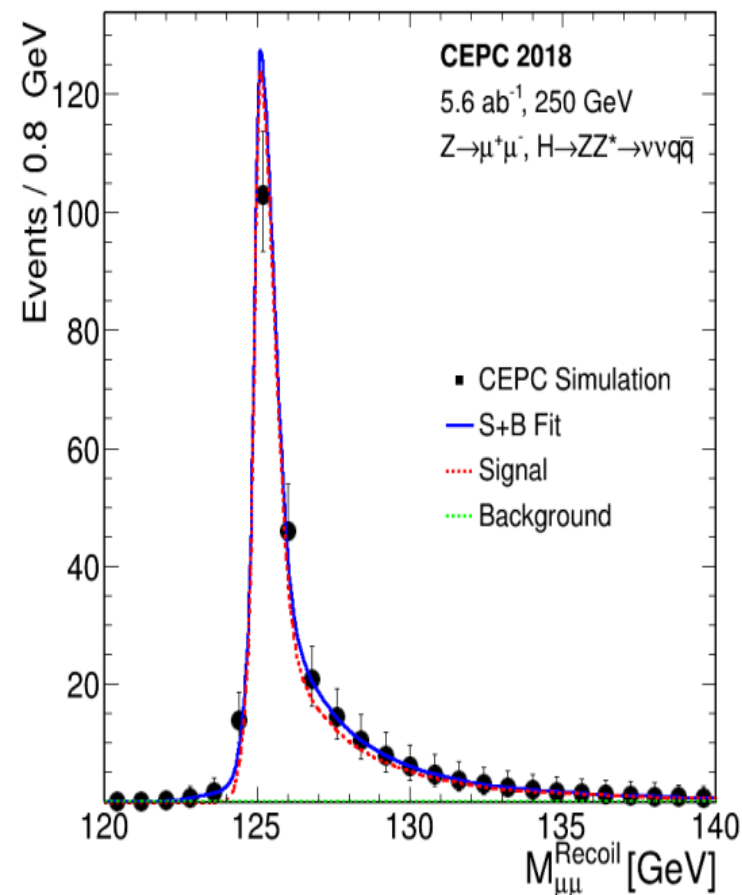
Expected relative precision on the $\sigma(\text{ZH}) \times \text{BR}(\text{H} \rightarrow \text{WW}^*)$ measurement from a CEPC dataset of 5.6 ab⁻¹

ZH production with $Z \rightarrow \nu\nu^-$ and $H \rightarrow \text{WW}^* \rightarrow \text{qqq}^- \text{q}^-$: distributions of the visible mass and the missing mass of selected events. The markers and their uncertainties represent the expected number of events in a CEPC dataset of 5.6 ab⁻¹, whereas the solid blue curves are the fit results. The dashed curves are the signal and background components. Contributions from other decays of the Higgs boson are included in the background.

- The combination of these decay final states leads to a precision of **0.9%**.
- This is likely a conservative estimate as many of the final states of the $\text{H} \rightarrow \text{WW}^*$ decay remain to be explored. Including these missing final states will no doubt improve the precision.



HIGGS PHYSICS: ZH PRODUCTION WITH $H \rightarrow ZZ^*$



ZH final state		Precision
$Z \rightarrow \mu^+ \mu^-$	$H \rightarrow ZZ^* \rightarrow \nu \bar{\nu} q \bar{q}$	7.2%
$Z \rightarrow \nu \bar{\nu}$	$H \rightarrow ZZ^* \rightarrow \ell^+ \ell^- q \bar{q}$	7.9%
Combination		4.9%

Expected relative precision on the $\sigma(\text{ZH}) \times \text{BR}(H \rightarrow ZZ^*)$ measurement from a CEPC at 5.6 ab⁻¹

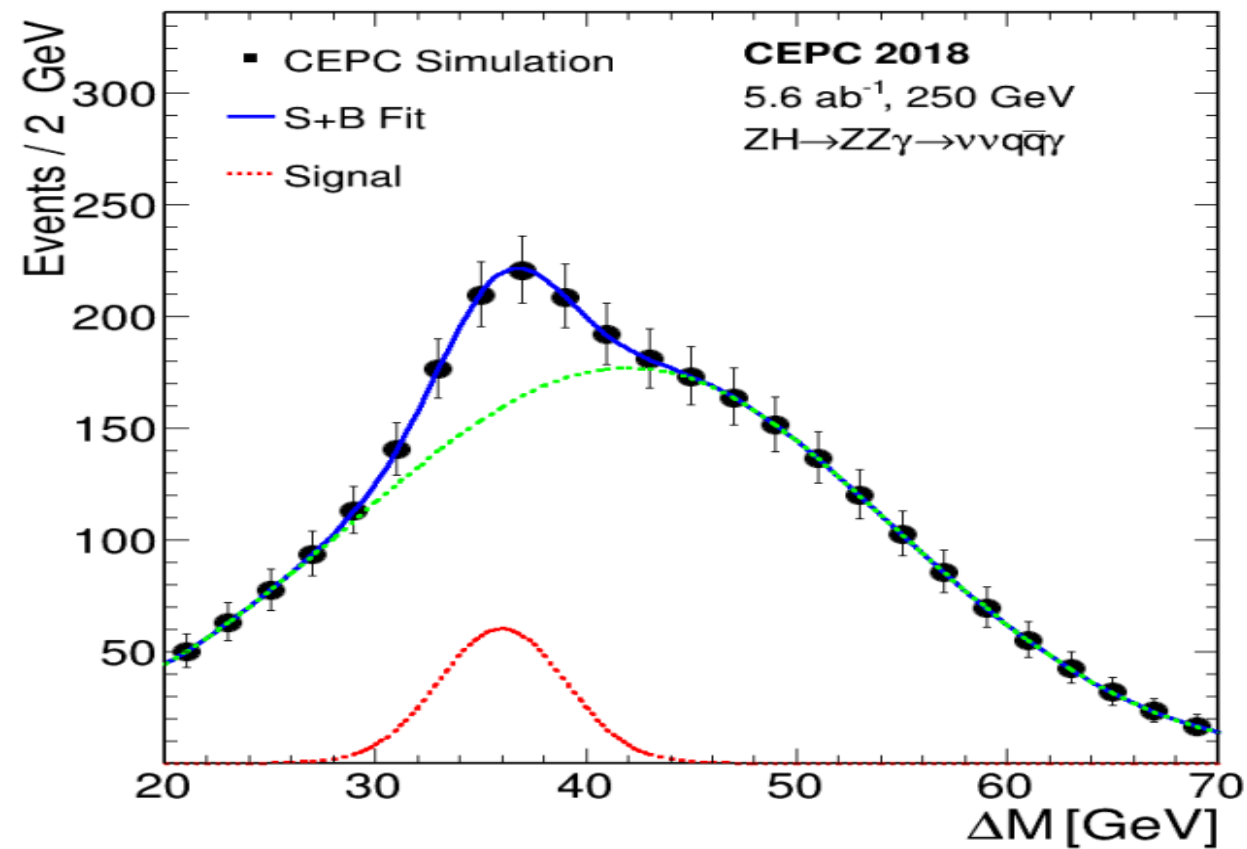
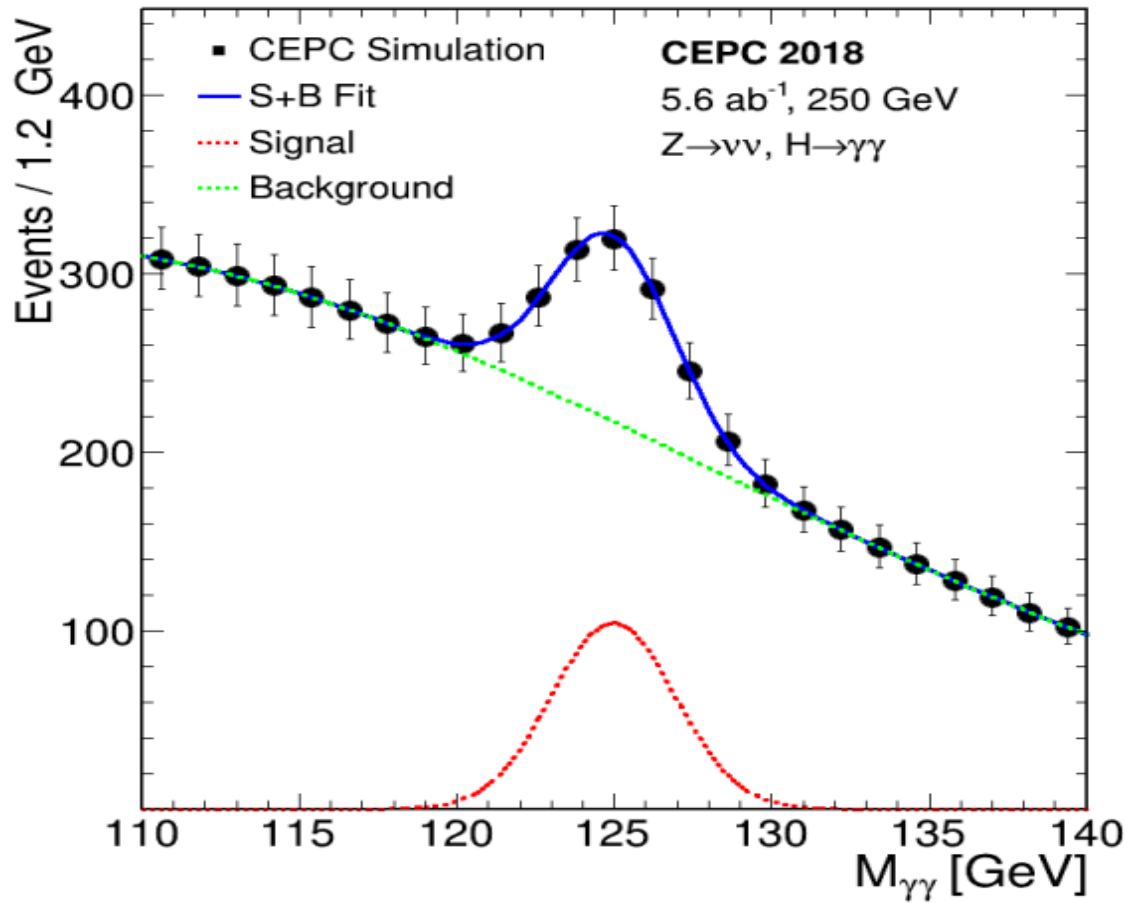
The combination of these final states results in a precision of about 4.9%.

The sensitivity can be significantly improved considering that many final states are not included in the current study. In particular, the final state of $Z \rightarrow qq^-, H \rightarrow ZZ^* \rightarrow qq^-\bar{q}^-$ which accounts for a third of all $ZH \rightarrow ZZZ^*$ decay is not studied. Moreover, there are further potential improvements by using multivariate techniques. The combination of these decay final states leads to a precision of 0.9%.

ZH production with $H \rightarrow ZZ^*$: the recoil mass distribution of the $\mu^+\mu^-$ system for $Z \rightarrow \mu^+\mu^-$; $H \rightarrow ZZ^* \rightarrow \nu\nu q^- q^-$; the invariant mass distribution of the $\mu^+\mu^- q^- q^-$ system for $Z \rightarrow \nu\nu$; $H \rightarrow ZZ^* \rightarrow \mu^+\mu^- q^- q^-$. The markers and their uncertainties represent the expected number of events in a CEPC dataset of 5.6 ab⁻¹, whereas the solid blue curves are the fit results. The dashed curves are the signal and background components. Contributions from other decays of the Higgs boson are included in the background.



HIGGS PHYSICS: ZH PRODUCTION WITH $H \rightarrow \gamma\gamma$



ZH production with $H \rightarrow \gamma\gamma$: the diphoton invariant mass distribution for the $Z \rightarrow \nu\nu$ decay. The markers and their uncertainties represent the expected number of events in a CEPC dataset of 5.6 ab⁻¹, whereas the solid blue curves are the fit results. The dashed curves are the signal and background components. **A relative precision of 6.2%** on $\sigma(\text{ZH}) \times \text{BR}(H \rightarrow \gamma\gamma)$ can be achieved.

The distribution of the mass difference ΔM ($M_{\text{qq}\bar{\gamma}} - M_{\text{qq}^-}$ & $M_{\nu\nu\bar{\gamma}} - M_{\nu\nu^-}$) of the selected $e^+e^- \rightarrow \text{ZH} \rightarrow \text{ZZ}\gamma \rightarrow \nu\nu \text{qq}\bar{\gamma}$ candidates expected in a dataset with an integrated luminosity of 5.6 ab⁻¹. The signal distribution shown is for the correct pairings of the Higgs boson decays.

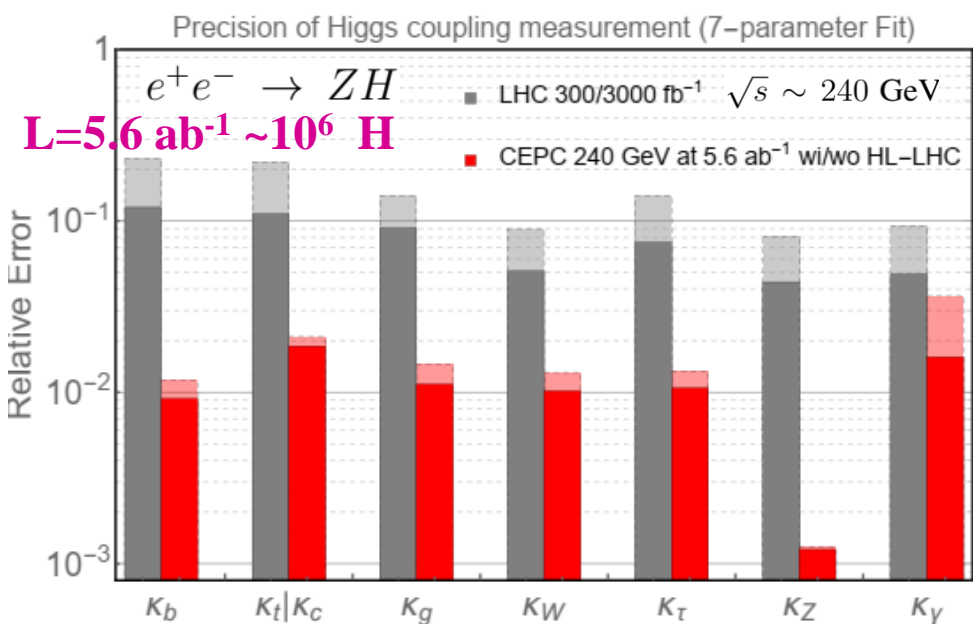
Similar to the $H \rightarrow \gamma\gamma$ decay, the $H \rightarrow Z\gamma$ decay in the SM is mediated by W-boson and top-quark loops and has a branching ratio of **0.154%**.



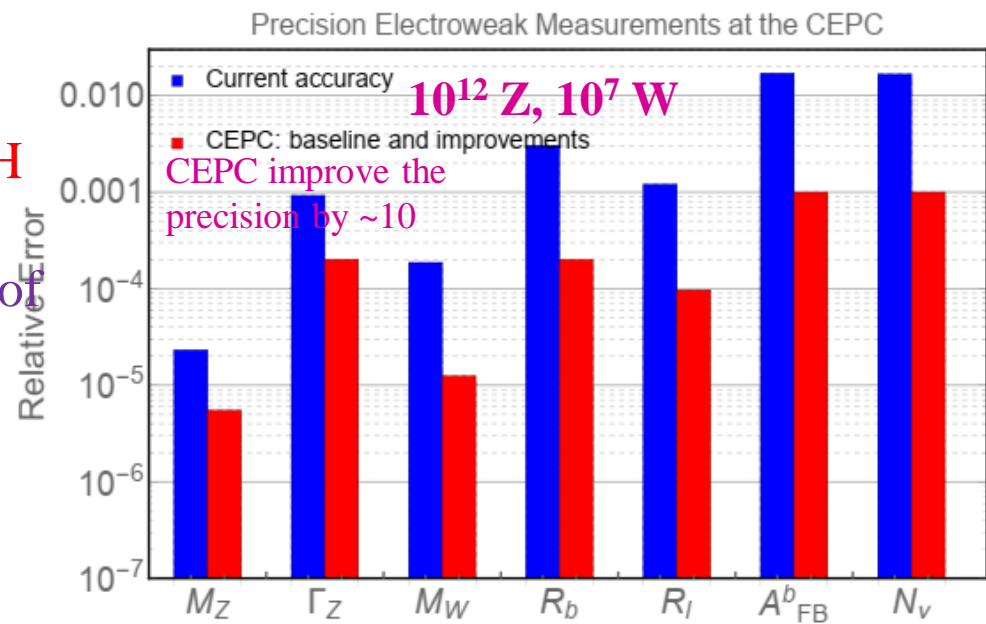
There is not a complete understanding of the nature of the EW phase transition.

- The discovery of a **spin zero Higgs boson**, the first elementary particle of its kind, has only sharpened these questions, *and their resolution* will necessarily involve new physics **BSM**.
- The precision measurement of Higgs boson properties will be a critical component of any road map for high energy physics in the coming decades.
- ❖ BSM physics can lead to *observable deviations in Higgs couplings* relative to SM expectations

$\delta = c \frac{v^2}{M_{NP}^2}$ v and M_{NP} are the vacuum expectation value of the H field & the typical mass scale of new physics. Need to probe new physics significantly beyond the LHC's reach requires measuring H couplings with *sub-percent-level accuracy*



- The **CEPC** has strong capability in detecting *invisible decays of the H*
- For $L=5.6 \text{ ab}^{-1}$, it can *improve the accuracy of the measurement of the H invisible branching ratio to 0.3%, more than 10 times better than the precision for HL-LHC.*



Higgs coupling extraction in the k-framework

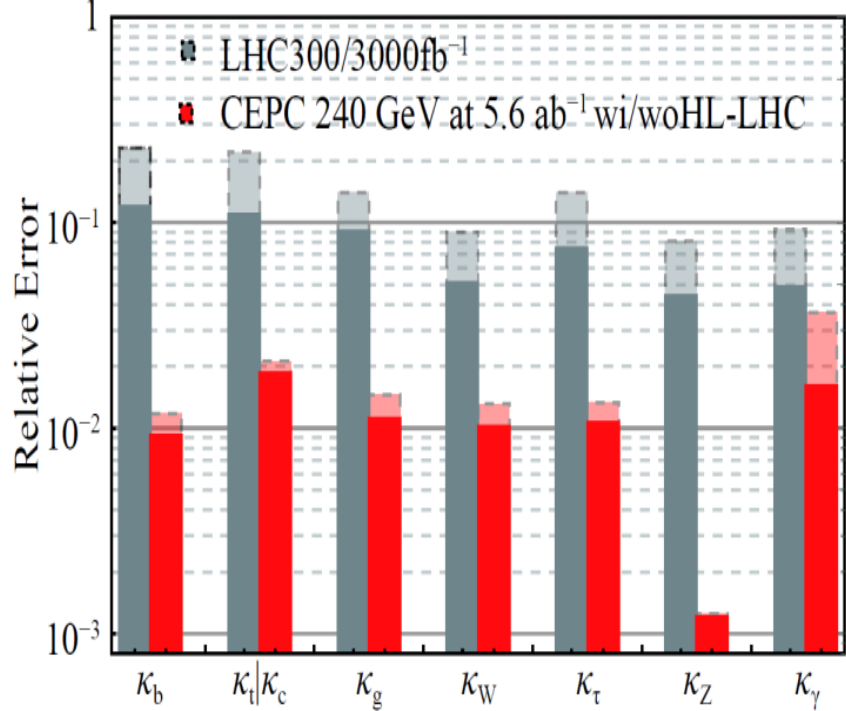
Projection for the precision of the Z-pole measurements



PHYSICS MOTIVATION

Higgs boson was discovered, but understanding its nature requires precision measurements of its properties at the (HL-)LHC or better at future lepton colliders, e.g. Higgs couplings:

Precision of Higgs coupling measurement (7-parameter Fit)

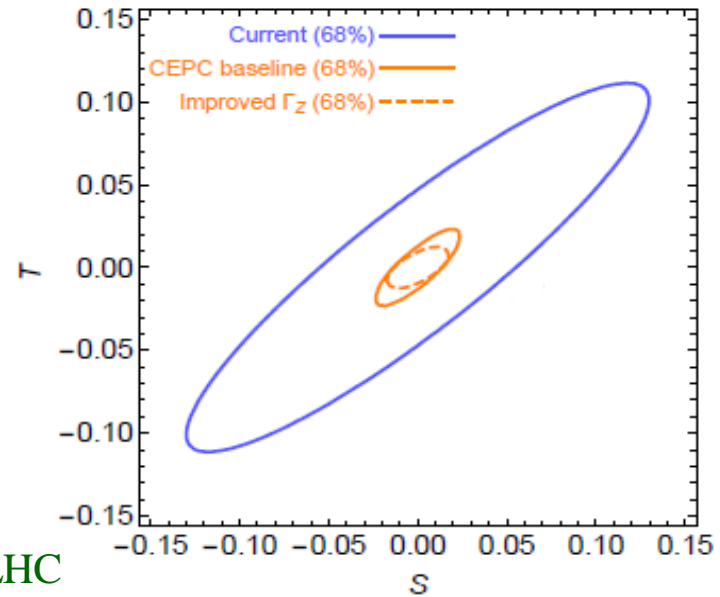


$$\kappa_f = \frac{g(hff)}{g(hff;SM)}$$

$$\kappa_V = \frac{g(hVV)}{g(hVV;SM)}$$

Anticipated accuracy on H-boson properties at CEPC & at LHC/HL-LHC

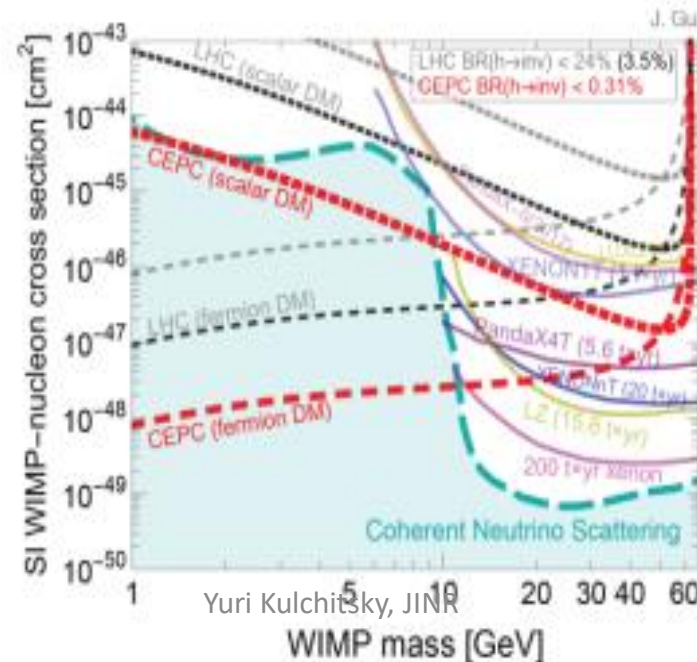
Electroweak Fit: S and T Oblique Parameters



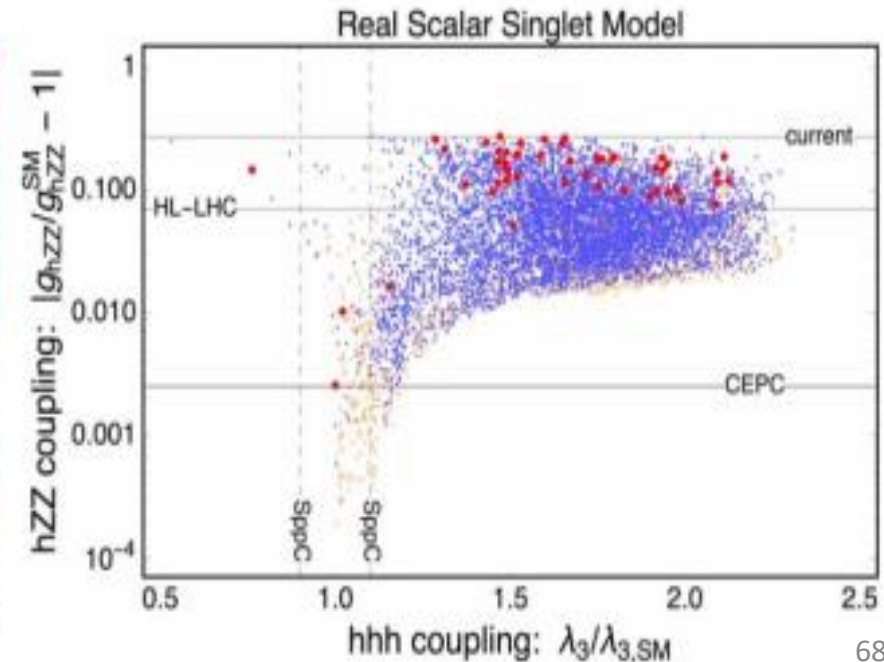
Electroweak measurement can be improved by a large factor

Direct or indirect probe to **dark matter** and **EWPT** etc, an order of magnitude more sensitive than the HL-LHC

31.10.2024



Yuri Kulchitsky, JINR



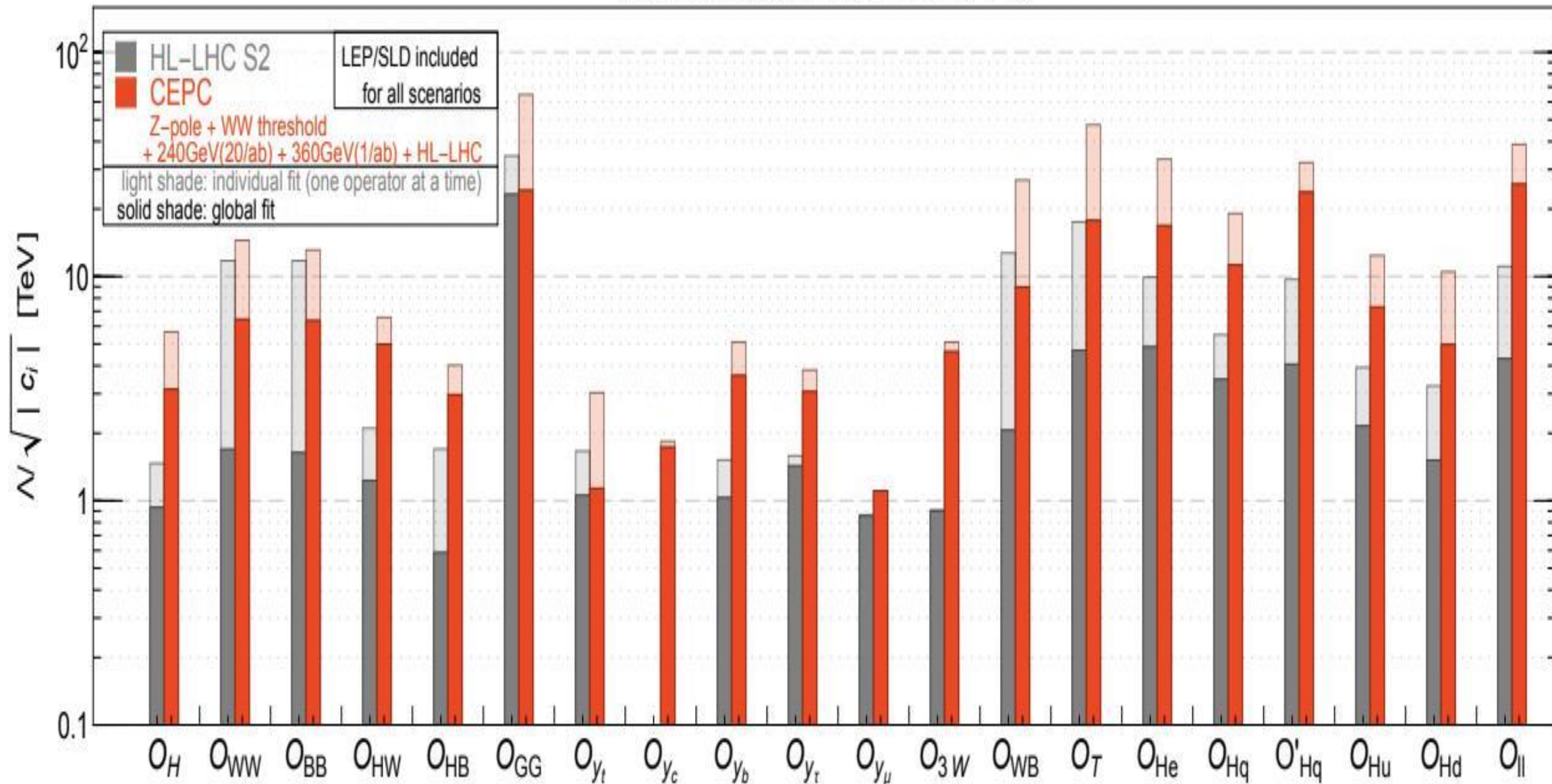


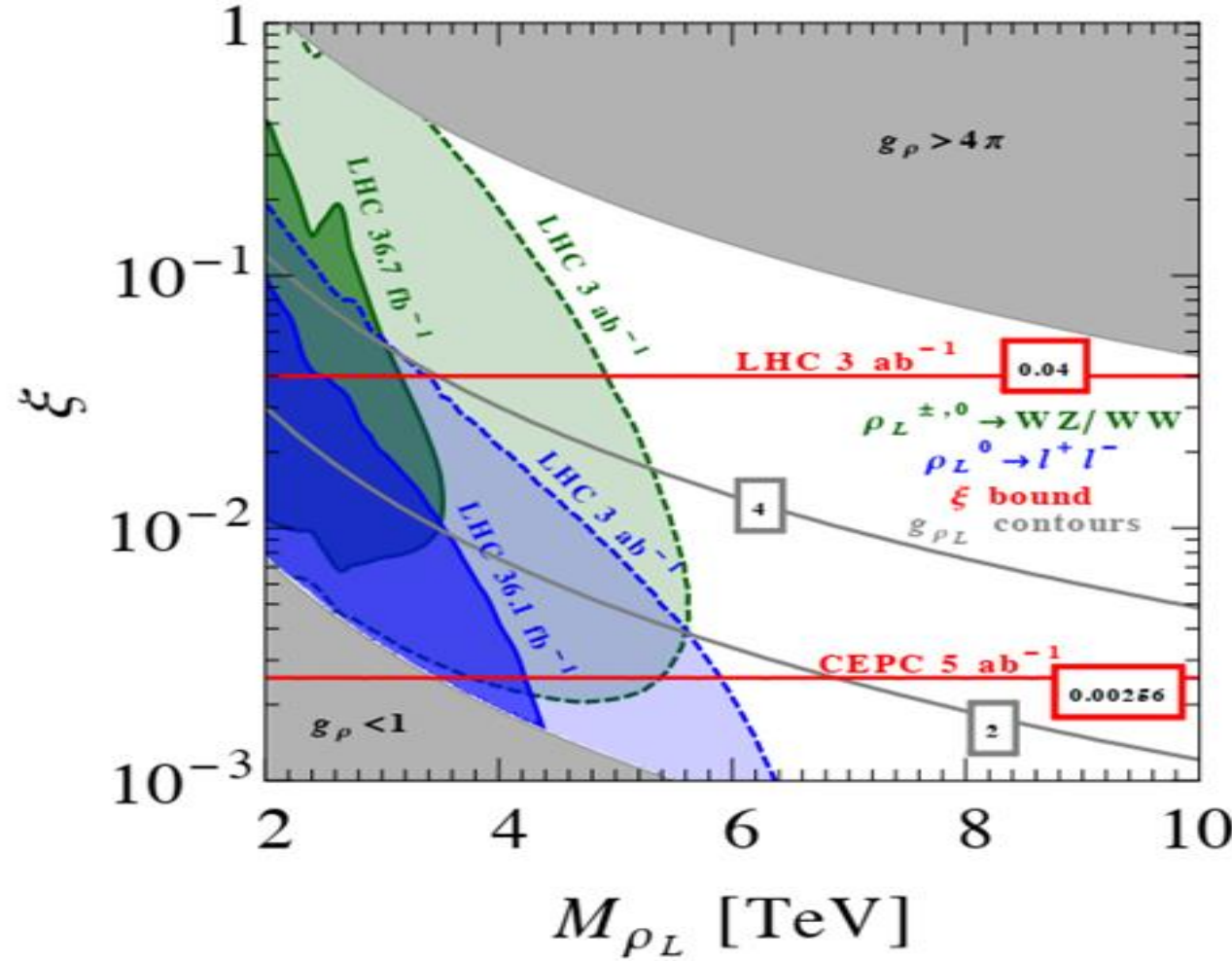
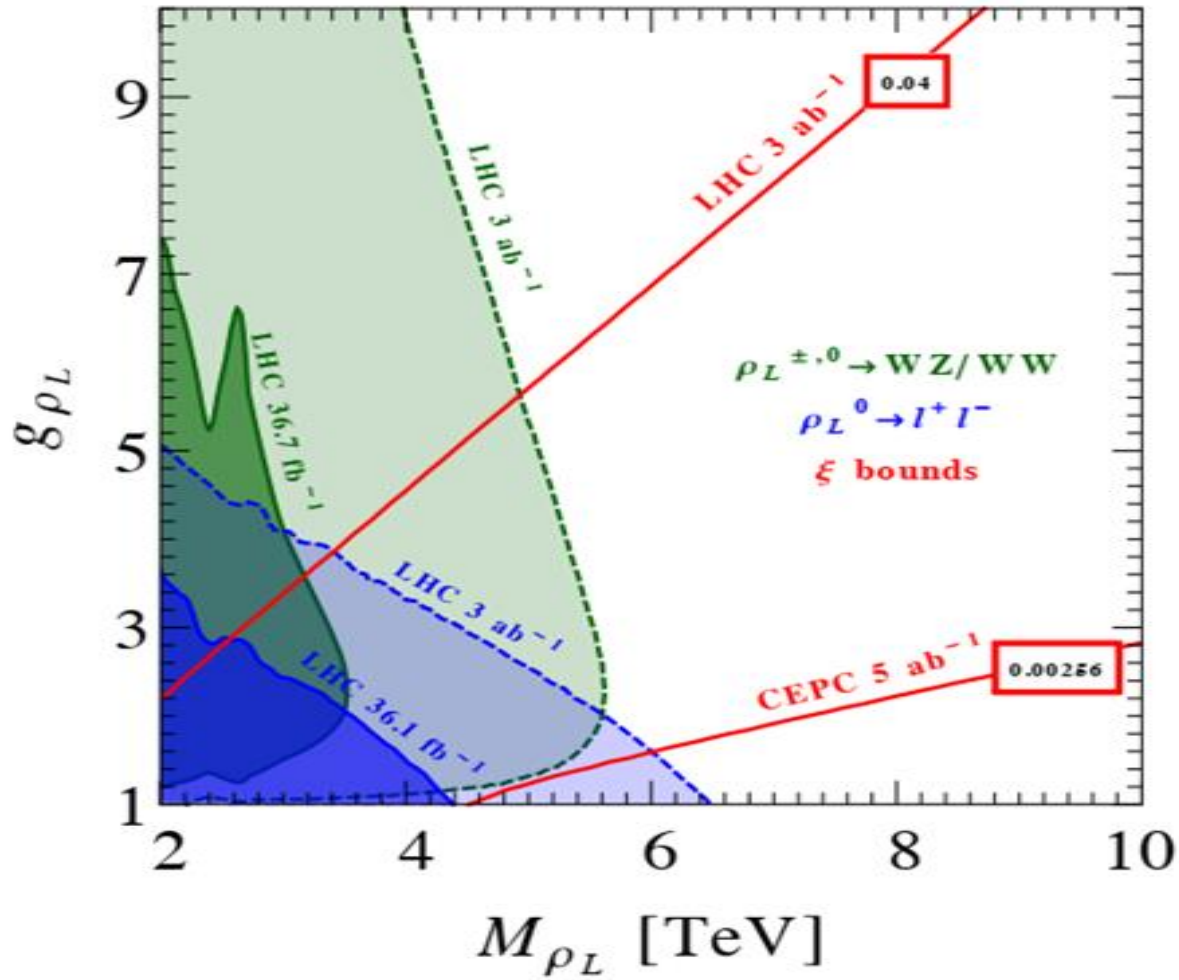
CEPC CAN REVEAL NEW PHYSICS AT ENERGY >10 TEV



Energy scale probed

95% CL reach from SMEFT fit





- Potential coverage of composite-type *global symmetry models* in terms of *resonance mass* $M_{\rho L}$ and *coupling parameter* $g_{\rho L}$;
- *Mixing parameter* $\xi \equiv v_2/f_2$ via direct searches at the LHC (blue & green shaded regions) and precision Higgs measurement constraints (red lines).



KEY SCIENTIFIC ISSUES AND TECHNOLOGICAL ROUTE



Physics → Detector → MDI → Accelerator

New Physics
~10 TeV

- ✓ Dark Matter
- ✓ Extended Higgs
- ✓ Composite Higgs
- ✓ Supersymmetry
-

High Precision
~1%

- ✓ Higgs: 1%-0.1%
- ✓ EW: $O(10^2-10^3)$ vs current
- ✓ Flavor
-

Detector
Particle Flow

- ✓ High Granularity
- ✓ Good Resolution
- ✓ Reliable PID
-

High Lumi.
~ $10^{34-36} \text{cm}^{-2}\text{s}^{-1}$

- ✓ Higgs: 20 ab^{-1}
- ✓ Z: 100 ab^{-1}
- ✓ W: 6 ab^{-1}
- ✓ Top: 1 ab^{-1}

Design & Implementation
Detector & Accelerator

- ✓ Multi-purposed Acc.
- ✓ New concept Detector
- ✓ Cost, added values
- ✓ Spill-over
-
- ✓ Management
- ✓ Collaboration
-

Accelerator
2 IPs/100 km

- ✓ Switchable Operations
- ✓ Upgradability
- ✓ Large Piwiniski angle with Crab-waist
-

Operation mode	Z	W	Higgs
Center-of-mass energy (GeV)	91	160	240
Operation time (year)	2	1	10
Instantaneous luminosity/IP ($10^{34} \text{cm}^{-2}\text{s}^{-1}$)	115	16.0	5.0
Integrated luminosity (ab^{-1} , 2 IPs)	60	3.6	12
Event yield (30 MW)	2.5×10^{12}	1.0×10^8	2.5×10^6
Event yield (50 MW)	4.0×10^{12}	1.6×10^8	4.0×10^6



□ Excellent **acceptance** and **luminosity control**

➤ E.g. ECAL inner radius known at 15 μm

□ **B** ~ 2T for beam emittance preservation

➤ Maximize **tracking volume**

□ Bunch spacing at Z pole ~ 25 ns

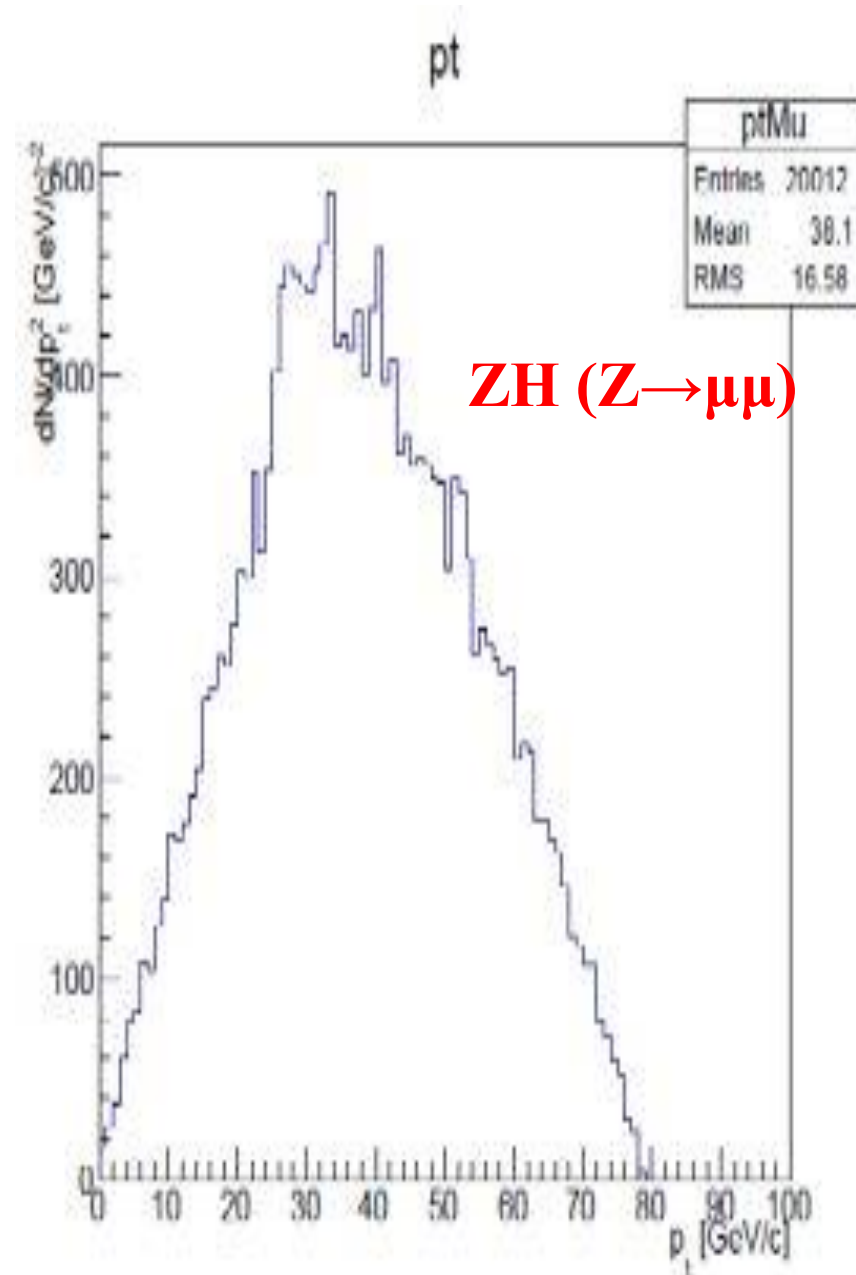
➤ Limited **drift-time**

□ **PID** & π^0 ID for HF/ τ physics

➤ dE/dx or TOF

□ Muons in **ZH** events have rather small p_T

➤ **Transparency** more relevant than asymptotic resolution



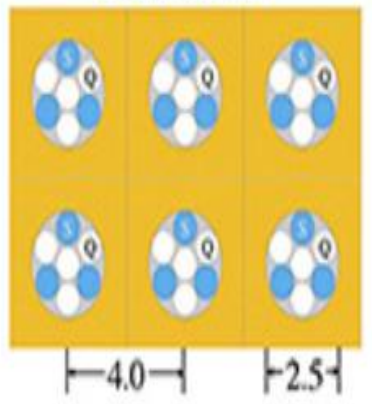


DUAL-READOUT CALORIMETERS

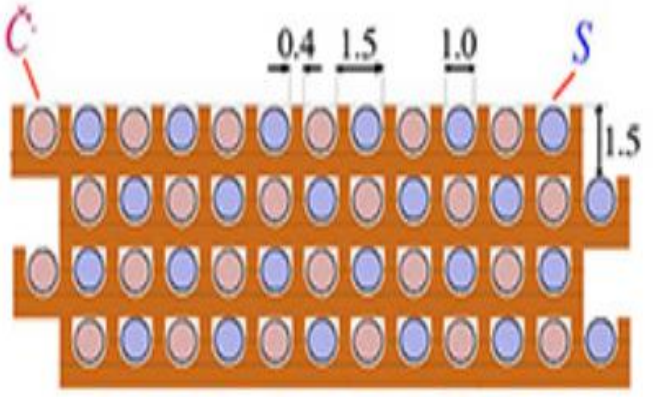
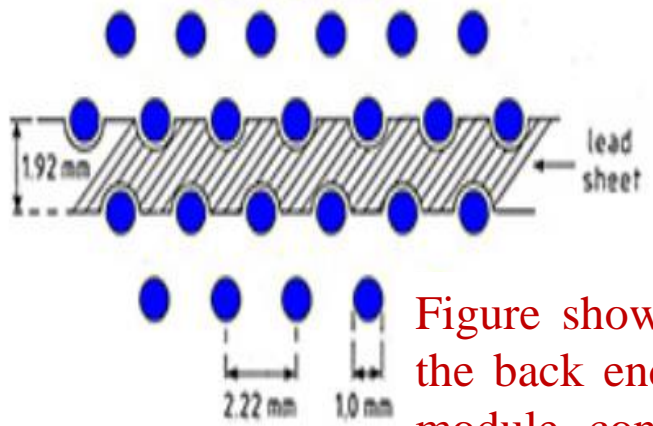
$$\frac{\sigma}{E} = \frac{a}{\sqrt{E}} \quad \text{with} \quad a = 0.027 \sqrt{d/f_{\text{samp}}}$$



DREAM



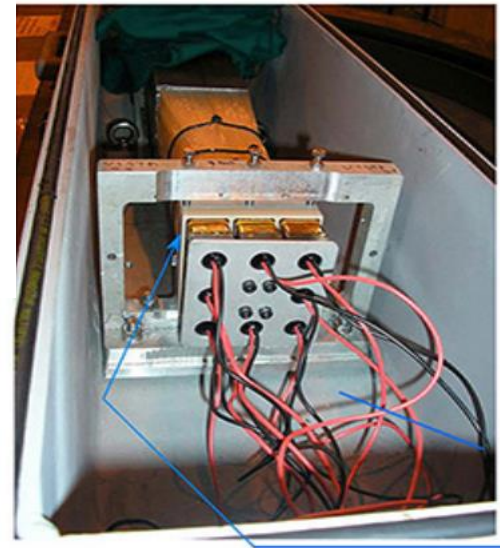
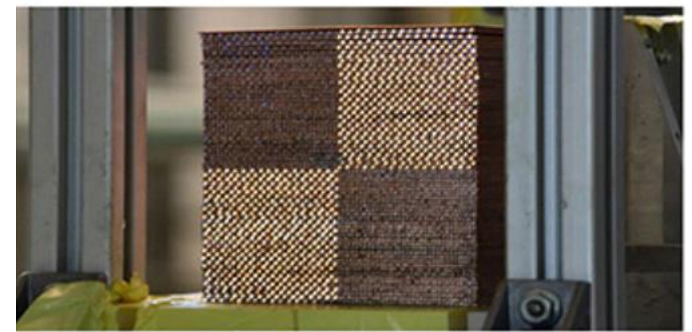
SPACAL



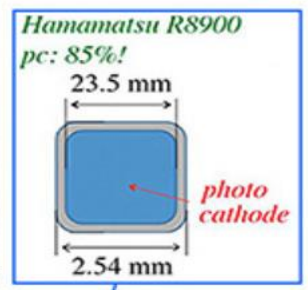
Fiber pattern RD52

Compared RD52 with DREAM, the number of fibers per unit volume, and thus the sampling fraction, is approximately **twice as large in the RD52 calorimeter**. And since each fiber is now separately embedded in the absorber structure, the sampling frequency has also considerably increased. Since both factors determine the electromagnetic energy resolution, one should thus expect a substantial resolution improvement

Figure shows pictures of the front face and the back end of a calorimeter module. Each module consists of four towers, and each tower produces a scintillation and a Cerenkov signal. The transverse dimension of the module was chosen such that the eight PMTs would fit within its perimeter, and the maximum fiber density was determined by the total photocathode surface of these PMTs (which corresponds to more than half of the module's lateral cross section)



9.3 x 9.3 x 250 cm
150 kg
4 towers, 8 PMTs
2 x 2048 fibers



Front and rear view of one of the **RD52** fiber calorimeter modules. The tower structure is made visible by shining light on two of the eight fiber bunches sticking out at the back end. See text for more details.

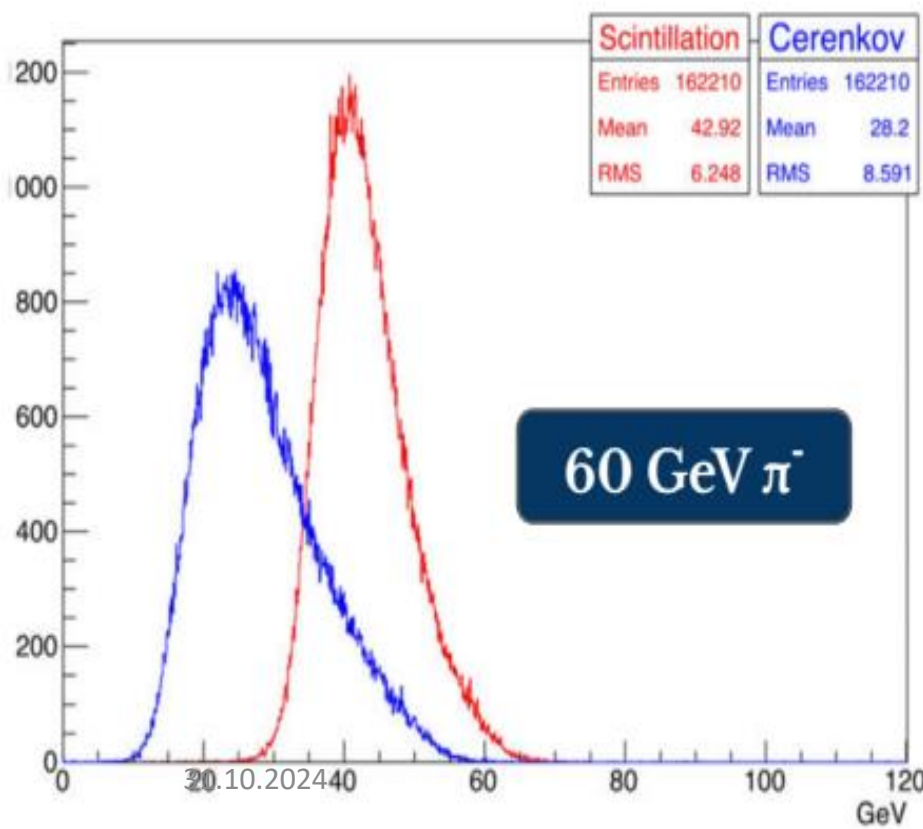
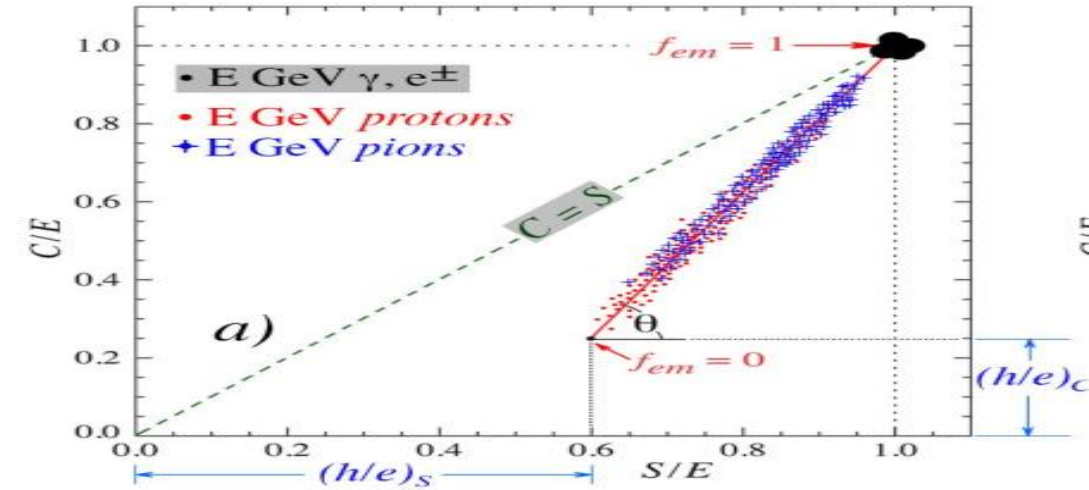
Yuri Kulchitsky, JINR

The structure of the **RD52** fiber calorimeter (copper based modules), compared to that of two other fiber calorimeters: DREAM [NIM A537, 5376 2005] and SPACAL [NIM A308, 4816 1991].



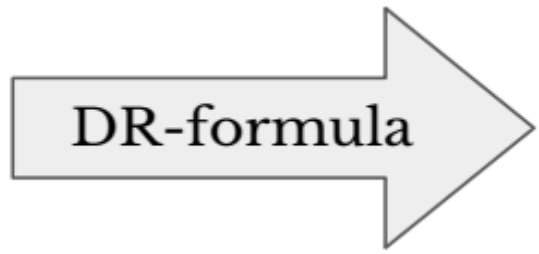
DUAL READOUT CALORIMETRY

- ❑ Calibration with electrons of known energy for both **em** and **hadronic** showers
 - Potential to use as ECAL and HCAL combined
 - Universal for all hadron types
- ❑ Restored Gaussian and linear response to hadrons
- ❑ **Improved energy resolution**

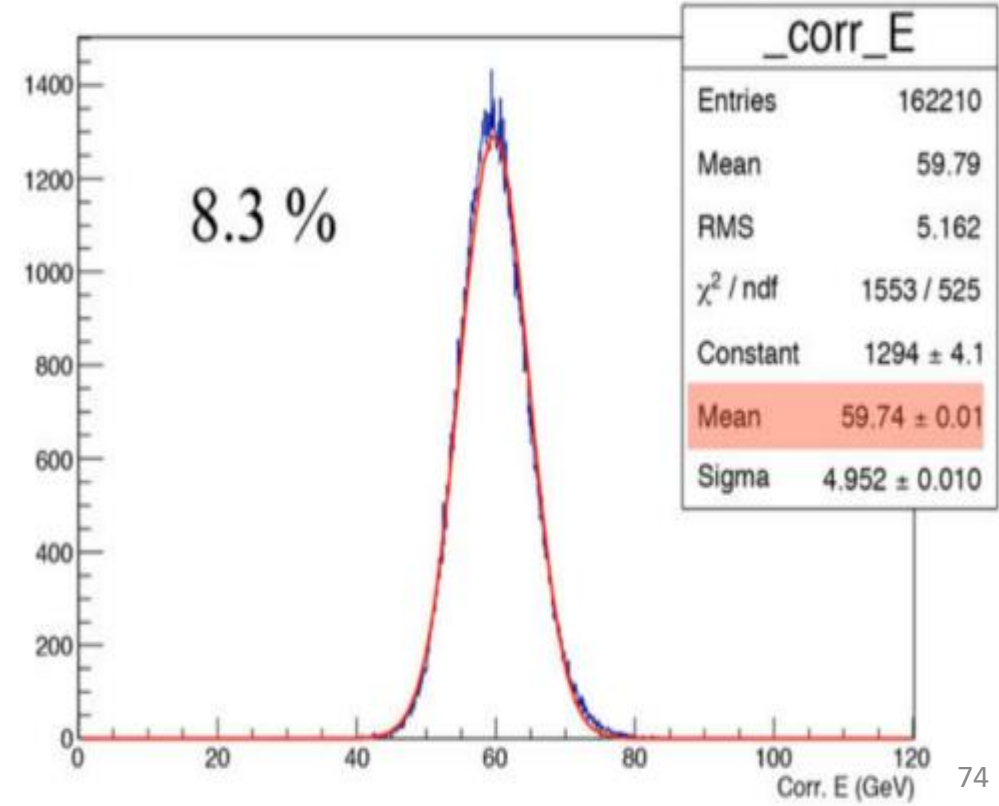


$$\cot \theta = \frac{1 - (h/e)_s}{1 - (h/e)_c} = \chi$$

$$E = \frac{S - \chi C}{1 - \chi}$$



Yuri Kulchitsky, JINR





Two technology options are being explored for the **CEPC calorimetry system**:

I. the **Dual-readout (DR) concept**

- ❖ The dual-readout approach aims for a **combined and homogeneous calorimeter with excellent performance for both electromagnetic and hadronic particle showers.**

II. the **Particle Flow Algorithm (PFA) concept**

- ❖ The PFA approach aims to develop **high-granularity electromagnetic and hadronic calorimeters capable of measuring individual particles in a jet.**

❖ **CEPC, Conceptual Design Report, Volume II - Physics & Detector, IHEP-CEPC-DR-2018-02, IHEP-EP-2018-01, IHEP-TH-2018-01, The CEPC Study Group, October 2018, e-Print: 1811.10545 [hep-ex], 424 pages**

Chapter 5: Calorimetry

5.3: Particle flow oriented electromagnetic calorimeter;

Jianbei Liu liujianb@ustc.edu.cn,

University of Science and Technology of China, Hefei

Tao Hu hut@ihep.ac.cn,

Institute of High Energy Physics, Chinese Academy of Sciences, Beijing

5.4: Particle flow oriented hadronic calorimeter

Haijun Yang, haijun.yang@sjtu.edu.cn,

Department of Physics and Astronomy, Shanghai Jiao Tong University, Shanghai,
Tsung-Dao Lee Institute, Shanghai Jiao Tong University, Shanghai

5.5: Dual-readout calorimeter

Franco Bedeschi bed@fnal.gov,

INFN - Sezione di Pisa, Universita' di Pisa and Scuola Normale Superiore

Roberto Ferrari roberto.ferrari@cern.ch,

INFN - Sezione di Pavia and University of Pavia



Requirements

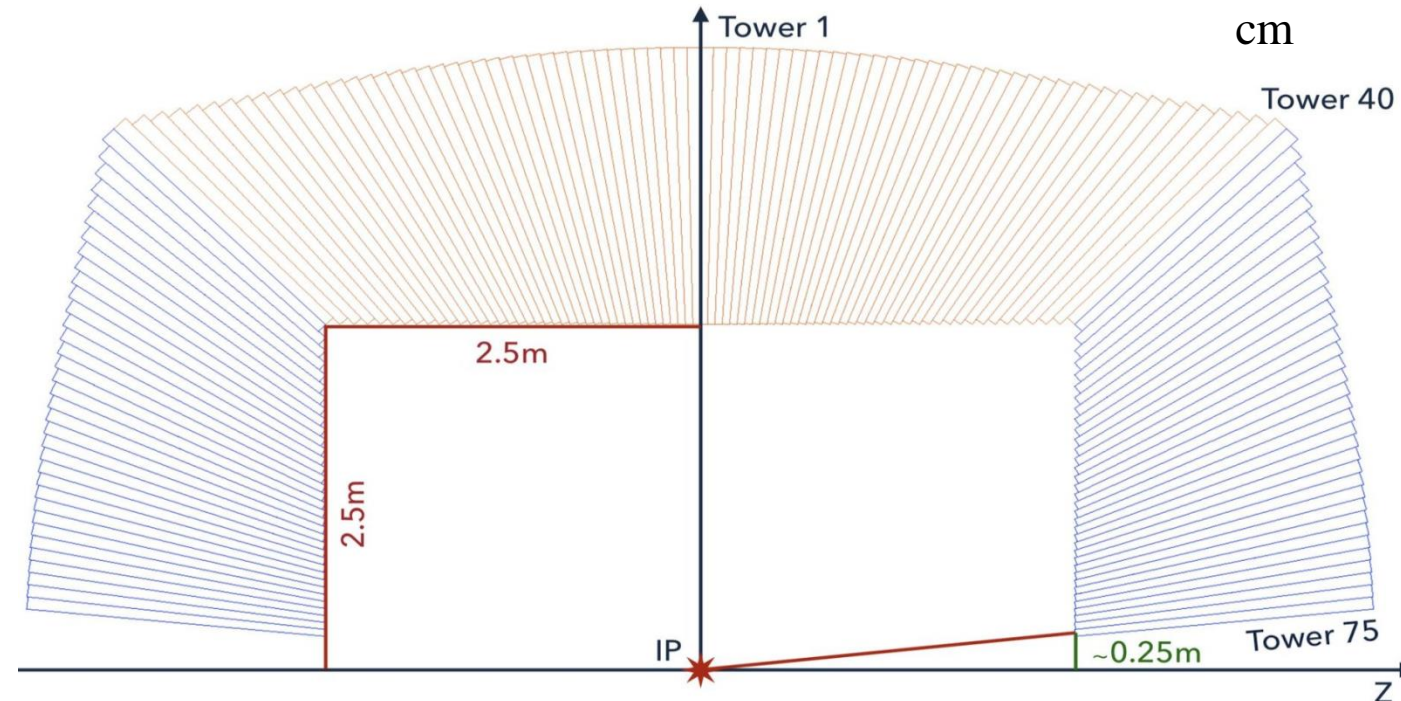
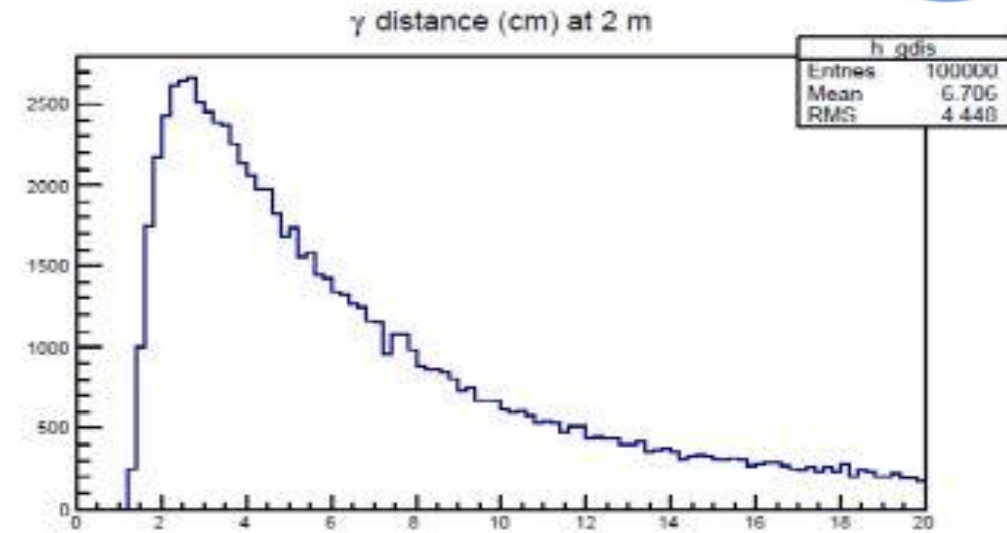
- $\sigma_{EM} \sim 10\text{-}15\%/\sqrt{E}$ sufficient for Higgs physics
- $\sigma_{jets} \sim 30\text{-}40\%/\sqrt{E}$ to clearly identify W, Z, H in 2 jets decays
- Transverse granularity < 1 cm for π^0 from τ and HF
- All electronics in the back to simplify cooling and services

Satisfied by a dual readout fiber calorimeter

- w/SiPM readout

Baseline option

- DR fiber calorimeter
 - ❖ ~ 130 M fibers
 - ✓ 1 mm \varnothing , 1.5 mm pitch
- Copper absorber
- 75 projective towers x 36 slices
 - ✓ $\Delta\vartheta = 1.125^\circ$, $\Delta\phi = 10.0^\circ$
 - ✓ ϑ coverage: ~ 0.100 rad
- G4 simulation available
- ✓ Tuned to RD52 TB data





The CEPC ECAL *to have is required*

1. a good intrinsic energy resolution,
2. precise energy measurement of electrons and photons,
3. excellent shower imaging capability that would allow to identify photons from close-by showers, reconstruct detailed properties of a shower and distinguish electromagnetic showers from hadronic ones effectively.

□ Extensive and focused R&D will be conducted on developing a tungsten-based (**Wolframium**) high-granularity sampling calorimeter with either silicon or scintillator as active medium.

❖ Design optimization and common R&D

1. Optimization of primary detector parameters with full detector simulation;
2. Thermal studies of detector and electronics components through both simulation

❖ Prototyping;

1. Cooling design based on the above studies and prototyping;
2. Development of technological prototypes to address power, cooling and front-end electronics issues;
3. Design of detector modules. Development of technology for fabricating large-size detector modules.

❖ Silicon-Tungsten ECAL

1. Full characterization of a physics Silicon-Tungsten ECAL prototype using its existing test beam data.

❖ Scintillator-Tungsten ECAL

1. Development of a SiPM-scintillator coupling scheme that allows very large dynamic range;
2. Development of technology of fabricating high-quality scintillator strips with required fine structures;
3. Design, construction and characterization of a small size physics prototype



High granularity HCAL is an essential part of the PFA-based CEPC calorimetry system

- **Currently R&D activities** for HCAL system includes **sampling calorimeters** with **stainless steel** as the **absorber** and **gaseous detector** (RPC or GEM) or **scintillator tiles** with embedded electronics as **active sensors**.
- Two technology options are considered, one is **SDHCAL** based on **gaseous detector** and the other is **AHCAL** based on **scintillator with SiPM**.
- **The future R&D plans** for HCAL system include design, construction and performance studies of various prototypes with the CALICE collaboration.

The following R&D program is being pursued in order to address and clarify several issues before the TDR

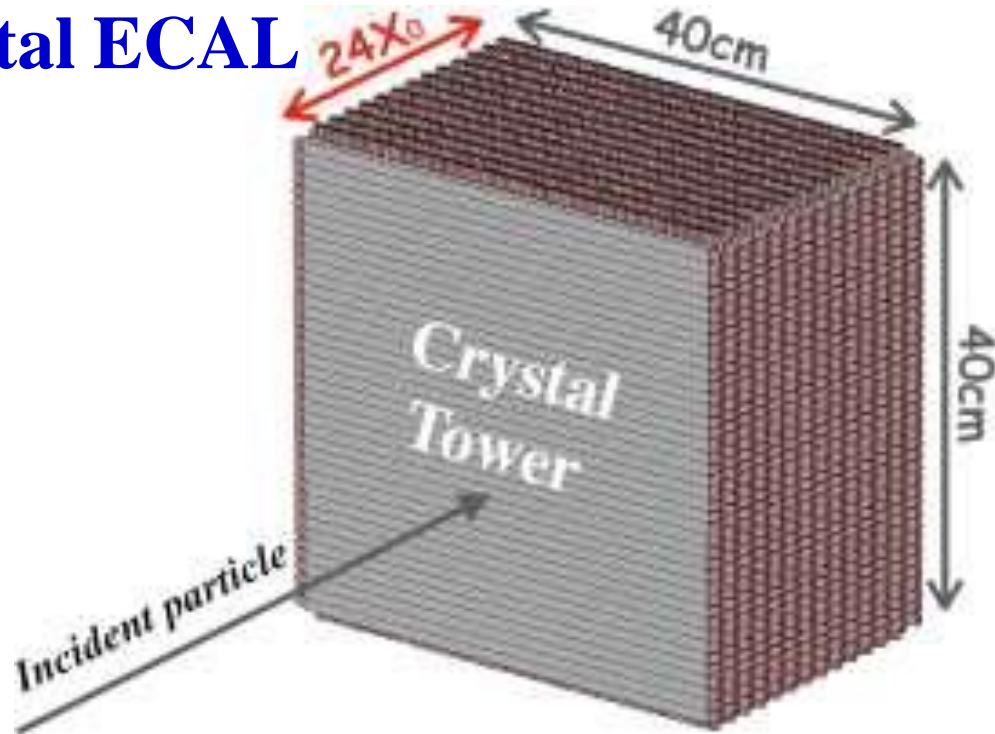
1. Make performance study of **SDHCAL** technological prototype based on RPC using MC and test beam data samples;
2. Design and construction of a small-size **AHCAL** prototype using **scintillator and SiPM**, make performance study with test beam and MC samples;
3. **Optimize the geometry and cell size** of **SDHCAL** and **AHCAL** designs;
4. **Design active cooling system** for both **SDHCAL** and **AHCAL** prototypes to address ASIC and front-end electronics heating issues;
5. **Develop large size Resistive Plate Chamber (RPC)** (2-3 m²), optimize gas distribution and circulation system to improve gas uniformity;
6. Develop **Multi-layer RPC** with excellent time resolution (~50 ps) which may help to **identify showers from neutrons**;
7. Explore ASIC chips with time information (PETIROC), design and develop corresponding PCB and front-end electronics;
8. Develop THGEM with very compact structure and stable operation.
9. Explore new types of SiPM (eg. NDL SiPM) with better performance/price ratio.



CALORIMETERS WITH PARTICLE FLOW ALGORITHM (PFA)



Crystal ECAL



Energy resolution $\frac{\sim 3\%}{\sqrt{E}} \oplus \sim 1\%$

Features

- Good energy resolution
- 3D shower info. with limited readout channel
- Shower separation < 4 cm

Main issues for R&D

- Jet reconstruction and PFA algorithm

Scintillation Glass HCAL

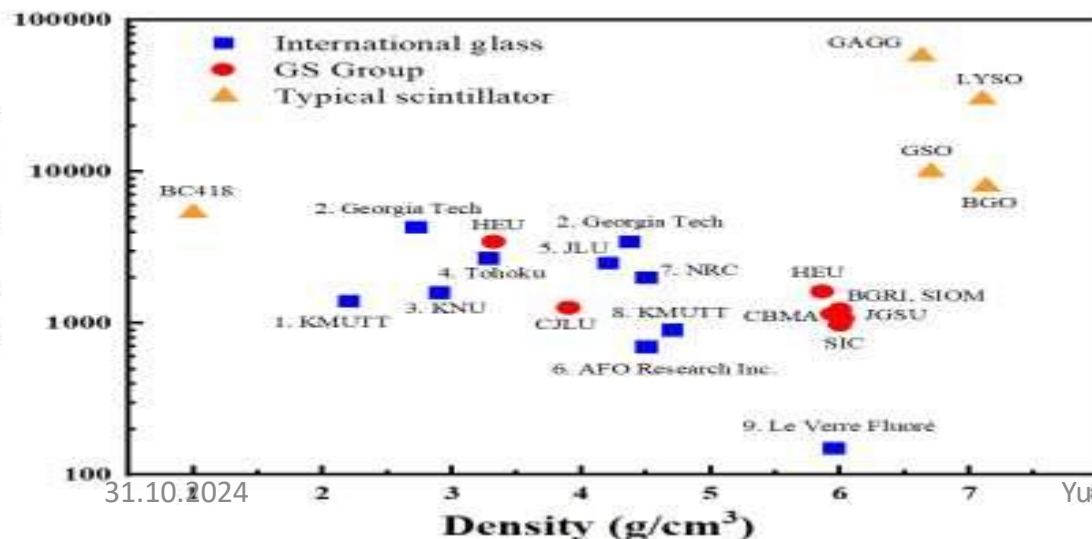
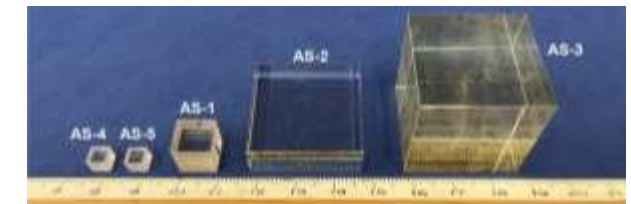
Energy resolution $\sim 40\%/\sqrt{E} \pm \sim 2\%$

Features :

- Large sampling ratio at low cost

Main issues for R&D

- high density, high light yield, radiation hardness, production



31.10.2024

Yuri Kulchitsky, JINR



DIGITAL ECAL CONCEPT

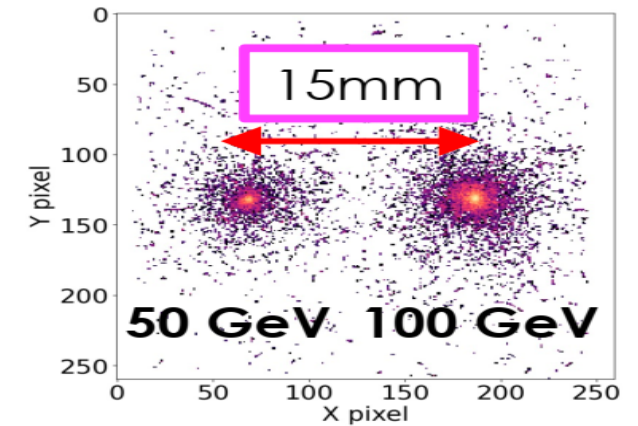
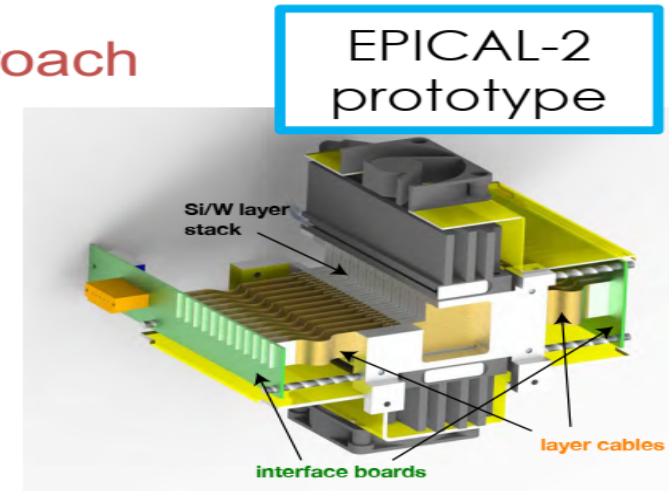
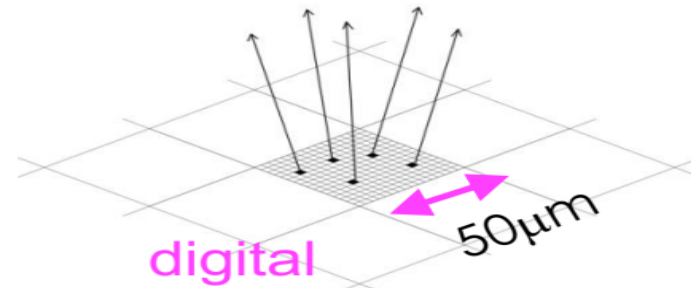
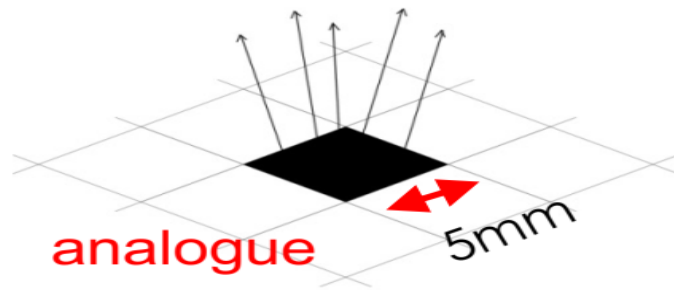
- Calorimeter samples energy between ~ 30 W absorber layers
- **Analogue**, e.g. CMS HGCAL (\sim ex-ILC), **sum energy** in **5×5 mm² Si cells**
- **Digital: count every individual particle** in EM shower

Need ultra-small pixels! Ideally 1 particle/pixel \rightarrow binary approach

EM shower core density at 500GeV $\sim 100/\text{mm}^2$

Pixels $< 100 \times 100 \mu\text{m}^2$ for no saturation

$\sim 10^{12}$ pixels for ECAL barrel



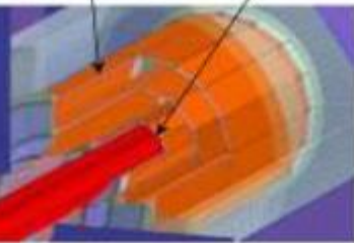
- Using CMOS MAPS, simpler construction, + expect lower cost
- A 'tracking calorimeter', separates boosted decays, e.g. $\tau, \pi^0 \rightarrow \gamma\gamma \dots$
- 20 X_0 **prototype** calorimeter in testbeams



VERTEX DETECTOR AND TRACKER



2 layers / ladder $R_n \sim 16$ mm



JadePix-3 Pixel size $\sim 16 \times 23 \mu\text{m}^2$



Tower-Jazz 180nm CIS process
Resolution 5 microns, 53 mW/cm^2

Goal: $\sigma(\text{IP}) \sim 5 \mu\text{m}$ for high P track

CDR design specifications

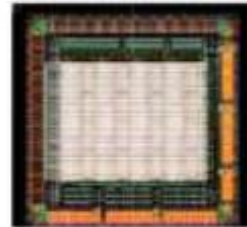
- Single point resolution $\sim 3 \mu\text{m}$
- Low material ($0.15\% X_0$ / layer)
- Low power ($< 50 \text{ mW/cm}^2$)
- Radiation hard (1 Mrad/year)

Silicon pixel sensor develops in 5 series:
JadePix, TaichuPix, CPV, Arcadia, CEPCPix

TaichuPix-3, FS $2.5 \times 1.5 \text{ cm}^2$
 $25 \times 25 \mu\text{m}^2$ pixel size



CPV4 (SOI-3D), 64×64 array
 $\sim 21 \times 17 \mu\text{m}^2$ pixel size



Develop CEPCPix for a CEPC tracker
based on ATLASPix3 CN/IT/UK/DE
TSI 180 nm HV-CMOS process



Arcadia by Italian groups
for IDEA vertex detector
LFoundry 110 nm CMOS



Full vertex detector prototype (TaichuPix-3, JadePix-3) has TB at DESY in Dec. 2022.

TEST BEAM

DESY II

MEMOGA Telescope

JADEPIX Telescope

TaichuPix-3 Telescope (6 layers)

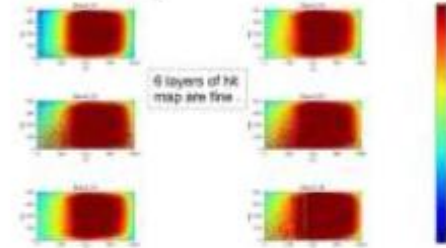
Ar open window in backside of PCB with size of $12 \text{ mm} \times 3 \text{ mm}$

18.6 mm

20.7 mm

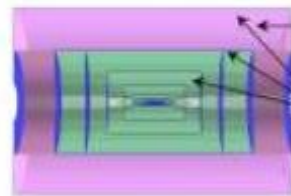


Hitmap of 4 GeV e^+e^- beam



Goal: $3\sigma \pi/K$ separation up to $\sim 20 \text{ GeV/c}$.

- Cluster counting method, or dN/dx , measures the number of primary ionization
- Can be optimized specifically for PID: larger cell size, no stereo layers, different gas mixture
- Garfield++ for simulation, realistic electronics, peak finding algorithm development.



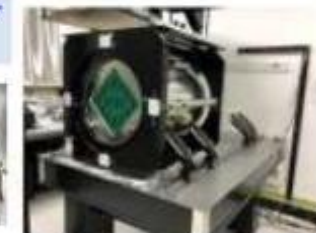
A DC between 2 outer layers

Full silicon trackers

Baseline main tracker
 $\sigma(r-\phi) \sim 100 \mu\text{m}$

470 cm

$R=23-180 \text{ cm}$

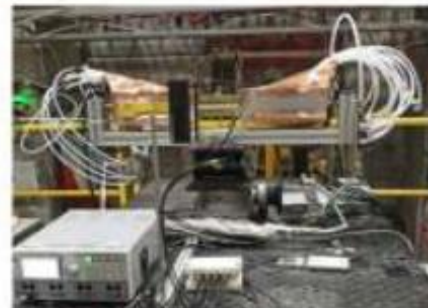
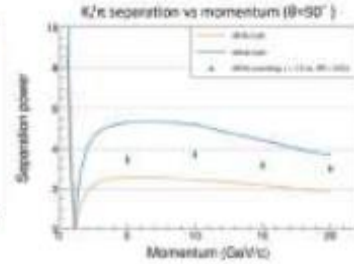
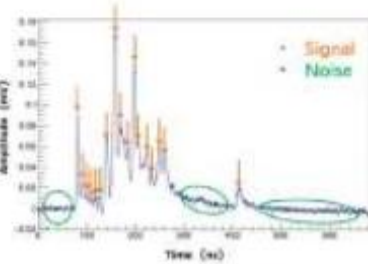


GEM-MM cathode TPC Prototype + UV laser beams

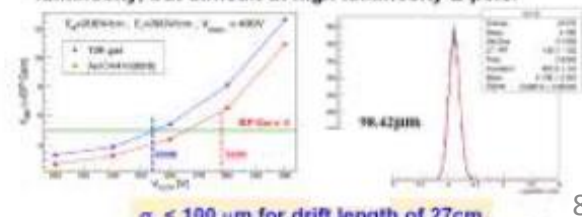
MOST 1 (IHEP+THU)



Low power FEE ASIC



Challenge: Ion backflow (IBF) affects the resolution. It can be corrected by a laser calibration at low luminosity, but difficult at high luminosity Z-pole.



IHEP and Italian INFN groups have close collaboration and regular meetings. IHEP joined the TB (led by INFN group) in 2021 and 2022

Yuri Kulchitsky, JINR